Technical Report CHL-98-16
July 1998

US Army Corps
of Engineers
Waterways Experiment
Station

Wave Refraction at Redondo Beach, California (Comparison of Field Measurements with Models)

by Joon P. Rhee, William D. Corson

Approved For Public Release; Distribution Is Unlimited

Prepared for Headquarters, U.S. Army Corps of Engineers

Technical Report CHL-98-16
July 1998

Wave Refraction at Redondo Beach, California (Comparison of Field Measurements with Models)

by Joon P. Rhee, William D. Corson

U.S. Army Corps of Engineers
Waterways Experiment Station
3909 Halls Ferry Road
Vicksburg, MS 39180-6199

Final report

Prepared for U.S. Army Corps of Engineers
Washington, DC 20314-1000

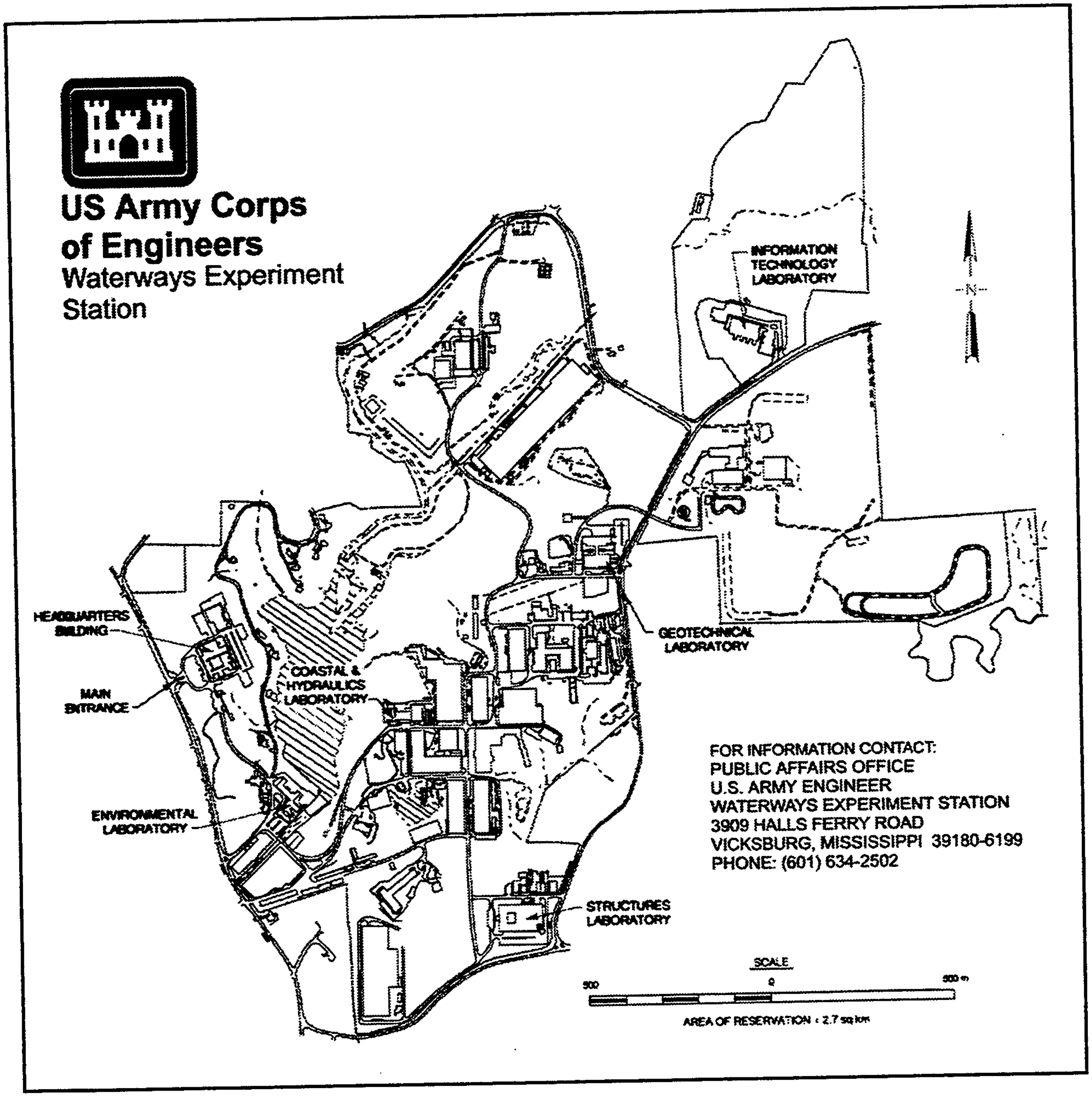

Waterways Experiment Station Cataloging-in-Publication Data

Rhee, Joon P.
Wave refraction at Redondo Beach, California (comparison of field measurements with models) / by Joon P. Rhee, William D. Corson ; prepared for U.S. Army Corps of Engineers.
87 p. : ill. ; 28 cm. — (Technical report ; CHL-98-16)
Includes bibliographic references.
1. Redondo Beach King Harbor (Calif.) 2. Ocean waves — Measurements. 3. RCPWAVE (Computer program) 4. STWAVE (Computer program) I. Corson, William D. II. United States. Army. Corps of Engineers. III. U.S. Army Engineer Waterways Experiment Station. IV. Coastal and Hydraulics Laboratory (U.S. Army Engineer Waterways Experiment Station) V. Title. VI. Series: Technical report (U.S. Army Engineer Waterways Experiment Station) ; CHL-98-16.
TA7 W34 no.CHL-98-16

Contents

Preface

This report was prepared in the Coastal and Hydraulics Laboratory (CHL), U.S. Army Engineer Waterways Experiment Station (WES). The CHL was formed in October 1996 with the merger of the WES Coastal Engineering Research Center and Hydraulics Laboratory. This report is a product of the Redondo Beach, CA, Work Unit of the Monitoring Completed Navigation Projects (MCNP) Program. The MCNP Program Manager during the conduct of the study was Ms. Carolyn M. Holmes, CHL. MCNP Program Manager at the time of publication was Mr. E. Clark McNair, Jr. Technical Monitors of the MCNP at Headquarters, U.S. Army Corps of Engineers, are Messrs. John H. Lockhart, Jr., Charles B. Chesnutt, and Barry W. Holliday.

Dr. J. P. Rhee and Mr. W. D. Corson authored this report under the supervision of Mr. William L. Preslan, Chief of the Prototype Measurement and Analysis Branch (PMAB), CHL, and Mr. Thomas W. Richardson, Chief, Coastal Sediments and Engineering Division (CSED), CHL. Mr. Charles C. Calhoun, Jr., and Dr. James R. Houston are Assistant Director and Director, respectively, of CHL.

The authors wish to thank Dr. T. E. White, Mr. W. E. Grogg, and Mr. W. L. Preslan, PMAB; Mr. G. L. Howell, CSED, Dr. Robert E. Jensen, Navigation and Harbors Division, CHL, and Mr. A. Shak, U.S. Army Engineer District, Los Angeles, for their valuable contributions to this project.

At the time of publication of this report, Director of WES was Dr. Robert W. Whalin, and Commander was COL Robin R. Cababa, EN.

1 Introduction

In January 1988, a powerful storm swept the coast of Southern California, extensively damaging both public and private property. Large storm waves, combined with high tides and winds, struck the man-made Redondo Beach King Harbor breakwaters, severely impairing the function of the harbor, and destroying numerous boats and permanent structures inside the harbor. The U.S. Army Corps of Engineers performed a feasibility study to find various measures for storm damage reduction for the Redondo Beach King Harbor area. The study included numerical model investigations of the effects of local bathymetry on the transformation of deepwater swell. Documents produced by the U.S. Army Engineer District (USAED), Los Angeles (1988, 1990) point out some discrepancies between the model computations and observations during the 1988 storm and a March 1983 storm, and raise questions about the accuracy of theoretical models in general, for areas of complex bathymetry such as Redondo Beach. The studies (USAED, Los Angeles 1988, 1990) also argue that the results from Regional Coastal Processes Wave Transformation Model, RCPWAVE (Ebersole, Cialone, and Prater 1986; Cialone et al. 1994), the wave propagation model employed for the study, "misrepresent actual conditions." Although there are questions about the reliability of the data supporting the conclusion, it undoubtedly deserves attention. The growing consensus since then has been to call for testing the capability of models. This report is a response to that call and, with prototype measurements, gives statistical guides to the evaluation of model computations. Prior to the present effort, no systematic attempt has been made to test RCPWAVE using field measurements.

Despite many successes in practical applications, modeling wave transformation over a variable sea bottom is still a difficult task in most cases. Analytical solutions limit themselves only to simple geometry; numerical treatments, unless in the context of long waves, must base their predictions on the fundamental assumption of 'slowly varying' sea depth; that is, the wavelength under consideration is far smaller than the characteristic horizontal distance of sea-depth variation. The assumption is severe in many cases. In particular, the present study region, though relatively small (11 km by 13 km) and clear of any offshore islands, which are typical in the Southern California Bight, presents a unique challenge to propagation models because of its steep topography. The difficulty of modeling is also heightened by the presence of a deep submarine canyon, which stretches almost linearly to the coastline from offshore and affects waves from the west or southwest, the dominant directions. The description of the flow around the canyon may be beyond the limit of linear theory. Hence, everyone involved in formulating this MCNP investigation expected some amount of discrepancy between model results and field measurements for the Redondo Beach site. The purpose of the project was to investigate the magnitude of the discrepancy and to provide guidance for evaluating model results for sites with steep, complex topography.

The project's data report (Sabol 1996) details the acquisition of the field data, completed in June 1994 after the winters of 1992-1993 and 1993-1994. The present report characterizes the field wave data mainly through the use of a statistical test and lends its findings to ready comparisons with computations from RCPWAVE. In addition, the study includes tests of the simulation results from a spectral refraction model, STWAVE (Resio 1990, Cialone et al. 1994), which treats the propagation of a spectral wave rather than a monochromatic wave as in RCPWAVE.

2 Wave Data Selected

The objective of this report is to determine statistical relationships from wave data of concurrent measurements from deep and shallow waters. Naturally, swell—distinguished from local *sea*—is the project's prime concern for testing a wave propagation model. Therefore, the study pays a great deal of attention to the identification of swell waves, especially those of lower frequency, which undergo more transformation effects in shallow water.

The study bases its evaluation and selection of "well-defined swell waves" on two features of a wave spectrum: the narrowness of the spectral density and the frequency at which a spectrum has its peak. Only 'sufficiently narrow-banded' waves are chosen through visual inspection[1] combined with the use of theoretical parameters defining spectral widths. The higher frequency limit used for truncation of a wave spectrum is 0.15 Hz (~6.7 sec). Also, swell records showing contamination by wave energy of frequencies higher than 0.15 Hz are discarded. This frequency limit is applied to both the deep- and shallow-water wave spectra, assuming that the nonlinear spectral evolution is negligible because of the short propagation distance.

The swell height is defined as four times the standard deviation of the free surface elevation with the cutoff frequency 0.15 Hz. The mean wave direction is calculated by using conventional means (Longuet-Higgins, Cartwright, and Smith 1963) at a spectral peak.

For detailed descriptions of gauge locations and wave data, the reader is referred to Sabol (1996). What follows is a brief complement to Chapter 1 of Sabol (1996), regarding the availability of swell wave data and the background of the shallow-water gauge sites (Figures 1 and 2).

Swell Waves in Deep Water

The study assumes that the water waves outside the bathymetry grid for model computations are homogeneous and can be represented by deep ocean

[1] This practice, with no precise definitions on swell waves, seems somewhat ambiguous. The intuitive view, however, is found to be more reliable than other theoretical restrictions.

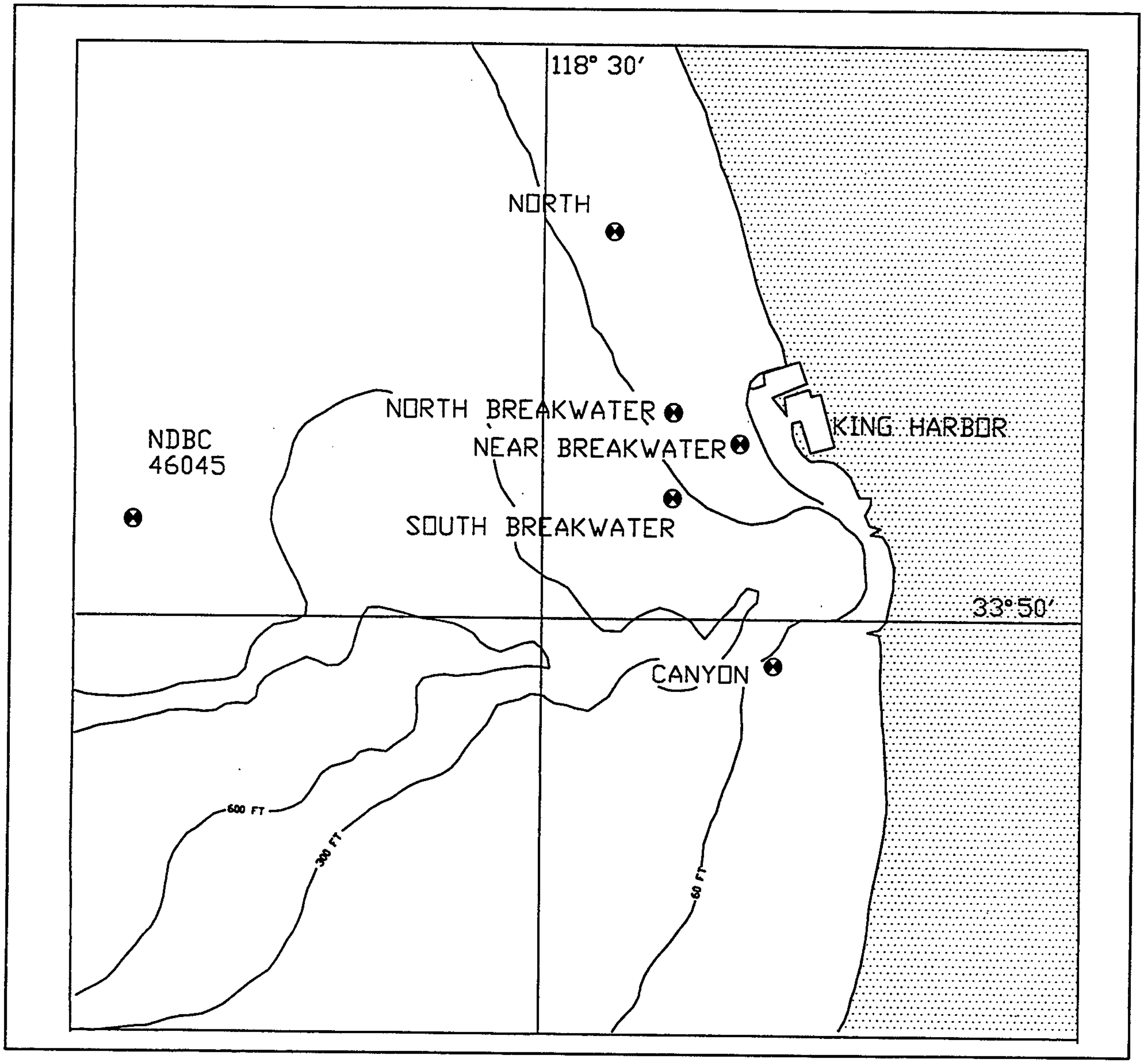

Figure 1. Locations of nearshore wave gauges

measurements at the National Data Buoy Center (NDBC)46025.[1] From late October 1992 to early April 1993, more than 1,200 hourly measurements from NDBC46025, which represent nearly one third of the available wave records, contain well-defined swell waves with the peak frequency ranging from 0.05 to 0.11 Hz and the swell height from ≈0.2 m to ≈3.3 m. Table 1 lists the swell cases which last for more than 5 hr. The swell direction covers from ≈140 deg to ≈320 deg, but mostly concentrates narrowly on a band between ≈250 deg and

[1] Uncertainty forces the study to reject the measurements at NDBC46045, which was initially intended to check the waves in the 80-m depth (approximately 4.5 km from the shallow gauges). A few times during the experiment, the buoy was mounted by many sea lions, which is suspected to result in erroneous data. Future work could involve determining the quality of the data from NDBC46045 for model comparisons. For this report, all offshore data are from NDBC46025.

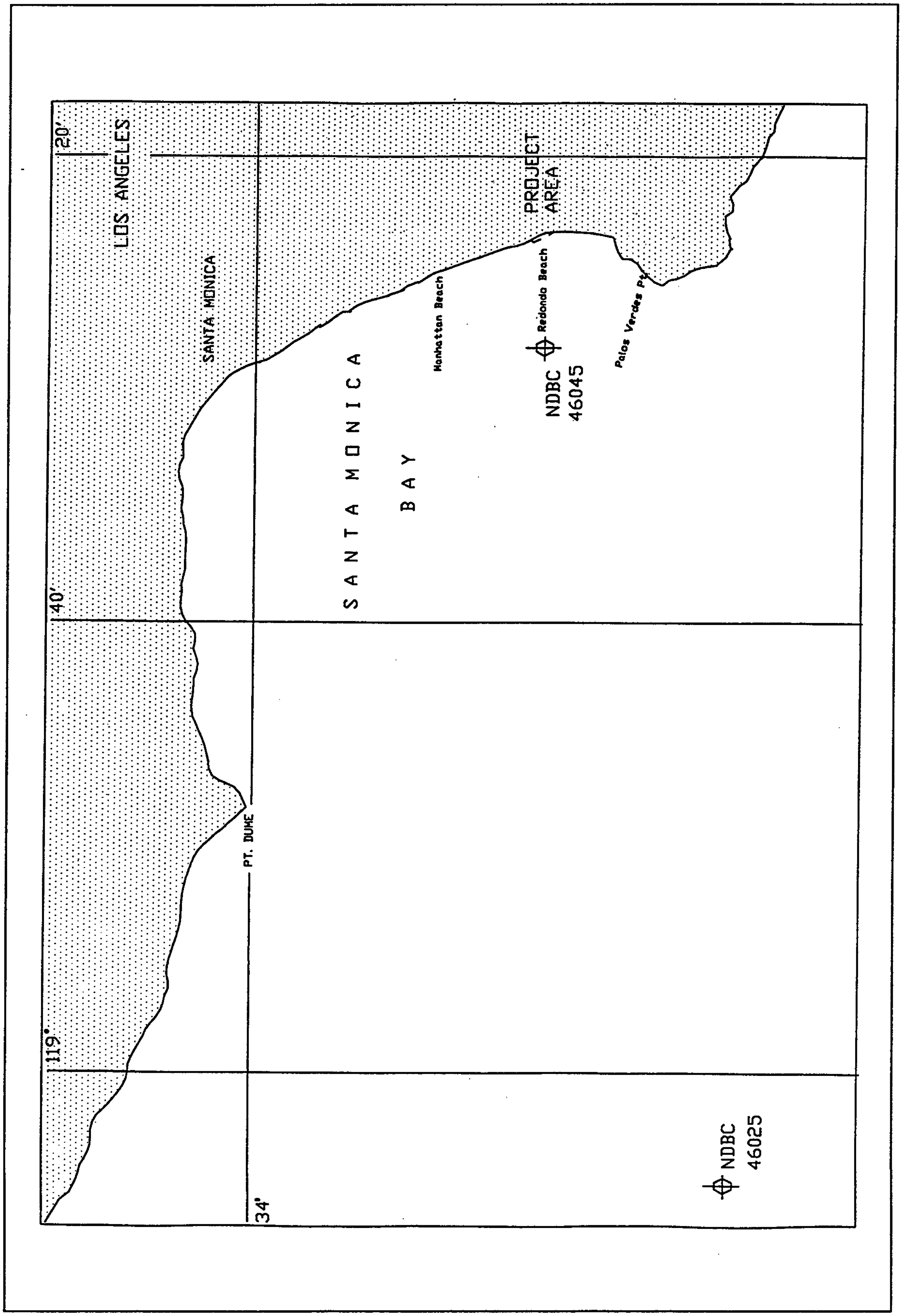

Figure 2. Location of deepwater wave gauge

≈270 deg. For reference, spectral width parameters, ε_p and Q_p, defined in Cartwright and Longuet-Higgins (1956) and Goda (1970), are listed. By definition, as $\varepsilon_p \rightarrow 0$ and $Q_p \rightarrow \infty$, the spectrum becomes narrow-banded.

Shallow-water Wave Gauges

The selection of the four gauge sites (Figure 1) is based on previous numerical computations and observations as presented in Hales (1987) and USAED, Los Angeles (1989).

In a comprehensive study for wave effects, which includes RCPWAVE computations for various cases of incident wave angle, wave period, and tide elevation, Hales (1987) finds that the greatest wave heights due to refraction occur at the north breakwater between the curved portion and the harbor entrance. In addition, Hales' results confirm the observations that the most significant and frequent storm damages occur "at, and slightly south of, the curved portion of the north breakwater" (see also USAED, Los Angeles 1990). Two locations were selected to monitor this highly converging wave energy: the **north breakwater site**, approximately 500 m west of the curved portion of the north breakwater and the **south breakwater site**, approximately 500 m west of the southern portion of the north breakwater.

Hales (1987) reports that, in the region of the tip (head) of the canyon, (**canyon site**), waves are greatly reduced in height due to the divergence of wave rays. The phenomenon is more pronounced for longer-period waves. With the extremely steep topography, waves in this region are the most difficult to accurately simulate.

The shallowest is the **north site**, located farther from the canyon than the three aforementioned sites. Waves may become overly steepened and thus unstable in this area, but, because of the smooth sea bottom, linear theory is expected to have the least difficulty.

Grid for RCPWAVE

A bathymetric grid was prepared from the National Ocean Survey database, for a rectangular region 10.64 km by 12.845 km between latitude 33.7667°N to 33.8818°N and longitude 118.3853°W to 118.5°W. The covered region contains a total of 54 by 65 rectangular grid cells, 200 m by 200 m in size (Figure 3).

Table 1
Swell Waves in Deep Water from NDBC Buoy 46025

Time (GMT)	Number of Records[1]	Frequency[2] (Hz)	Direction (degrees)	Swell Height[3] (m)	Q_p[4]	ε_p[4]
2300 10/25/92 - 1700 10/30/92	112	0.05 - 0.09	231 - 303	0.73 - 1.70	1.7 - 3.3	0.38 - 0.56
1600 10/31/92 - 0200 11/01/92	11	0.07 - 0.08	272- 280	1.22 - 1.72	2.4 - 2.8	0.42 - 0.48
2200 11/06/92 - 1300 11/07/92	13	0.07 - 0.10	213 -257	0.46 - 0.55	2.2 - 2.7	0.42 - 0.50
1200 11/12/92 - 0900 11/17/92	111	0.06 - 0.09	187- 288	0.35 - 0.98	1.9 - 5.0	0.30 - 0.51
0200 11/22/92 - 0800 11/22/92	7	0.07 - 0.08	135 -281	0.54 - 0.63	2.6 - 3.0	0.43 - 0.46
0600 11/24/92 - 0300 11/28/92	93	0.06 - 0.10	232 - 288	0.71 - 1.26	2.0 - 4.2	0.35 - 0.52
1800 11/30/92 - 0300 12/05/92	95	0.06 - 0.10	187 - 284	0.51 - 1.52	2.1 - 3.3	0.40 - 0.53
1700 12/06/92 - 0100 12/07/92	9	0.07 - 0.08	200 - 245	0.62 - 0.84	2.3 - 3.0	0.47 - 0.51
1200 12/14/92 - 0700 12/15/92	20	0.08 - 0.11	263 - 278	0.75 - 1.07	2.4 - 2.9	0.37 - 0.43
0200 12/27/92 - 0800 12/29/92	55	0.06 - 0.08	177 - 258	0.25 - 0.82	2.1 - 12.0	0.00 - 0.55
1400 01/05/93 - 0800 01/06/93	19	0.08 - 0.08	146 - 196	0.36 - 0.44	2.5 - 3.8	0.39 - 0.47
1500 01/15/93 - 2200 01/15/93	13	0.08 - 0.09	236 - 253	0.98 - 1.95	2.5 - 3.2	0.36 - 0.41
1900 01/18/93 - 1200 01/19/93	17	0.08 - 0.09	249 - 265	2.56 - 3.16	2.4 - 3.5	0.36 - 0.43
1100 01/21/93 - 2200 01/22/93	36	0.07 - 0.08	249 - 265	1.26 - 1.91	2.4 - 3.7	0.40 - 0.48
1300 01/23/93 - 1000 01/24/93	21	0.08 - 0.09	251 - 274	0.82 - 1.65	2.6 - 3.1	0.36 - 0.42
1800 01/25/93 - 0800 02/04/93	216	0.06 - 0.10	233 - 288	0.49 - 1.49	2.0 - 4.4	0.30 - 0.56
1400 02/04/93 - 0200 02/08/93	81	0.05 - 0.10	238 - 262	1.01 - 2.86	1.7 - 4.0	0.33 - 0.61
1700 02/09/93 - 1300 02/10/93	20	0.07 - 0.09	250 - 270	1.83 - 3.27	2.3 - 3.2	0.41 - 0.51
2300 02/22/93 - 0800 02/23/93	10	0.06 - 0.07	231 - 259	1.14 - 1.48	2.5 - 3.1	0.53 - 0.58
1300 03/02/93 - 2400 03/03/93	36	0.06 - 0.08	220 - 289	0.91 - 1.40	2.1 - 3.0	0.41 - 0.55
0900 03/04/93 - 2200 03/05/93	38	0.06 - 0.08	251 - 287	1.59 - 2.97	2.1 - 3.3	0.47 - 0.59
0700 03/06/93 - 2200 03/10/93	101	0.06 - 0.09	210 - 320	0.70 - 1.62	2.0 - 3.6	0.36 - 0.56
0100 03/13/93 - 0800 03/14/93	29	0.06 - 0.08	223 - 279	0.50 - 0.79	2.4 - 3.2	0.39 - 0.53
2000 03/15/93 - 0800 03/16/93	13	0.10 - 0.11	245 - 265	0.75 - 1.07	2.5 - 4.8	0.29 - 0.42
2000 03/17/93 - 0800 03/18/93	13	0.07 - 0.08	242 - 271	0.64 - 0.79	2.6 - 4.1	0.49 - 0.55
Total	1189					

[1] Cases where swell lasts for more than 5 hr.
[2] Frequency at which a spectrum has the maximum peak.
[3] Four times the standard deviation of the free surface elevation with the cutoff frequency 0.15 Hz.
[4] $Q_p = (2/m_o^2) \int fS^2 df$ and $\varepsilon_p = \sqrt{1 - m_2^2/m_0 m_4}$ with m_n as the n-th order spectral moment, f the frequency, and S the spectral density.

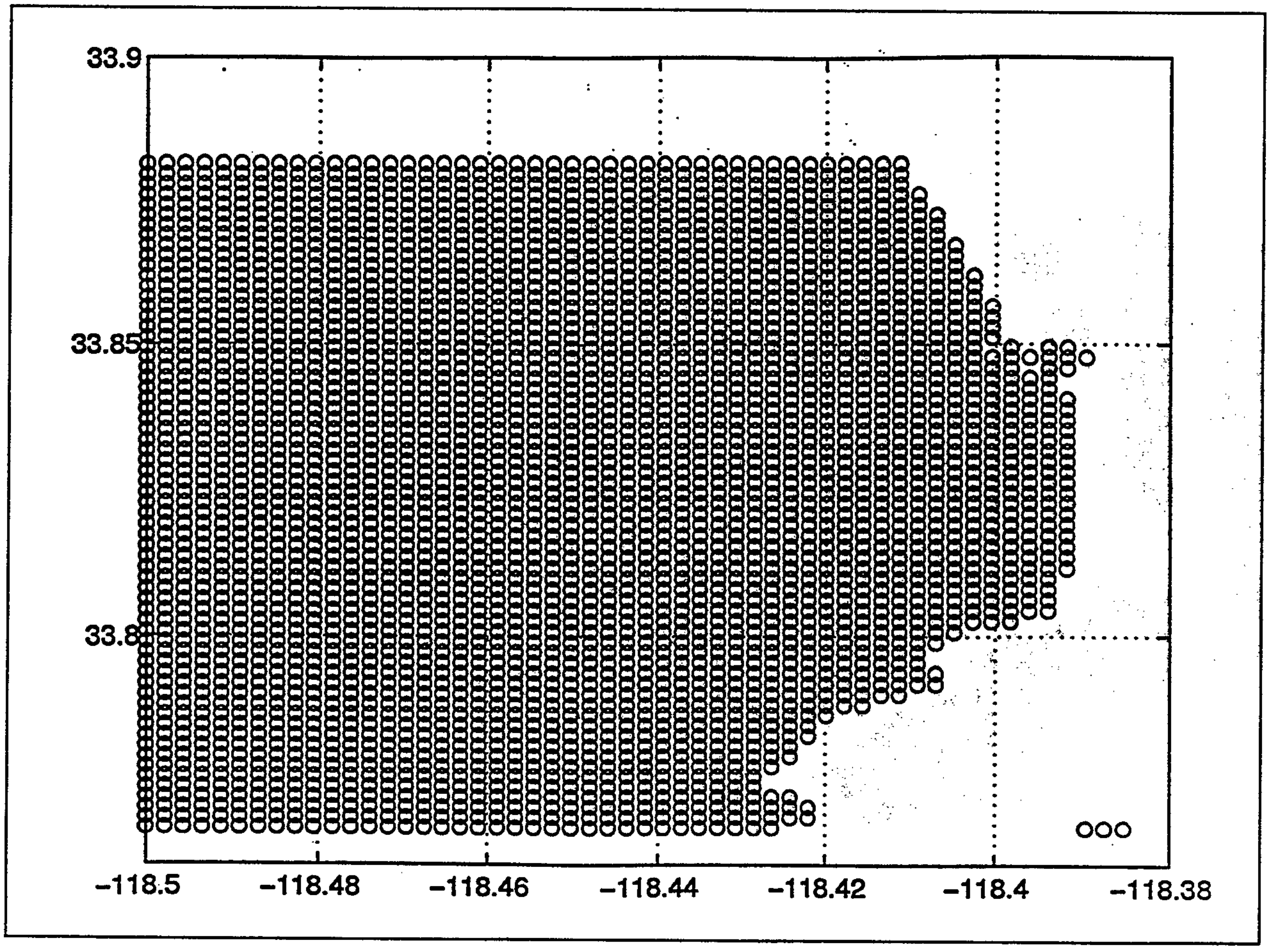

Figure 3. Grid for numerical computations

Data Pairing

Wave height and wave direction[1] are of primary interest, particularly the dependence of the shallow-water height H and direction θ on the deep wave height H_O and direction θ_O.[2] Pairing these deep and shallow quantities such as (H_O, H), however, requires approximation. For example, the travel time[3] for a group of swell waves of frequencies centered on, say, 0.10 Hz is about 130 min according to deepwater theory. This lag is approximated as 2 hr to pair the deep- and shallow-water records, both of which start on the hour. Throughout the study, 1- or 2-hr lag times were used, depending upon the swell frequency.

[1] Wave directions are defined as those from which waves propagate toward the origin at angle measured with respect to the north.

[2] In subsequent discussions, the subscript 0 is appended to the deepwater quantities.

[3] Approximately 62 km between the deepwater gauge NDBC46025 and the shallow-water gauge sites.

3 Comparison

With the range of swell frequencies listed in Table 1 and, in particular, with the relatively large water depths (>15 m) over the study region, changes in wave energy during propagation, such as depth-induced wave breaking and reflection, appear to be minimal. In addition, nonlinear interactions among different frequency components can be safely assumed negligible because of the short propagation distance. This means that, given conditions of an incident wave, i.e., the wave height H_0, the frequency f_0, and the direction θ_0 in deep water, numerical computations find the wave height of interest H in the form $H = \kappa H_0$, where κ is constant.[1] Thus, the study first attempted to find this seemingly intense relationship from the field measurements, seeking a possibility of comparing the observed κ with model computations. Nevertheless, in testing the regression coefficients of a simple linear regression analysis, it has been observed that in many cases the assumption of the regression model $H = \kappa H_0$ may be too strong and a non-zero intercept or higher-order model would be more appropriate. With the limited breadth of the data,[2] efforts here are far from exhaustive and subject to further investigations, but the present observations do not support the assumption that $H = \kappa H_0$.

In the next section of this chapter, results of the aforementioned tests are briefly presented. In the two sections that follow, direct comparisons between model computations and observations are presented for particular time periods during the experiment. In the final section of this chapter, the linear regression is revisited by assuming $H = \kappa H_0$ and comparing κ with model computations. A note about using a refraction formula is also added.

Tests of Linear Regression

The data are grouped primarily by dividing the deepwater directions θ_0 into small groups, with adjustment to give a reasonable sample size to each group for

[1] κ is equivalent to the product of a shoaling coefficient κ_s and a refraction coefficient κ_r in Ebersole et al. (1985).

[2] In all cases analyzed, the deepwater swell height H_0 rarely exceeds 3 m and in most cases is less than 2 m, widening the confidence intervals beyond practical usage for any large storm waves.

a regression analysis. For the most part, 10 deg is found to be reasonable for a group.

Redividing each group into frequency intervals of 0.01 Hz width (which NDBC46025 uses), results in sample sizes that are too small. Thus, the effects of wave frequency are measured by redividing each group using an arbitrary criterion of 0.07 Hz, resulting in two subgroups, one where $f_0 \le 0.07$ Hz and the other where $f_0 > 0.07$ Hz. Although somewhat crude, this method appears adequate, considering the fact that the data are heavily concentrated between 0.06 - 0.09 Hz.

The bulk of the scatter plots are presented in Appendix A. Tables 2 and 3 summarize the regression results along with the test statistics obtained by taking the null hypothesis that the intercept term κ_0 of $H = \kappa_0 + \kappa H_0$ is zero. At a 5-percent significance level, a number of cases are found to reject the hypothesis for both $f_0 \le 0.07$ Hz and $f_0 > 0.07$ Hz.

Comparison During February and March 1993

Because of the uncertainty associated with the assumption that $H = \kappa H_0$, as shown in the observations, the model's performance may be best viewed through direct comparison of its predictions with observations for a certain time period. Using two time segments, 0000 2/2/93 - 0200 2/8/93 and 0900 3/4/93 - 2200 3/10/93, relatively few interruptions are found in the swell data. The predictions are computed with the actual water surface elevations available from the field measurements, though, as will be noted later, the influence of the water surface fluctuations appears to be negligible to the refraction in the Redondo area. For comparison of these computations with the field measurements, a number of statistical parameters may be introduced (cf, for example, Guillaume (1990)), but the following two parameters for the shallow-water wave height H and direction θ are found most useful for the present study:

$$r_H = \frac{|H_{model} - H_{obs}|}{H_{obs}} \quad \text{and} \quad \Delta_\theta = |\theta_{model} - \theta_{obs}| \tag{1}$$

where the subscript *obs* represents the observations. Note that for the wave height, the ratio appears to make more sense than the difference itself because the models' wave height is simply proportional to a deepwater input. Also note the absolute values, which appear to work better for purposes of comparison. Figures 4 through 11 present the time-series of wave height and wave direction for the four shallow-water gauge sites, and Table 4 summarizes the average values and the standard deviations of r_H and Δ_θ for each gauge site. Figure 12 shows the scatter plots for all four sites, for the observed versus predicted swell heights and directions.

Table 2
Results of Regression and Test of $\kappa_0 = 0$ of $H = \kappa_0 + \kappa H_0$ for Cases Where $f_0 \le 0.07$ Hz

$f_0 \le 0.07$ Hz							
θ_o	$\bar{f}_o$	Number of Observations	Corr.	κ_0	κ	t - test	$t_{(0.975)(d.f.)}$
NORTH							
≤200	0.064	16	0.816	0.237	0.417	3.690	2.15
200 - 225	0.068	41	0.891	0.035	0.630	0.750	2.02
225 - 235	0.070	38	0.871	0.041	0.661	0.772	2.03
235 - 245	0.069	60	0.807	0.191	0.549	4.081	2.00
245 - 255	0.068	93	0.841	0.055	0.729	1.186	1.99
255 - 265	0.068	115	0.855	0.127	0.659	3.234	1.98
265 - 275	0.068	87	0.848	0.154	0.583	3.719	1.99
275 - 285	0.067	40	0.773	0.263	0.469	3.237	2.02
> 285	0.067	40	0.865	0.274	0.497	4.716	2.02
NORTH BREAKWATER							
≤ 200	0.063	7	0.938	0.117	0.464	1.749	2.57
200 - 225	0.068	27	0.924	0.021	0.068	0.477	2.06
225 - 235	0.070	20	0.804	-0.089	0.798	-0.732	2.10
235 - 245	0.069	33	0.934	-0.273	1.057	-3.465	2.04
245 - 255	0.069	57	0.947	-0.287	1.066	-4.524	2.00
255 - 265	0.068	66	0.889	-0.061	0.856	-0.939	2.00
265 - 275	0.067	46	0.870	0.125	0.583	1.966	2.01
275 - 285	0.068	22	0.767	-0.247	0.915	-1.074	2.09
> 285	0.067	21	0.881	0.094	0.599	0.948	2.09
SOUTH BREAKWATER							
≤ 200	0.064	5	0.918	0.198	0.423	2.428	3.18
200 - 225	0.068	14	0.916	0.022	0.577	0.325	2.18
225 - 235	0.070	10	0.938	-0.149	0.850	-1.926	2.31
235 - 245	0.070	19	0.958	-0.226	0.953	-2.976	2.11
245 - 255	0.068	41	0.967	-0.120	0.848	-2.421	2.02
255 - 265	0.069	36	0.942	-0.084	0.826	-1.411	2.03
265 - 275	0.068	29	0.911	0.253	0.452	4.707	2.05

(Continued)

Table 2 (Concluded)

θ_o	$\bar{f}_0$	Number of Observations	Corr.	K_0	K	t - test	$t_{(0.975)\,(d.f.)}$
$f_0 \leq 0.07$ Hz							
SOUTH BREAKWATER							
275 - 285	0.068	11	0.843	0.123	0.556	0.718	2.26
> 285	0.068	13	0.802	0.127	0.529	0.856	2.20
CANYON							
≤ 200	0.064	16	0.839	0.000	0.460	0.004	2.15
200 - 225	0.068	40	0.871	-0.026	0.473	-0.674	2.02
225 - 235	0.070	38	0.883	0.009	0.441	0.254	2.03
235 - 245	0.070	65	0.931	0.059	0.385	2.903	2.00
245 - 255	0.069	118	0.955	0.003	0.443	-0.175	1.98
255 - 265	0.068	138	0.921	0.041	0.405	2.356	1.98
265 - 275	0.068	103	0.943	0.082	0.326	5.496	1.98
275 - 285	0.068	48	0.900	0.019	0.387	0.506	2.01
> 285	0.067	45	0.847	0.117	0.291	3.232	2.02

Note: θ_0 = Wave direction in deep water (NDBC46025) in degrees.
$\bar{f}_0$ = Average f_0.
corr. = Correlation coefficient.
d.f. = Degrees of freedom.

Predictions from a spectral wave model STWAVE are also displayed in Figures 4 to 11, 13, and Table 5, and are discussed in a later section of this chapter. A few points concerning the RCPWAVE's performance are as follows:

a. Overall, the model tends to overestimate the wave height (Figure 12) with the largest at the south breakwater site, where an average computed wave height during March 1993 is 62 percent greater than the observed. The model's only underestimation comes from the Canyon site. The reason for these overestimations is not clear, especially because the conditions used for the comparison are not severe to the testing of linear theory.[1] Because of this and the aforementioned mild sea conditions with only 3.2 m for the maximum swell height, it is unlikely that wave breaking is an important factor in the present study. In the study region, waves,

[1] The average swell periods observed are less than 15 sec for the group of $f_0 \leq 0.07$. With gauge depths ranging from 15 - 17 m, the conditions are closer to intermediate depth rather than the shallow water that the project wished to test. Thus, for most of the swell waves tested, the depth-to-wavelength ratio may be too large for them to 'feel' the seabed.

Table 3
Results of Regression and Test of $\kappa_0 = 0$ of $H = \kappa_0 + \kappa H_0$ for Cases Where $f_o > 0.07$ Hz

$f_o > 0.07$ Hz							
θ_o	$\bar{f}_o$	Number of Observations	Corr.	κ_0	κ	t - test	$t_{(0.975)(d.f.)}$
NORTH							
≤200	0.080	19	0.030	0.287	-0.039	2.426	2.11
200 - 225	0.080	11	0.719	0.083	0.562	0.666	2.26
225 - 235	0.081	17	0.780	0.039	0.715	0.328	2.13
235 - 245	0.083	36	0.904	-0.100	0.846	-1.534	2.03
245 - 255	0.084	132	0.916	-0.036	0.838	-1.102	1.98
255 - 265	0.086	185	0.920	0.021	0.749	0.781	1.97
265 - 275	0.085	104	0.936	0.055	0.697	2.042	1.98
275 - 285	0.084	48	0.869	0.126	0.568	2.700	2.01
> 285	0.083	9	0.957	-0.149	1.027	-1.681	2.37
NORTH BREAKWATER							
≤ 200	0.080	9	0.388	0.437	-0.524	2.464	2.37
200 - 225	0.080	6	0.898	0.074	0.475	1.005	2.78
225 - 235	0.081	9	0.851	-0.181	0.903	-1.198	2.37
235 - 245	0.082	14	0.630	-0.030	0.733	-0.123	2.18
245 - 255	0.084	74	0.971	-0.060	0.843	-1.860	1.99
255 - 265	0.085	95	0.960	-0.138	0.845	-4.244	1.99
265 - 275	0.085	59	0.930	0.072	0.609	1.824	2.00
275 - 285	0.083	23	0.875	0.154	0.479	2.659	2.08
> 285	0.083	4	0.895	-0.033	0.822	-0.134	4.30
SOUTH BREAKWATER							
≤ 200	0.080	6	0.131	0.290	-0.109	1.810	2.78
200 - 225	0.080	4	0.933	-0.076	0.720	-0.505	4.30
225 - 235	0.080	6	0.846	-0.034	0.726	-0.167	2.78
235 - 245	0.083	12	0.896	-0.214	0.975	-1.318	2.23
245 - 255	0.083	44	0.922	-0.013	0.730	-0.233	2.02
255 - 265	0.086	62	0.945	-0.095	0.810	-1.909	2.00
265 - 275	0.083	34	0.943	0.061	0.632	1.225	2.04

(Continued)

Table 3 (Concluded)

θ_0	$\bar{f}_0$	Number of Observations	Corr.	κ_0	κ	t - test	$t_{(0.975)(d.f.)}$
			$f_0 > 0.07$ Hz				
			SOUTH BREAKWATER				
275 - 285	0.083	21	0.850	0.081	0.563	1.124	2.09
> 285	0.087	3	0.989	-0.211	1.153	-1.493	12.71
			CANYON				
≤ 200	0.080	19	0.303	0.264	-0.226	4.063	2.11
200 - 225	0.080	11	0.860	-0.028	0.483	-0.424	2.26
225 - 235	0.081	17	0.852	-0.035	0.510	-0.526	2.13
235 - 245	0.083	37	0.892	-0.111	0.620	-2.133	2.03
245 - 255	0.084	154	0.915	0.055	0.475	2.537	1.98
255 - 265	0.086	199	0.923	0.054	0.483	2.814	1.97
265 - 275	0.084	113	0.910	0.051	0.463	2.135	1.98
275 - 285	0.083	52	0.819	0.082	0.391	2.135	2.01
> 285	0.083	10	0.711	0.152	0.338	1.431	2.31

Note: θ_0 = Wave direction in deep water (NDBC46025) in degrees.
$\bar{f}_0$ = Average f_0.
corr. = Correlation coefficient.
d.f. = Degrees of freedom.

though narrow-banded, may be difficult to accurately model through an approximation using a monochromatic wave.

b. Relatively good agreement is shown at the north breakwater site, with 19 percent and 26 percent overestimations during February 1993 and March 1993, respectively.

c. The model's accuracy appears to be sensitive to the input wave direction. Note that the deviations from observations in both wave height and wave direction are larger during March 1993 than February 1993, and that the deepwater wave directions show $\theta_0 > 270$ deg during 3/4/93 - 3/10/93 and $\theta_0 < 270$ deg during 2/2/93 - 2/8/93. Thus, it appears that accuracy improves when deepwater waves are directed more perpendicular to the shore.

d. The fluctuations shown by the model's wave directions have little correlation to observations (Figure 12), though in wave direction the deviations are considered small (the maximum value of the average

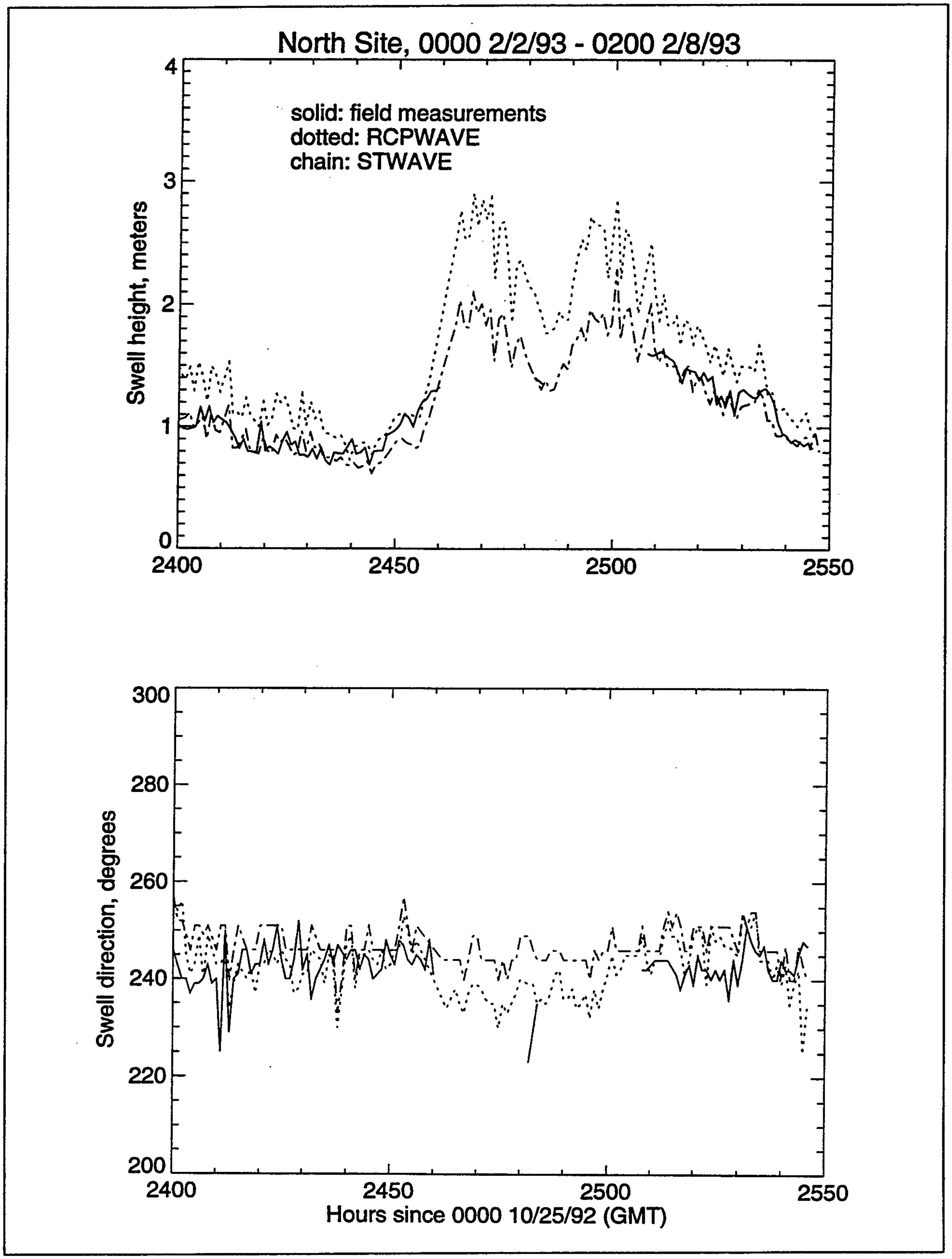

Figure 4. Wave height and wave direction, north site, February 1993

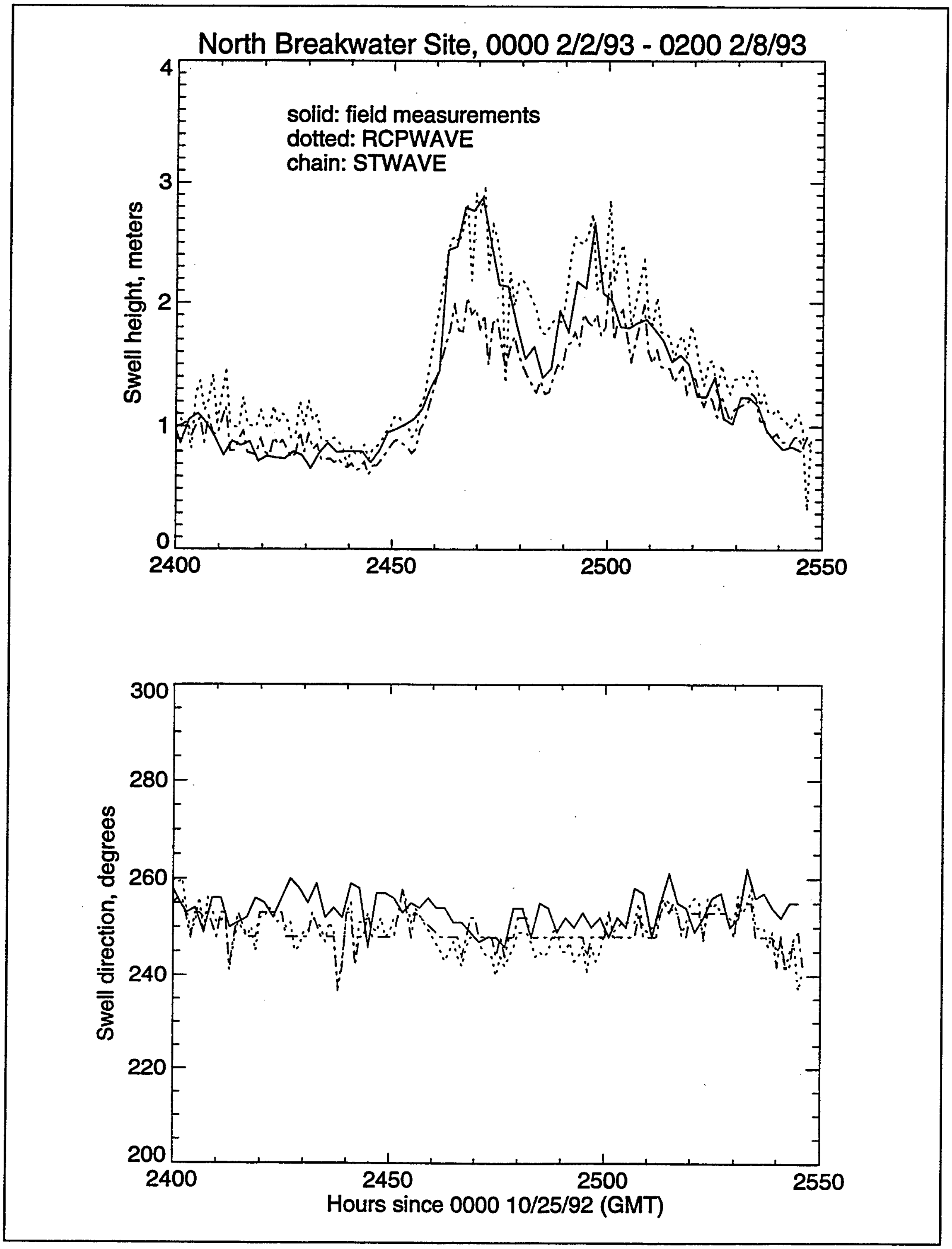

Figure 5. Wave height and wave direction, north breakwater site, February 1993

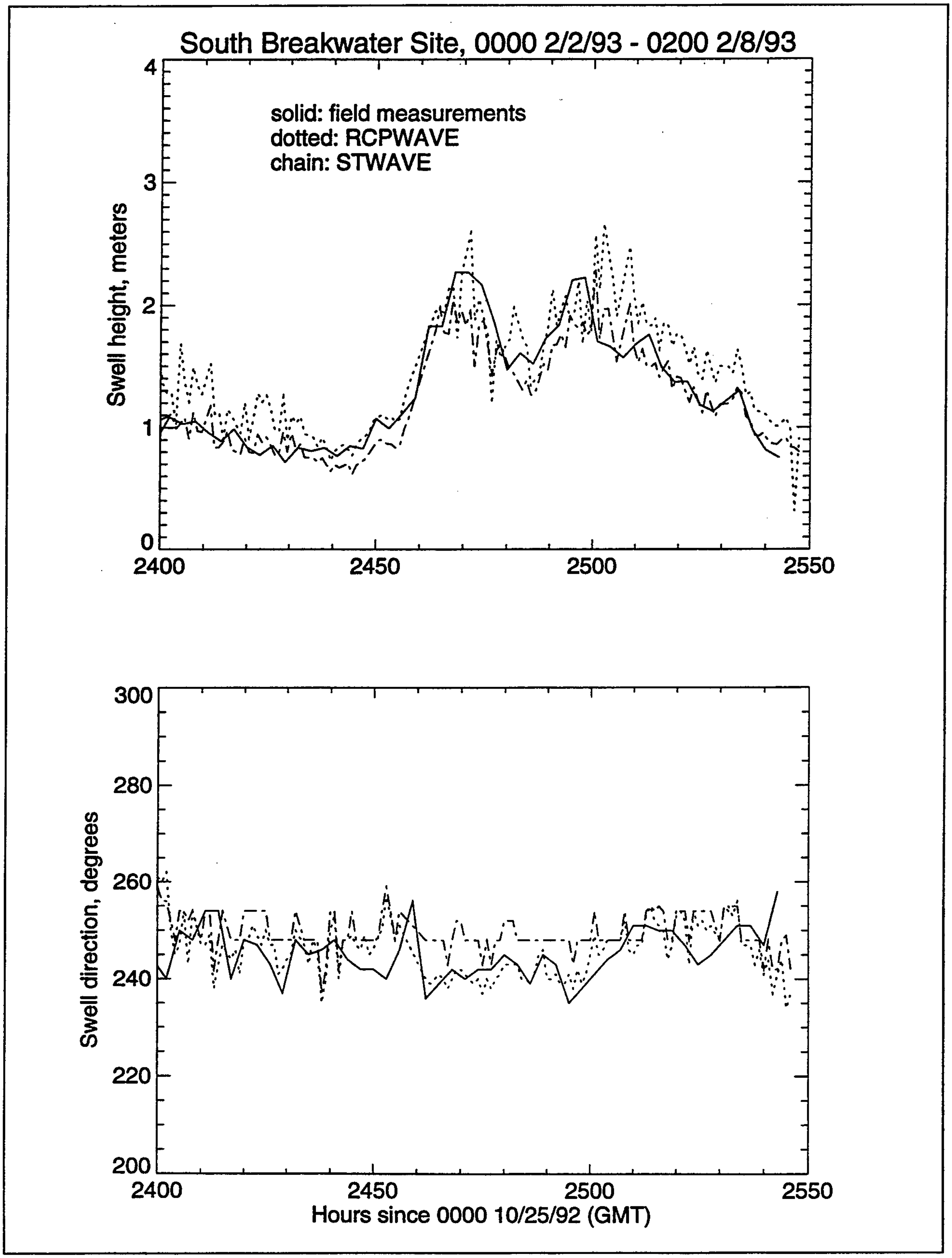

Figure 6. Wave height and wave direction, south breakwater site, February 1993

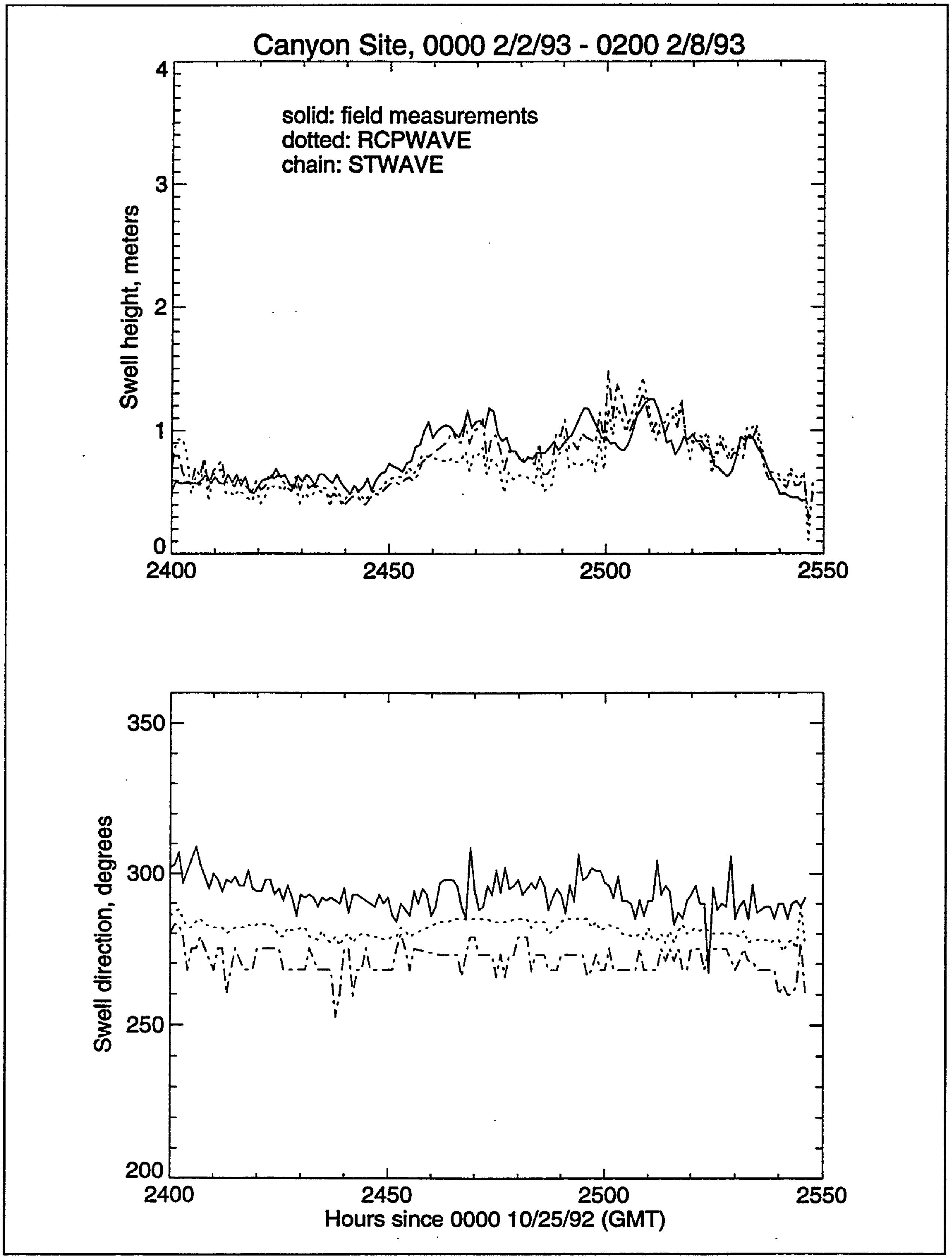

Figure 7. Wave height and wave direction, canyon site, February 1993

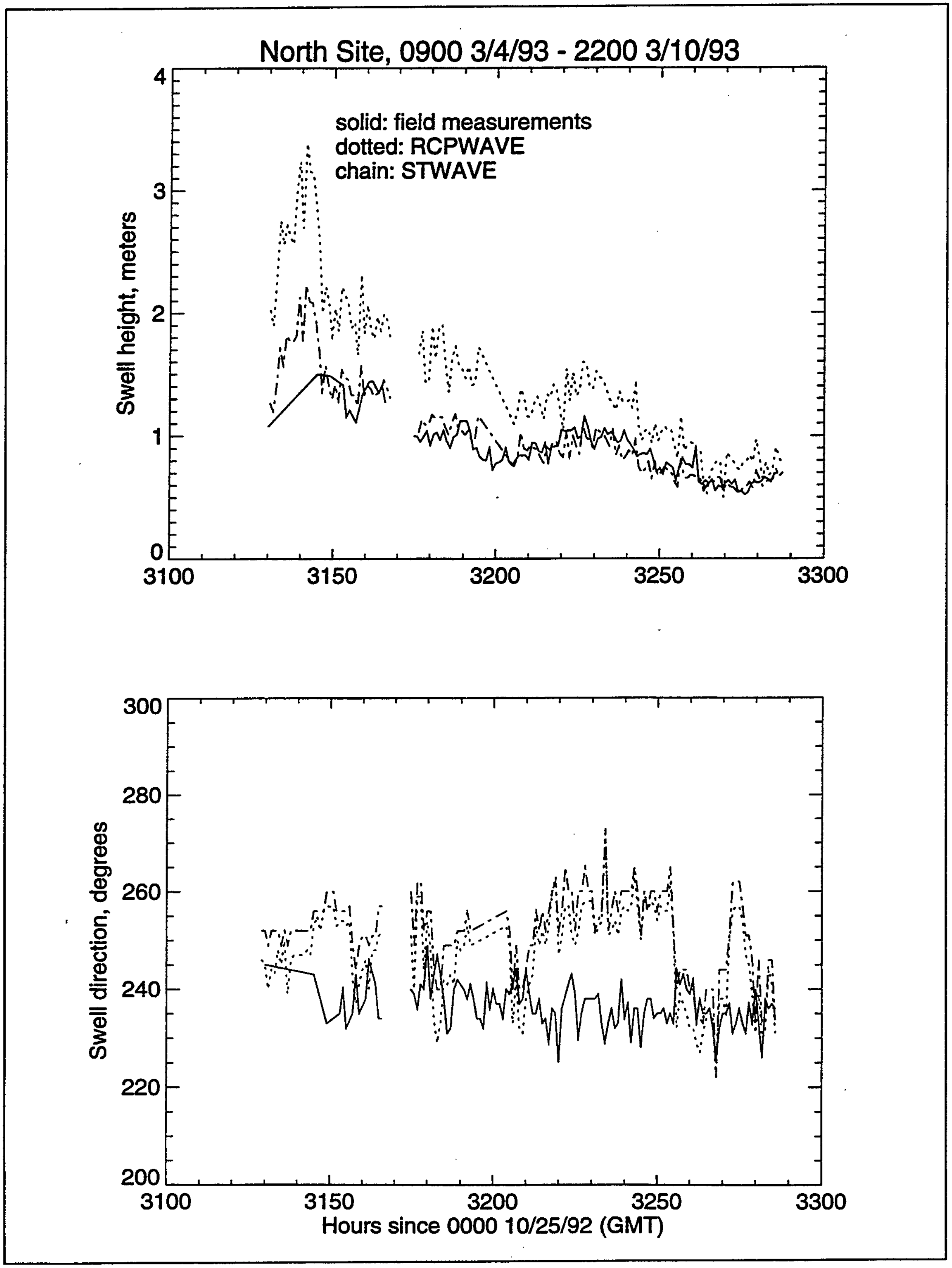

Figure 8. Wave height and wave direction, north site, March 1993

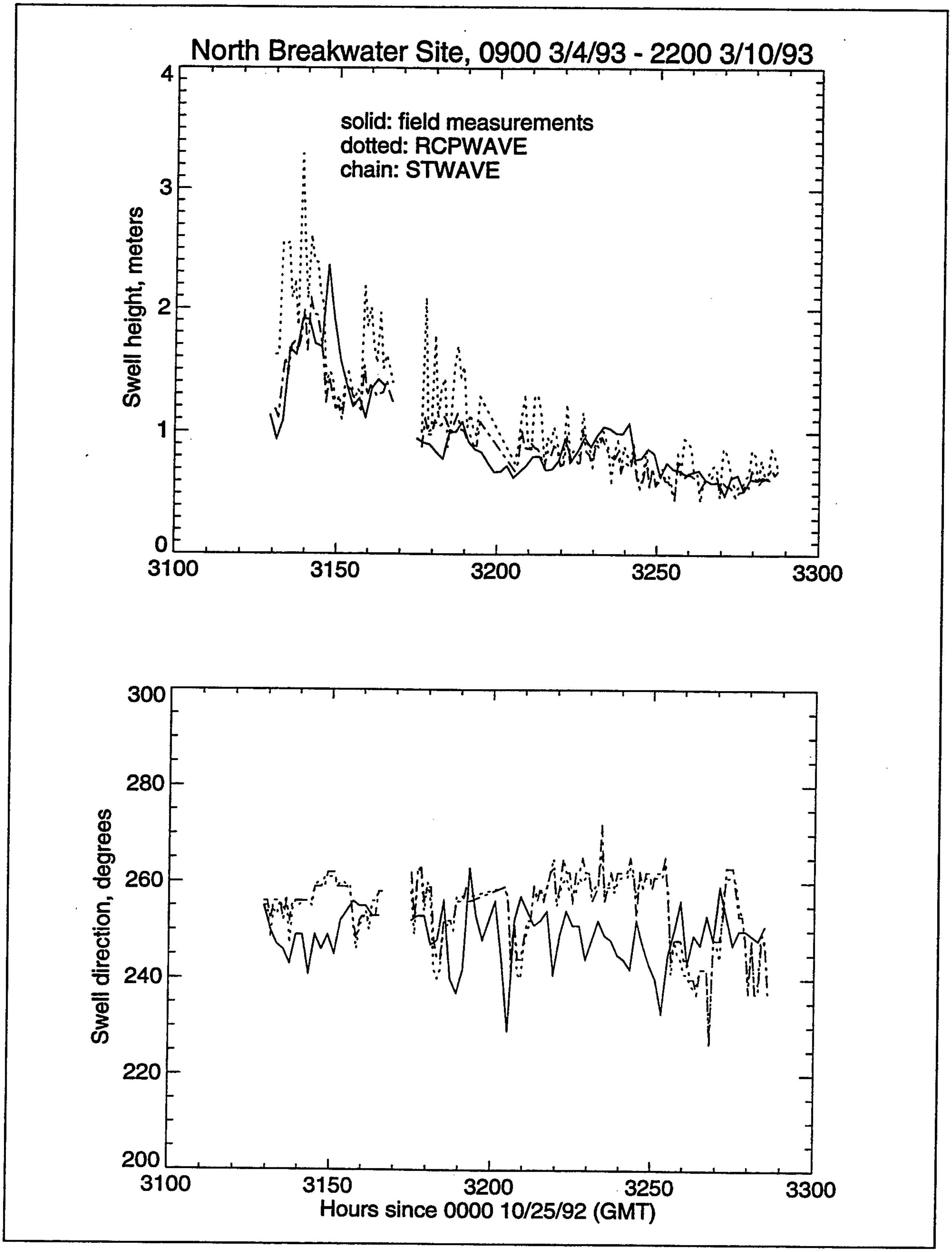

Figure 9. Wave height and wave direction, north breakwater site, March 1993

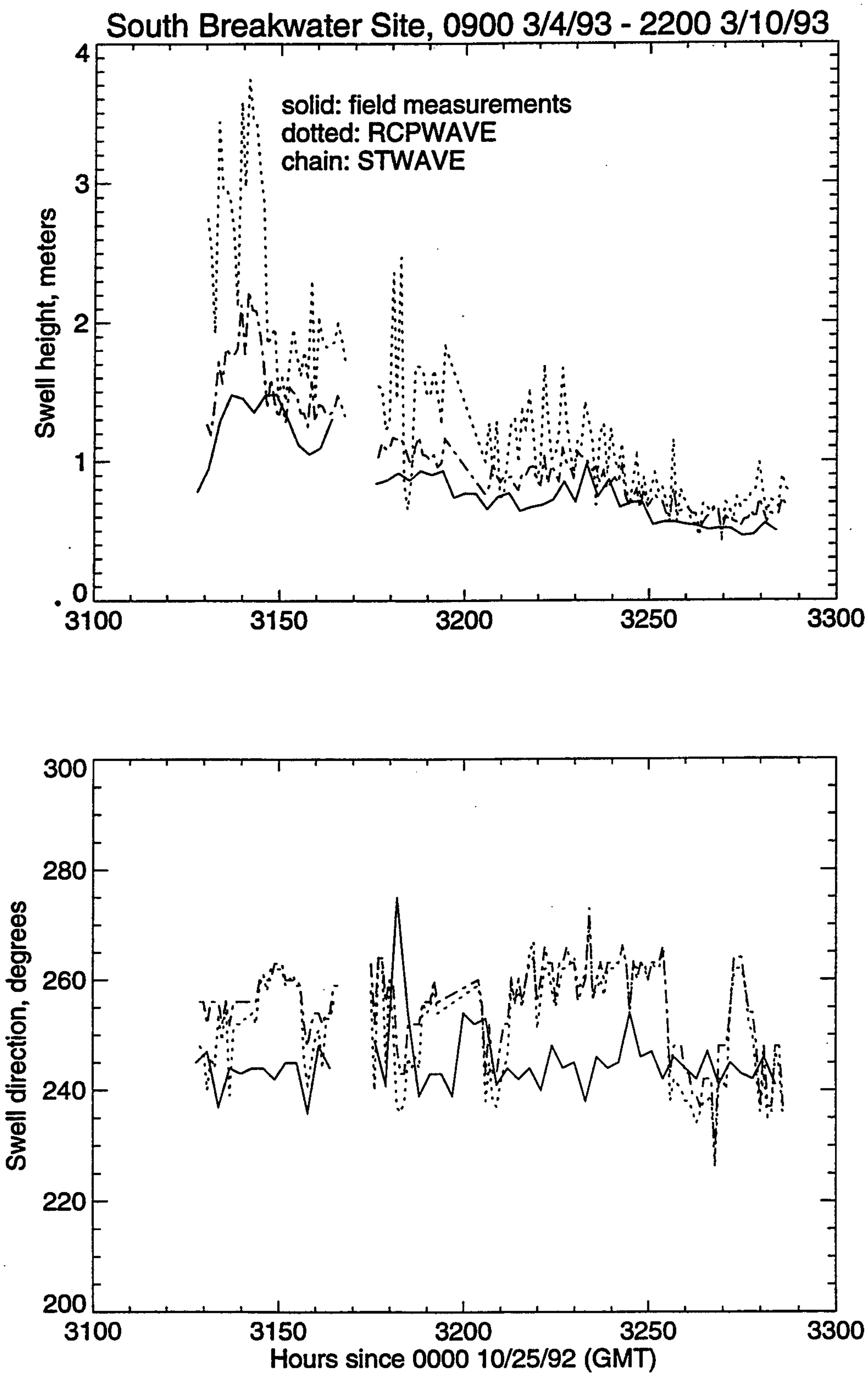

Figure 10. Wave height and wave direction, south breakwater site, March 1993

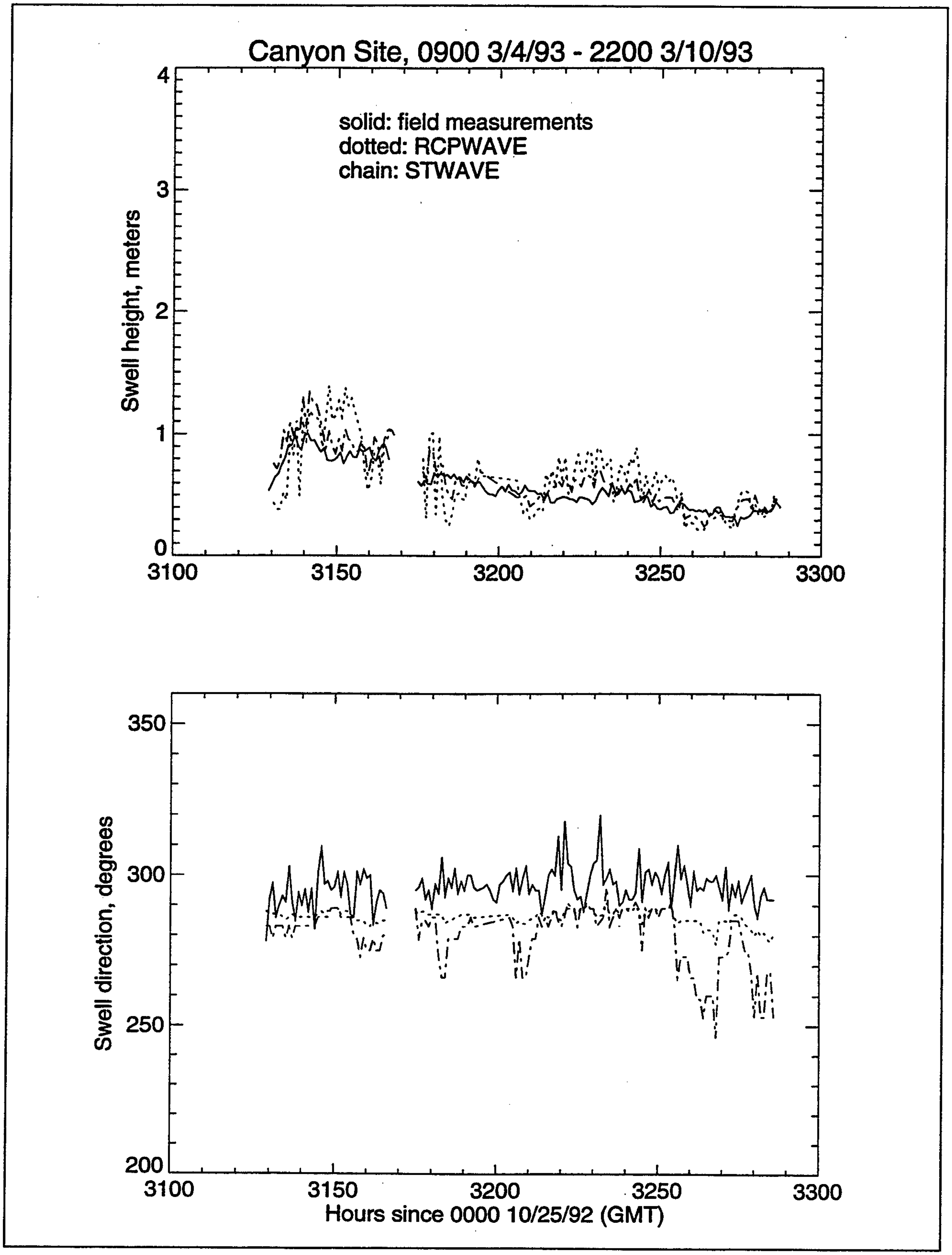

Figure 11. Wave height and wave direction, canyon site, March 1993

Table 4
Average Values of r_H and Δ_θ and Standard Deviations from RCPWAVE and Swell Observations

Gauge Site	Number of Occurrences	Average r_H	Standard Deviation r_H	Average Δ_θ	Standard Deviation Δ_θ
0000 2/2/93 - 0200 2/8/93					
North	112	0.25	0.16	7	5.6
North breakwater	75	0.19	0.17	5	3.3
South breakwater	50	0.26	0.21	6	5.2
Canyon	156	0.22	0.14	13	6.9
0900 3/4/93 - 2200 3/10/93					
North	114	0.41	0.22	13	8.2
North breakwater	68	0.26	0.28	9	5.6
South breakwater	46	0.62	0.42	11	7.3
Canyon	139	0.34	0.22	11	8.0

model deviation from the observation is 13 deg at the canyon site from the February 1993 data and the north site from the March 1993 data).

e. Model directions for the canyon site compare poorly to the observations, perhaps because of the computational difficulty contributed by the deep submarine canyon.

f. Coefficients of correlation with the observations are 0.805 and 0.902 for wave height and wave direction, respectively, for the data during this time period (see Figure 12). For data whose deepwater swell heights are greater than 1.5 m, however, the correlation becomes 0.350 for wave height and 0.462 for wave direction, obviously suggesting a poor agreement for larger (though less than 3 m) waves. Therefore, extrapolation of the regression analysis (presented in Tables 2 and 3 and in the next part of this chapter) beyond the present observation range must be exercised with care.

g. In summary, for the present study region, RCPWAVE appears to overestimate wave heights. The underestimation at the canyon site is not of primary significance for practical purposes because there is little wave energy left once the rays reach the site (the submarine canyon works as a natural breakwater for the canyon site). Note that these present findings contradict the criticism in the *General Design Memorandum*, which implicitly suggests that RCPWAVE underestimates wave heights (see Chapter 1, "Introduction").

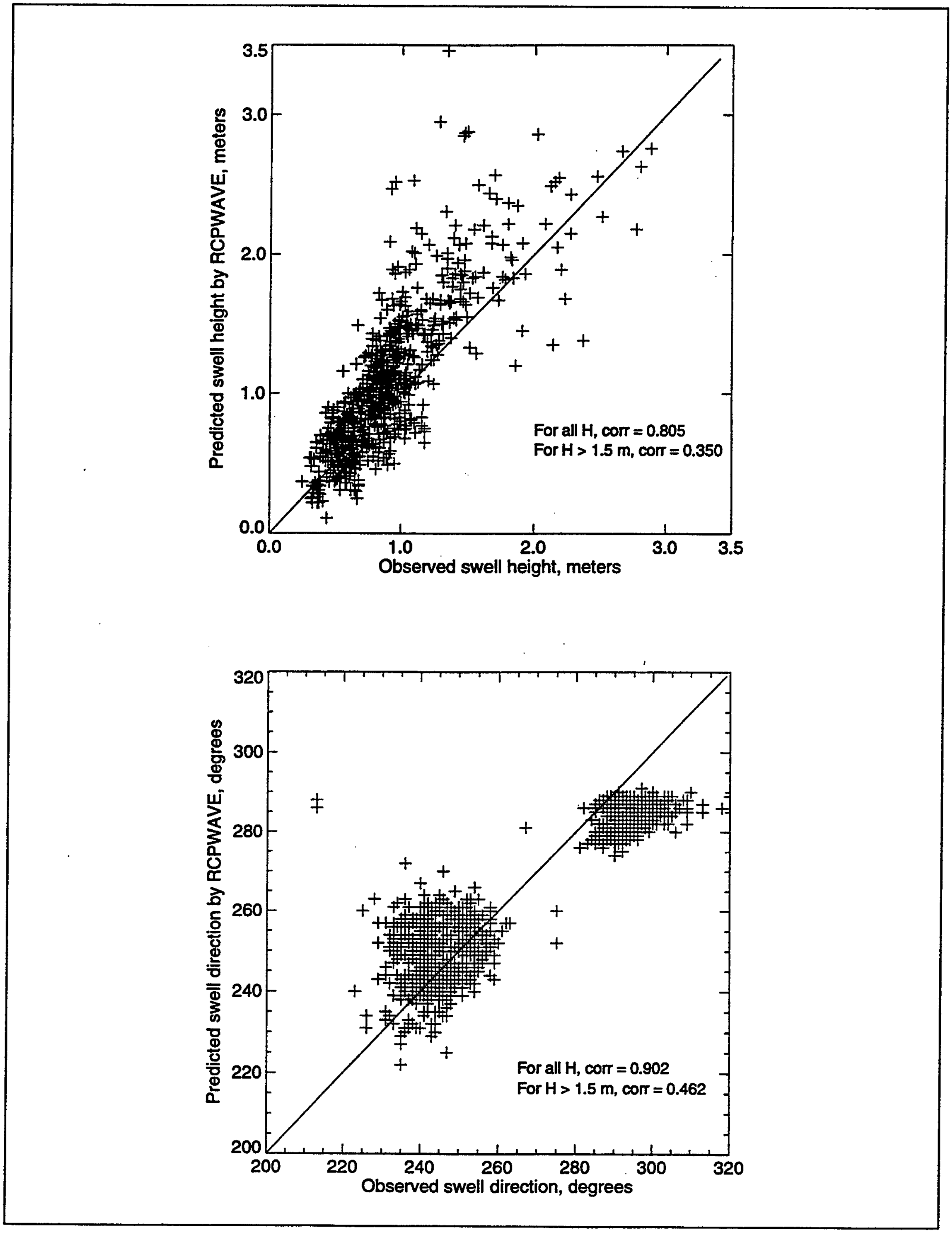

Figure 12. Observation vs RCPWAVE, during 000 2/2/93 - 0200 2/8/93 and 0900 3/4/93 - 2200 3/10/93 (corr = correlation coefficient)

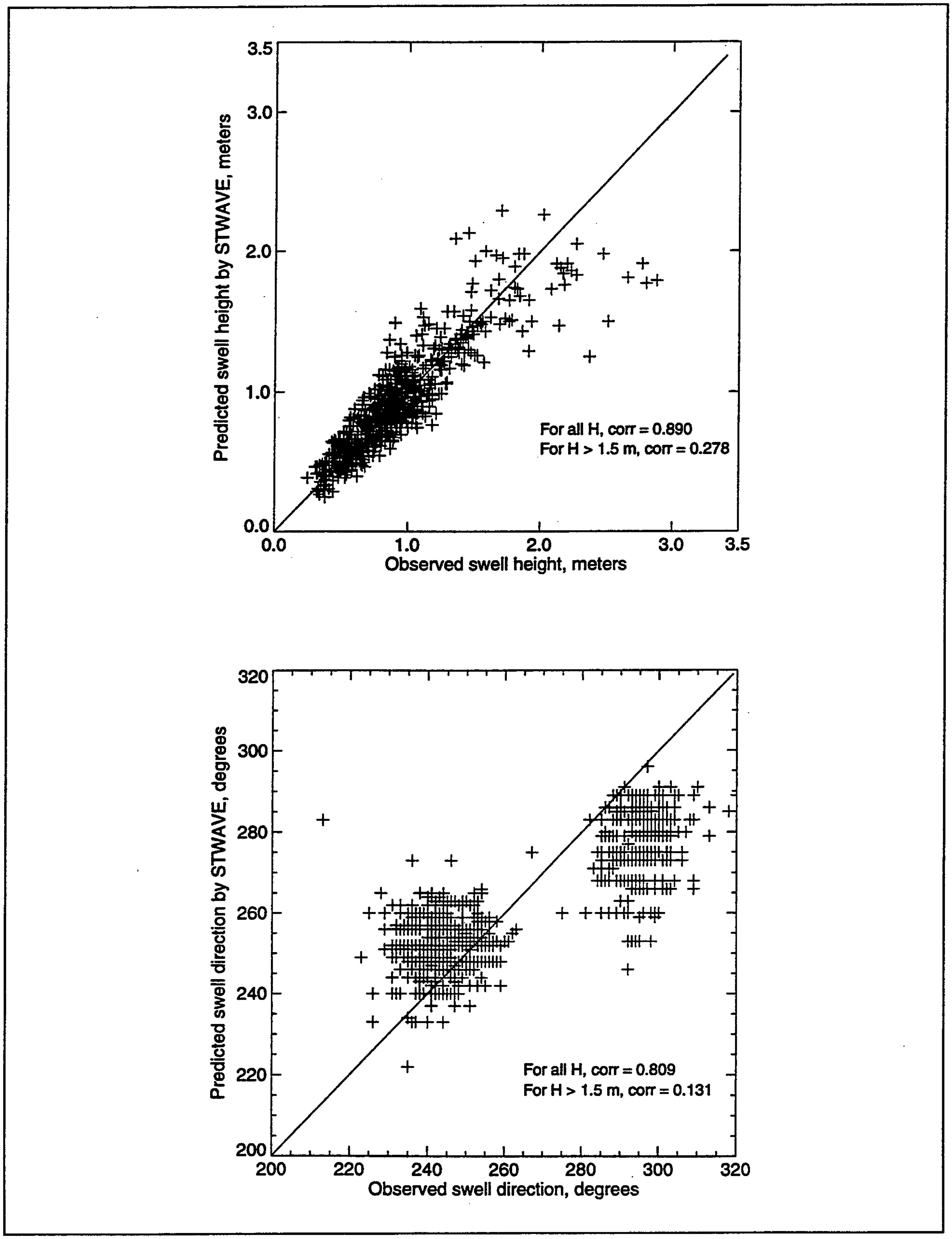

Figure 13. Observation vs STWAVE, during 000 2/2/93 - 0200 2/2/93 0900 3/4/93 - 2200 3/10/93 (corr = correlation coefficient)

Table 5
Average Values of r_H and Δ_θ and Standard Deviations from STWAVE and Swell Observations

Gauge Site	Number of Occurrences	Average r_H	Standard Deviation r_H	Average Δ_θ	Standard Deviation Δ_θ
0000 2/2/93 - 0200 2/8/93					
North	112	0.10	0.07	8	5.8
North breakwater	75	0.13	0.10	4	3.4
South breakwater	50	0.12	0.09	7	4.7
Canyon	156	0.15	0.12	22	7.5
0900 3/4/93 - 2200 3/10/93					
North	114	0.10	0.07	16	8.7
North breakwater	68	0.13	0.11	9	6.2
South breakwater	46	0.22	0.12	13	6.6
Canyon	139	0.18	0.13	17	11.7

Comparison with STWAVE

Although examining models other than RCPWAVE is not included as one of the project's primary purposes, it is of great interest to explore the differences between linear propagation models and to compare their results with the observations. In the text that follows, observations are statistically compared to predictions from STWAVE, a spectral refraction model that uses computational schemes based on a more realistic approach to describe a refraction wave field (i.e., a continuous wave spectrum rather than a monochromatic wave) (Resio 1990, Cialone et al. 1994, Longuet-Higgins 1957). Following is the summary of the comparisons displayed in Figures 4-13, and the statistics shown in Table 5.

a. For both February and March 1993 data, most of the STWAVE's average values of r_H are within 10 - 20 percent of the observations, which is a significant improvement compared to those of RCPWAVE. The reduced standard deviations also explain how the predictions become less scattered than RCPWAVE. The average values of Δ_θ for the two models appear to be about the same.

b. Overall, STWAVE tends to underestimate the wave height. This is more obvious in Figures 5 and 6, where the 13-percent and and 12-percent differences shown by the north breakwater and the south breakwater sites, respectively, are largely due to underestimations.

c. The coefficients of correlation with the observations are 0.805 and 0.902 for wave height and wave direction, respectively (see Figure 13), and appear to be close to those for RCPWAVE. For data whose swell heights are greater than 1.5 m, the correlation coefficients are 0.278 for wave height and 0.131 for wave direction.

d. In summary, STWAVE generally fits the observations better than RCPWAVE, but some underestimations are apparent.

Comparison Using $H = \kappa H_0$

Regression coefficients are estimated with the assumption that $H = \kappa H_0$ regardless of the test results presented in Tables 2 and 3. Table 6 summarizes the results, giving the slope κ (wave height ratio H/H_0) and the confidence intervals on κ for each group of the data grouped by the incident wave direction θ_0 and frequency f_0. Figures 14 through 17 reproduce the regression results presented in Table 6 to compare with the model predictions. Note that inputs to the model computations are the average values of the field data in each group; for example, at the north site, the average values of the group for θ_0 = 275 deg - 285 deg and $f_0 \leq 0.07$ Hz, we find $\theta_0 \approx 279$ deg and $f_0 \approx 0.068$ Hz.

For reasons addressed earlier, these regression results are somewhat questionable. Nevertheless, they are presented here because $\kappa_0 = 0$ is inherent in the model results. Findings are summarized as follows:

a. For the most part, the RCPWAVE's shallow-water wave heights exceed the observations, except for the cases of $\theta_0 < 270$ deg with $f \leq 0.07$ Hz at the canyon site. This confirms the previous results.

b. The model's wave heights are more sensitive to the incident wave direction (θ_0) than the observations. (For all gauge sites, the observed wave-height ratios remain nearly constant for all θ_0.)

c. The model's wave heights have a relatively good agreement with the observations when $\theta_0 < 250$ deg, except for the **canyon** site, when $f_0 < 0.07$ Hz.

d. No noticeable difference is seen between the model performances for $f_0 > 0.07$ Hz and for $f_0 \leq 0.07$ Hz.

e. The largest difference is shown by the **south breakwater** site, where the computed H becomes approximately twice that measured for an incident wave of $f_0 \leq 0.07$ Hz approaching at an angle of 270 deg.

Comparison of θ

In most swell cases analyzed, the directional beam is narrow so that mean direction estimated at the frequency of the peak of a spectrum is sufficient to represent the directional distribution. Here we compare the computed

Table 6
Results of Regression for Wave Height Under the Assumption $H = \kappa H_0$

θ_0	$f_0 \leq 0.07$ Hz		$f_0 > 0.07$ Hz	
	Number of Observations	κ[1]	Number of Observations	κ[1]
NORTH				
≤ 200	16	0.69±0.070	19	0.72±0.045
200 - 225	41	0.67±0.034	11	0.68±0.087
225 - 235	38	0.71±0.039	17	0.76±0.071
235 - 245	60	0.76±0.034	36	0.75±0.039
245 - 255	93	0.79±0.024	132	0.81±0.021
255 - 265	115	0.78±0.022	185	0.77±0.017
265 - 275	87	0.72±0.026	104	0.75±0.021
275 - 285	40	0.66±0.035	48	0.69±0.040
> 285	40	0.71±0.025	9	0.84±0.095
NORTH BREAKWATER				
≤ 200	7	0.59±0.064	9	0.63±0.059
200 - 225	27	0.63±0.033	6	0.59±0.055
225 - 235	20	0.70±0.083	9	0.66±0.100
235 - 245	33	0.83±0.074	14	0.70±0.087
245 - 255	57	0.87±0.049	74	0.80±0.023
255 - 265	66	0.81±0.041	95	0.75±0.025
265 - 275	46	0.67±0.042	59	0.66±0.030
275 - 285	22	0.74±0.097	23	0.62±0.055
> 285	21	0.67±0.041	4	0.79±0.219
SOUTH BREAKWATER				
≤ 200	5	0.66±0.161	6	0.64±0.046
200 - 225	14	0.60±0.051	4	0.62±0.129
225 - 235	10	0.65±0.089	6	0.69±0.114
235 - 245	19	0.77±0.078	12	0.78±0.103
245 - 255	41	0.77±0.033	44	0.72±0.040
255 - 265	36	0.76±0.045	62	0.75±0.033
265 - 275	29	0.62±0.045	34	0.67±0.040
275 - 285	11	0.64±0.062	21	0.65±0.067
> 285	13	0.63±0.057	3	0.90±0.152

(Continued)

[1] κ is given with 95-percent confidence intervals

Table 6 (Concluded)				
	$f_0 \le 0.07$ Hz		$f_0 > 0.07$ Hz	
θ_0	Number of Observations	κ	Number of Observations	κ
CANYON				
≤ 200	16	0.46±0.051	19	0.47±0.030
200 - 225	40	0.45±0.028	11	0.44±0.045
225 - 235	38	0.45±0.024	17	0.47±0.039
235 - 245	65	0.44±0.017	37	0.51±0.035
245 - 255	118	0.44±0.011	154	0.51±0.016
255 - 265	138	0.44±0.011	199	0.52±0.013
265 - 275	103	0.38±0.011	113	0.50±0.019
275 - 285	48	0.40±0.014	52	0.47±0.030
> 285	45	0.38±0.015	10	0.49±0.118

shallow-water wave directions with the observed ones. Tables 7 and 8 list these directions for $f_0 \le 0.07$ Hz and $f_0 > 0.07$ Hz, respectively, along with the standard t-test (columns 6 and 7) statistics testing the null hypothesis that a computed wave direction (θ_{model}) equals an average value of the observations (θ_{obs}). The critical regions ($t_{(0.975)\,(d.f.)}$) found by using a 5-percent significance level are also listed for reference. In the tables, a number of cases reject the hypothesis. Considering the uncertainty on the accurate measurements of θ itself, however, it is difficult to construe these rejections as indicating strong differences.

Green's Law

A final note to the assumption $H = \kappa H_0$ is constructed as follows. For a simple geometry with little lateral variation and a smooth sea bottom, a formula, called Green's law (see Dean and Dalrymple 1984, Mei 1989), is well-known for the approximation of the wave height ratio, i.e.,

$$\frac{H}{H_0} \approx (C_{go} \sin \theta_0)^{1/2} (gh)^{-1/4} \qquad (2)$$

where C_{g0} is the group velocity for deep water, g the gravitational acceleration, and h the water depth. It is of interest to see how this simple formula fits the present complicated bathymetry. Figures 14-17 indicate that for each gauge site, the measured wave-height ratio κ remains nearly constant as the deepwater

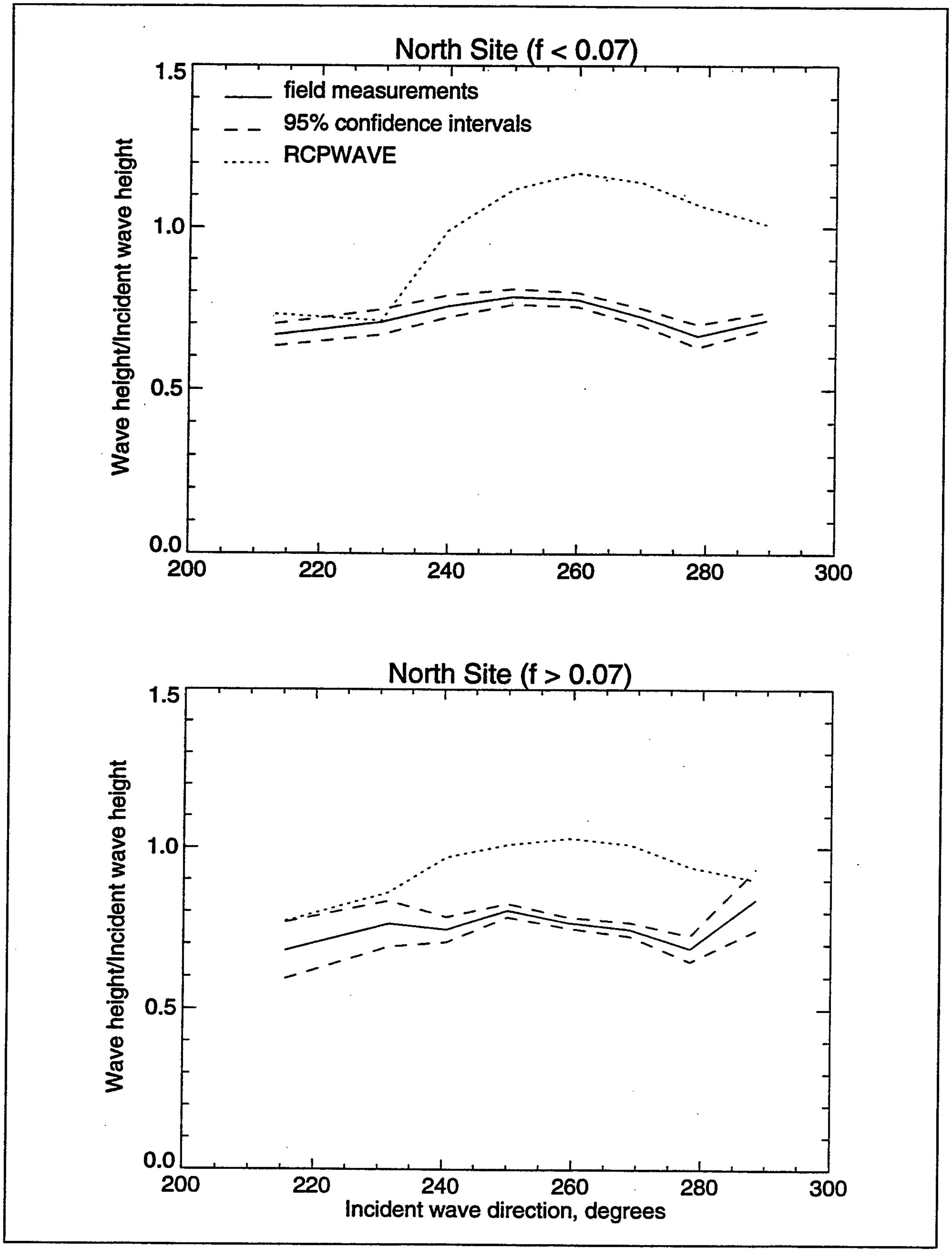

Figure 14. Regression results, north site

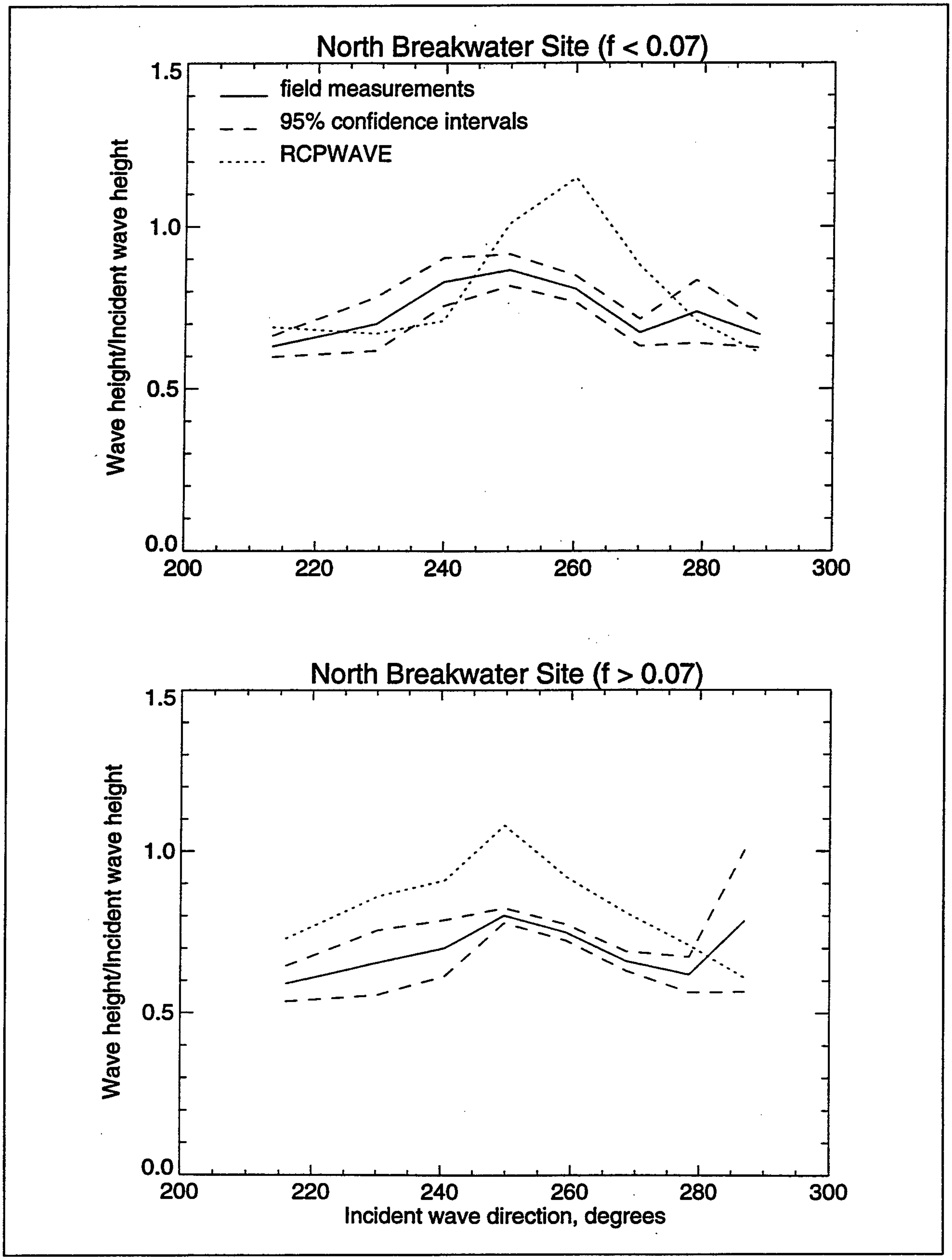

Figure 15. Regression results, north breakwater site

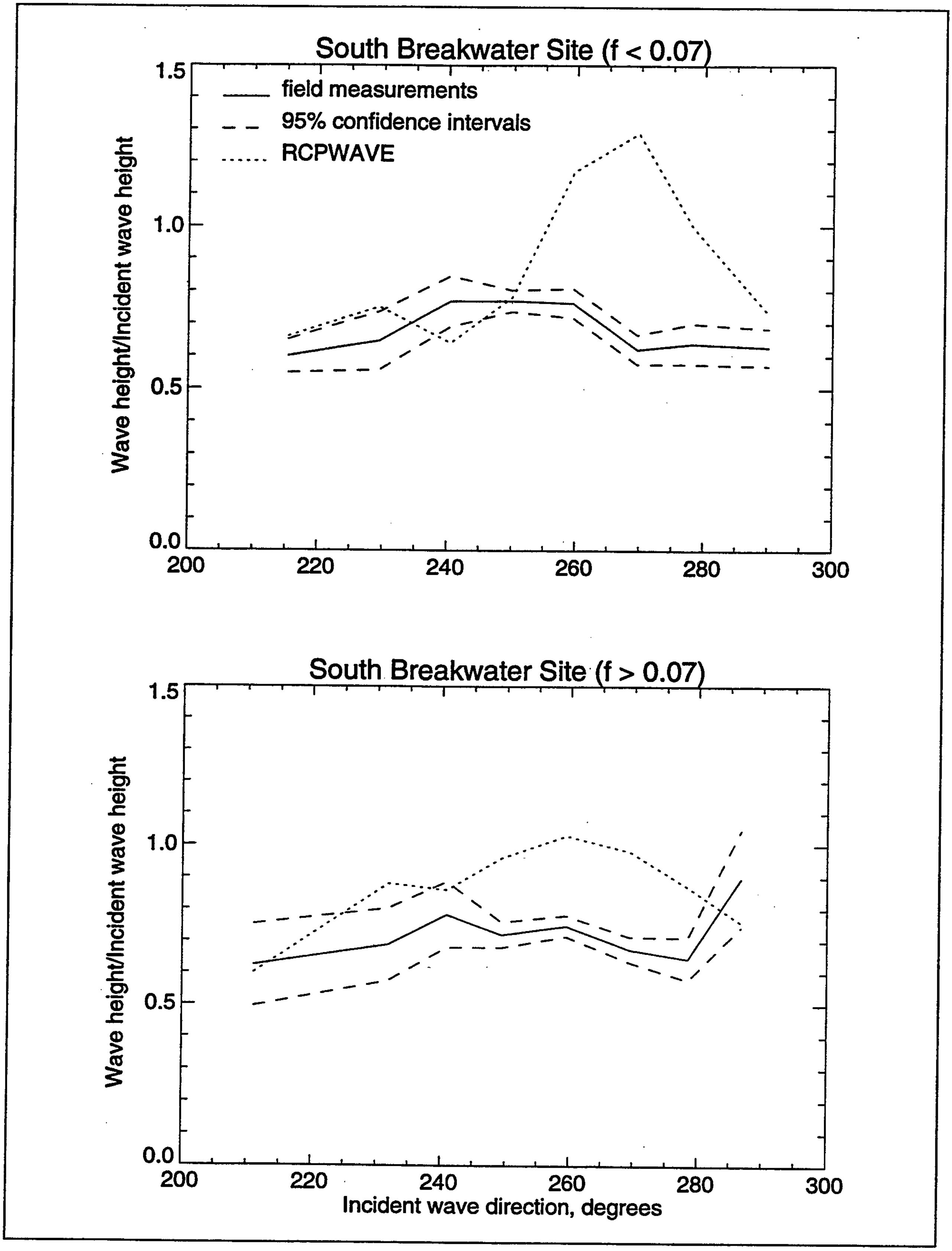

Figure 16. Regression results, south breakwater site

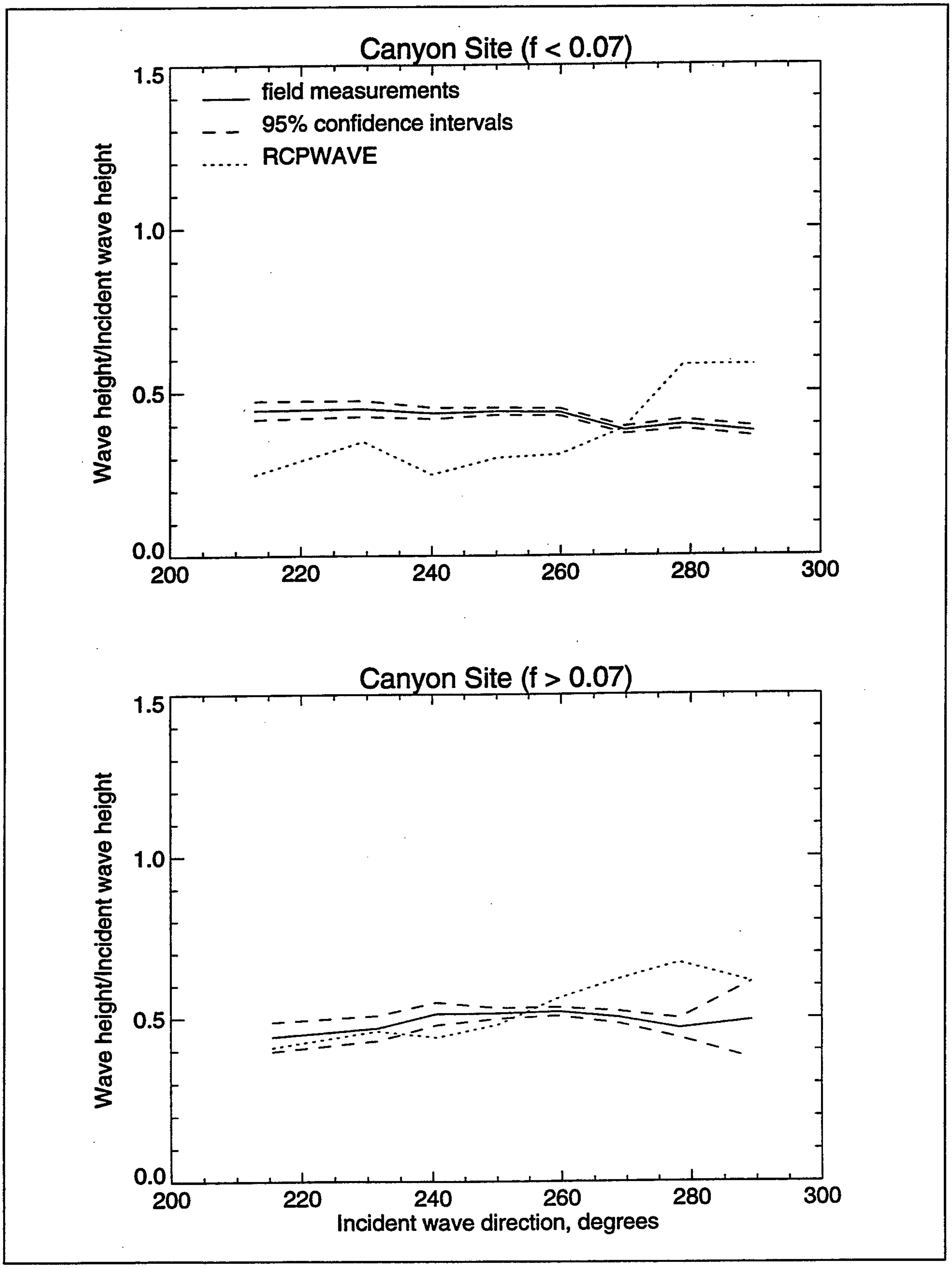

Figure 17. Regression results, canyon site

Table 7
Observed and RCPWAVE-Predicted Wave Directions, $f_0 \leq 0.07$ Hz[1]

θ_0	Number of Observations	θ_{obs}	std	θ_{model}	t-test	$t_{(0.975)\,(d.f.)}$
NORTH						
200 - 225	41	241	5	225	21.27	2.02
225 - 235	38	240	7	228	10.13	2.03
235 - 245	60	239	6	231	10.80	2.00
245 - 255	93	238	6	236	3.86	1.99
255 - 265	115	239	7	241	-3.22	1.98
265 - 275	87	239	7	247	-10.65	1.99
275 - 285	40	241	8	251	-7.66	2.02
> 285	40	238	6	256	-18.45	2.02
NORTH BREAKWATER						
200 - 225	27	243	16	234	2.80	2.06
225 - 235	20	247	6	238	7.18	2.09
235 - 245	33	256	33	241	4.50	2.04
245 - 255	57	250	6	245	6.61	2.00
255 - 265	66	248	6	251	-4.51	2.00
265 - 275	46	249	6	256	-7.54	2.01
275 - 285	22	248	6	258	-8.00	2.08
> 285	21	246	5	260	-12.57	2.09
SOUTH BREAKWATER						
200 - 225	14	251	10	230	7.47	2.16
225 - 235	10	249	9	235	4.93	2.26
235 - 245	19	248	7	238	6.05	2.10
245 - 255	41	245	6	239	6.92	2.02
255 - 265	36	245	6	245	-0.13	2.03
265 - 275	29	244	4	252	-10.69	2.05
275 - 285	11	250	13	258	-2.00	2.23
> 285	13	246	3	262	-18.04	2.18

(Continued)

[1] The hypothesis $\theta_{model} = \theta_{obs}$ is rejected if $|t\text{-test}| > t_{(0.975)\,(d.f.)}$.

Table 7 (Concluded)

θ_0	Number of Observations	θ_{obs}	std	θ_{model}	t-test	$t_{(0.975)\,(d.f.)}$
			CANYON			
200 - 225	40	288	59	286	0.23	2.02
225 - 235	38	297	11	285	6.70	2.03
235 - 245	65	299	8	285	13.96	2.00
245 - 255	118	298	8	286	15.01	1.98
255 - 265	138	297	7	286	18.94	1.98
265 - 275	103	294	31	287	2.26	1.98
275 - 285	48	295	7	288	6.65	2.01
> 285	45	294	14	289	2.45	2.02

Note: θ_{model} = Predicted wave direction by the model, deg; std = Standard deviation of θ_{obs}.

wave direction θ_0 varies. Assuming normal incidence to the shore, i.e., sin θ_0 = 1, we find, for instance, the wave height ratio κ about 0.8 for a 15-sec wave at the 15-m water depth, which is close to the observations found for all three sites, except the canyon site.

Table 8
Observed and RCPWAVE-Predicted Wave Directions, $f_0 > 0.07$ Hz[1]

θ_0	Number of Observations	θ_{obs}	std	θ_{model}	t-test	$t_{(0.975)\,(d.f.)}$
NORTH						
200 - 225	11	237	10	224	4.34	2.23
225 - 235	17	240	7	230	5.63	2.12
235 - 245	36	243	6	235	7.81	2.03
245 - 255	132	244	8	241	4.24	1.98
255 - 265	185	244	7	248	-8.24	1.97
265 - 275	104	245	7	253	-12.73	1.98
275 - 285	48	247	7	258	-10.92	2.01
> 285	9	245	6	263	-8.36	2.31
NORTH BREAKWATER						
200 - 225	6	241	15	231	1.65	2.57
225 - 235	9	248	10	237	3.35	2.31
235 - 245	14	252	4	242	7.96	2.16
245 - 255	74	251	7	248	3.59	1.99
255 - 265	95	253	8	254	-1.61	1.99
265 - 275	59	254	6	259	-6.14	2.00
275 - 285	23	253	5	262	-8.03	2.07
> 285	4	254	4	264	-5.19	3.18
SOUTH BREAKWATER						
200 - 225	4	249	9	227	5.16	3.18
225 - 235	6	255	13	235	3.82	2.57
235 - 245	12	245	15	239	1.50	2.20
245 - 255	44	249	7	243	5.24	2.02
255 - 265	62	250	7	251	1.75	2.00
265 - 275	34	251	7	258	-5.27	2.04
275 - 285	21	248	6	263	-11.01	2.09
> 285	3	253	6	268	-4.67	4.30

(Continued)

[1] The hypothesis $\theta_{model} = \theta_{obs}$ is rejected if $|t\text{-test}| > t_{(0.975)\,(d.f.)}$.

Table 8 (Concluded)						
θ_0	Number of Observations	θ_{obs}	std	θ_{model}	t-test	$t_{(0.975)\,(d.f.)}$
			CANYON			
200 - 225	11	295	11	279	4.88	2.23
225 - 235	17	296	5	281	12.64	2.12
235 - 245	37	294	6	281	13.76	2.03
245 - 255	154	294	6	281	27.38	1.98
255 - 265	199	293	22	282	7.04	1.97
265 - 275	113	292	26	285	2.84	1.98
275 - 285	52	294	13	287	3.86	2.01
> 285	10	297	7	290	3.03	2.26

Note: θ_{model} = Wave direction by the model, deg; std = Standard deviation of θ_{obs}.

4 Tides

Wind speeds and directions (available from NDBC46025) are not included for the present study, considering the short distance of propagation (approximately 62 km from NDBC46025 to the shallow water gauges) and the study by Hasselman et. al. (1973) which reports "only a marginal indication of an increase of the decay rate with the swell energy" by the wind fetching parallel to the swell direction.

Tides, though the range is not large,[1] are sought as a possible physical parameter affecting swell energy and directions because the previous studies by Hales (1987) and USAED, Los Angeles (1989) indicate that the water surface elevation is an important factor in wave damage to breakwaters during storms.[2] Water-depth data (specifically, the hourly recordings from DWG1s, which provide excellent information on tides), are used to examine the correlation between the regression parameters and the water surface level.

Are (observed) wave heights H and directions θ in shallow water influenced by the currents induced by tides and the fluctuation of the mean water surface level (mwl)? For this test, the data are divided into three nonoverlapping groups so that the first group contains data whose mwls are higher than the mean high water (mhw), the second group contains mwls between the mean low water (mlw) and mhw, and the third group contains data whose mwls are lower than mlw. The observations of each group are assumed to be represented by a regression model $H = \kappa_0 + \kappa H_0$ with a non-zero intercept term.

Table 9 shows the results of testing the following three hypotheses: (a) homogeneity for variances of the three tide groups (Bartlett's test, χ^2-statistics), (b) one regression line for all observations of the three groups (denoted by F-test(1)), (c) the same slopes (κ) for the three groups (denoted by F-test(2)).

In most of the cases tested, the values of the χ^2 statistics are less than those of the χ^2 distribution at a 5-percent level of significance ($\chi^2_{(.95)(2)} = 5.99$), suggesting

[1] 1.6 m between mean lower low water (mllw) and the mean higher high water (mhhw).
[2] Hasselman et al. (1973), however, report no tidal modulation of the swell decay rate in their JONSWAP study, in which the horizontal measuring distance is 160 km.

Table 9
Test of Tidal Influence on the Shallow-Water Wave Height *H*

Incident Wave Direction, θ_0	χ^2-test	F-test(1)	F-test(2)	ν_2
North Site, $f_0 \le 0.07$ Hz				
245 - 255	0.271	0.862	0.079	87
255 - 265	1.457	1.611	0.772	109
265 - 275	1.532	1.521	0.773	81
275 - 285	0.071	0.365	0.532	34
North Site, $f_0 > 0.07$ Hz				
245 - 255	4.087	0.559	0.732	126
255 - 265	1.337	0.697		179
265 - 275	3.561	2.444	2.185	98
275 - 285	2.111	2.058	2.527	42
Canyon, $f_0 \le 0.07$ Hz				
245 - 255	0.241	1.878	1.291	112
255 - 265	5.873	2.446	4.361	132
265 - 275	1.179	2.650	0.060	97
275 - 285	2.031	1.680	0.054	42
Canyon, $f_0 > 0.07$ Hz				
245 - 255	3.997	1.039	1.282	148
255 - 265	4.835	4.181	7.700	193
265 - 275	4.314	3.453	2.739	107
275 - 285	1.817	0.559	0.830	46
North Breakwater Site, $f_0 \le 0.07$ Hz				
245 - 255	1.571	2.382	2.369	51
255 - 265	2.460	10.895	18.966	60
265 - 275	3.703	5.562	6.084	40
275 - 285	1.166	1.187	0.223	16
North Breakwater Site, $f_0 > 0.07$ Hz				
245 - 255	10.508	1.940		68
255 - 265	7.128	1.067	1.605	89
265 - 275	2.921	2.049	3.672	53
275 - 285	1.474	2.371	2.239	17

(Continued)

Table 9 (Concluded)				
Incident Wave Direction, θ_0	**χ^2-test**	***F*-test(1)**	***F*-test(2)**	**v_2**
South Breakwater Site, $f_0 \le 0.07$ Hz				
245 - 255	1.049	1.504	2.784	35
South Breakwater Site, $f_0 > 0.07$ Hz				
245 - 255	0.932	7.702	8.800	38
255 - 265	1.514	0.851	1.336	56
θ_0 = Wave direction in the deep water (NDBC46025) in degrees.				

the variances of the shallow-water wave height H of the three different tide groups are equal. The rejections shown by the two cases (north breakwater site, 245 - 255 and 255 - 265 with $f_0 > 0.07$ Hz) are considered to result from nonnormality, rather than from nonhomogeniety of variance. Regardless of these outcomes, we proceed further for the second (F-test(1)) and third (F-test(2)) tests, which find a few cases rejecting the hypotheses at the 5-percent level of significance ($F_{(0.95)(v1,v2)}$, where v_1 and v_2 denote degrees of freedom with $v_1 = 4$ for F-test(1) and $v_1 = 2$ for F-test(2). The values of v_2 are listed in the table).

Table 10 lists the results for the tidal influence on the wave directions. Two tests are performed: Bartlett's test and an F-test against a null hypothesis that the three wave directions (averaged in each group) are equal. As can be seen in the table, there are some rejections in both tests, especially for the canyon site, though many cases accept the hypotheses.

It is suspected that the few rejections seen, especially in the χ^2-tests, are caused by false detections due to failure of the data to meet the underlying assumptions of the tests. Though a complete discussion requires further checks on the data such as the testing of normality, at this stage it may be concluded from the foregoing tests that the data available fall short in supporting any noticeable influence by the tide-induced currents or sea level changes on the characteristics of swell waves observed. The RCPWAVE computations, using different water levels within the tide range, also show negligible differences between results from different water levels. RCPWAVE results shown in the previous discussion were obtained with the water depth set at mllw.

Table 10
Test of Tidal Influence on the Shallow-Water Wave Direction θ

Incident Wave Direction, θ_0	χ^2-test	F-test	v_2
North Site, $f_0 \leq 0.07$ Hz			
245 - 255	1.654	6.527	90
255 - 265	4.601	3.802	112
265 - 275	0.681	9.406	84
275 - 285	2.506	2.232	37
North Site, $f_0 > 0.07$ Hz			
245 - 255	22.830	1.125	129
255 - 265	0.738	1.854	182
265 - 275	1.962	0.450	101
275 - 285	2.506	1.255	45
Canyon, $f_0 \leq 0.07$ Hz			
245 - 255	20.313	2.735	115
255 - 265	3.737	8.585	135
265 - 275	33.774	0.287	110
275 - 285	10.699	4.273	45
Canyon, $f_0 > 0.07$ Hz			
245 - 255	0.558	31.985	151
255 - 265	115.790	1.029	196
265 - 275	82.813	0.305	110
275 - 285	17.904	0.209	49
North Breakwater Site, $f_0 \leq 0.07$ Hz			
245 - 255	2.433	1.604	54
255 - 265	6.492	8.286	63
265 - 275	4.712	1.643	43
275 - 285	5.756	1.180	19
North Breakwater Site, $f_0 > 0.07$ Hz			
245 - 255	4.290	0.267	71
255 - 265	9.615	2.806	92
265 - 275	1.337	2.547	56
275 - 285	3.028	8.720	20

(Continued)

Table 10 (Concluded)

Incident Wave Direction, θ_0	χ^2-test	F-test(2)	v_2
South Breakwater Site, $f_0 \leq 0.07$ Hz			
245 - 255	6.793	3.767	38
265 - 275	2.520	1.499	26
275 - 285	12.089	14.101	8
South Breakwater Site, $f_0 > 0.07$ Hz			
245 - 255	3.495	0.251	41
255 - 265	1.051	1.817	59
265 - 275	4.406	3.553	31
275 - 285	1.205	0.238	18

θ_0 = Wave direction in the deep water (NDBC46025) in degrees.

5 Conclusions

The study compares statistical results from the refraction model RCPWAVE to measured waves near the Redondo breakwaters. The study also evaluates results from the spectral refraction model STWAVE against the same measurements. Redondo Beach was specifically chosen as a site which gives a difficult challenge to linear propagation models. Therefore, it is no surprise that RCPWAVE and STWAVE did not agree well with the field measurements. Nevertheless, the present results indicate how model results may be related to actual wave propagation in the presence of complex topography. Following are summary points from comparisons of model results to measured waves.

a. Computations from both RCPWAVE and STWAVE are in poor agreement (low correlation coefficients) with the field measurements for $H > 1.5$ m.

b. RCPWAVE tends to overestimate wave heights in general.

c. STWAVE wave heights appear to be more accurate than RCPWAVE, but their underestimations may be unacceptable in some cases.

d. Both the field measurements and the model computations indicate no significant tidal influence on wave transformation.

e. Field measurements fail to support the wave-height relationship $H = \kappa H_0$ inherent in the model computations.

f. Correlation changes significantly with increasing measured wave height. Therefore, extrapolation of the present results beyond those measured (3.3 m for maximum H_0) requires caution.

References

Cartwright, D. E., and Longuet-Higgins, M. S. (1956). "The statistical distribution of the maxima of a random function." *Proc. Roy. Soc. London*, Ser. A, Vol 237, 212-232.

Cialone, M. A., et al. (1994). "Coastal Modeling System (CMS) User's Manual," Instruction Report CERC-91-1, U.S. Army Engineer Waterways Experiment Station, Vicksburg, MS.

Dean, R. G., and Dalrymple, R. A. (1984). *Water wave mechanics for engineers and scientists.* Prentice-Hall, Englewood Cliffs, NJ.

Ebersole, B. A., Cialone, M. A., and Prater, M. D. (1986). "Regional coastal processes numerical modeling system; Report 1, RCPWAVE-A linear wave propagation model for engineering use," Technical Report CERC-86-4, U.S. Army Engineer Waterways Experiment Station, Vicksburg, MS.

Goda, Y. (1970). "Numerical experiments on wave statistics with spectral simulation," *Report of Port and Harbour Research Institute* 16(2), 3-26.

Guillaume, A. (1990). "Statistical tests for the comparison of surface gravity wave spectra with application to model validation," *J. Atmospheric and Ocean Tech.* 7, 551-567.

Hales, L. Z. (1987). "Water wave effects at Redondo Beach King Harbor, California," Miscellaneous Paper CERC-87-2, U.S. Army Engineer Waterways Experiment Station, Vicksburg, MS.

Hasselmann, K., et al. (1973). "Measurements of wind-wave growth and swell decay during the Joint North Sea Wave Project (JONSWAP)," Deutsches Hydrographisches Institut, Reiche A (8°), Nr. 12, Hamburg, Germany.

Longuet-Higgins, M. S. (1957). "On the transformatin of a continuous spectrum by refraction." *Proc. Cambridge Philos. Soc.*, 53(1), 226-229.

Longuet-Higgins, M. S., Cartwright, D. E., and Smith, N. D. (1963). "Observations of the directional spectrum of sea waves using the motions of a floating buoy." *Ocean wave spectra.* Prentice Hall, 111-136.

Longuet-Higgins, M. S., Cartwright, D. E., and Smith, N. D. (1963). "Observations of the directional spectrum of sea waves using the motions of a floating buoy." *Ocean wave spectra.* Prentice Hall, 111-136.

Mei, C. C. (1989). *The applied dynamics of ocean surface waves.* World Scientific, Singapore, Teaneck, NJ.

Resio, D. T. (1990). "A steady-state spectral model for near-coast wave simulations," prepared by Offshore and Coastal Technologies, Inc., for the Coastal Engineering Research Center, U.S. Army Engineer Waterways Experiment Station, Vicksburg, MS.

Sabol, M. A. (1996). "Redondo Beach, California, 1992-1994 wave data," Technical Report CERC-96-4, U.S. Army Engineer Waterways Experiment Station, Vicksburg, MS.

U.S. Army Engineer District, Los Angeles. (1988). "Feasibility report storm damage reduction, Redondo Beach - King Harbor area, Los Angeles County, CA," Los Angeles, CA.

__________. (1990). "General Design Memorandum No. 3; Storm damage reduction for King Harbor (Redondo Beach) area," Los Angeles, CA.

Appendix A
Scatter Plots of Nearshore and Offshore Wave Heights

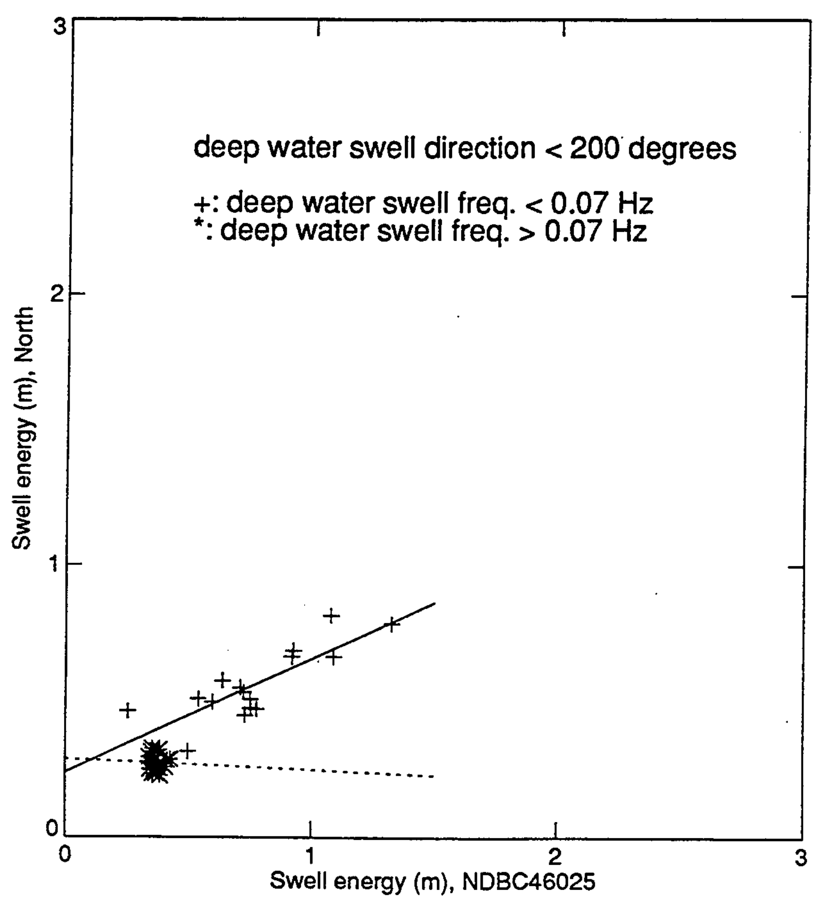

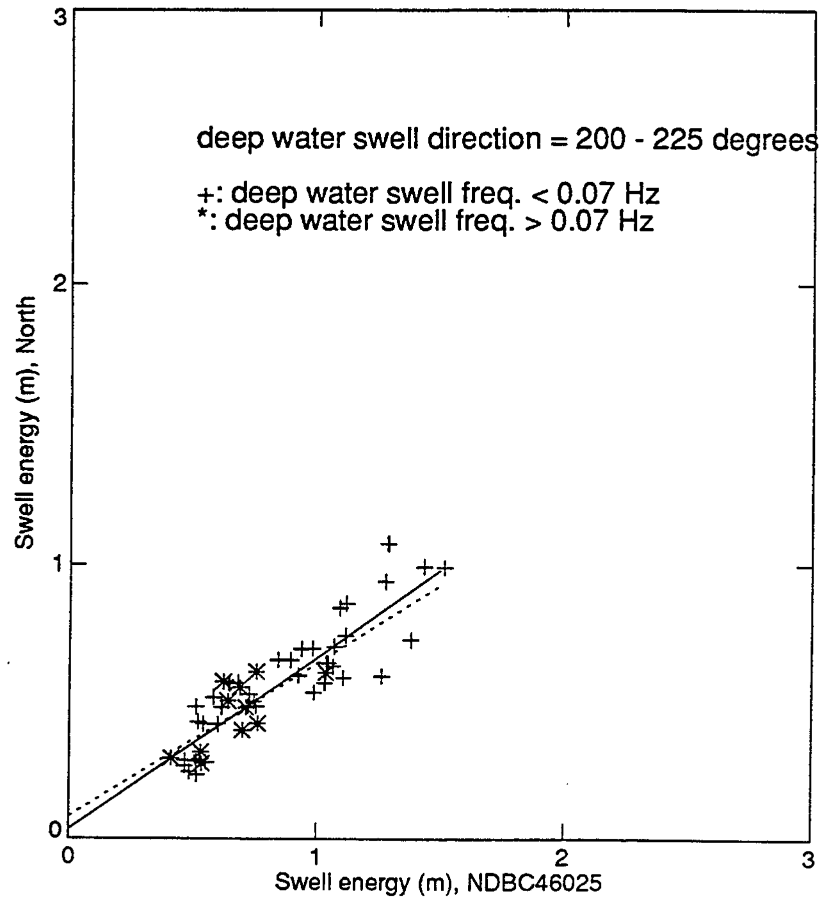
deep water swell direction = 200 - 225 degrees
+: deep water swell freq. < 0.07 Hz
*: deep water swell freq. > 0.07 Hz
Swell energy (m), North
Swell energy (m), NDBC46025
0
1
2
3
0
1
2
3

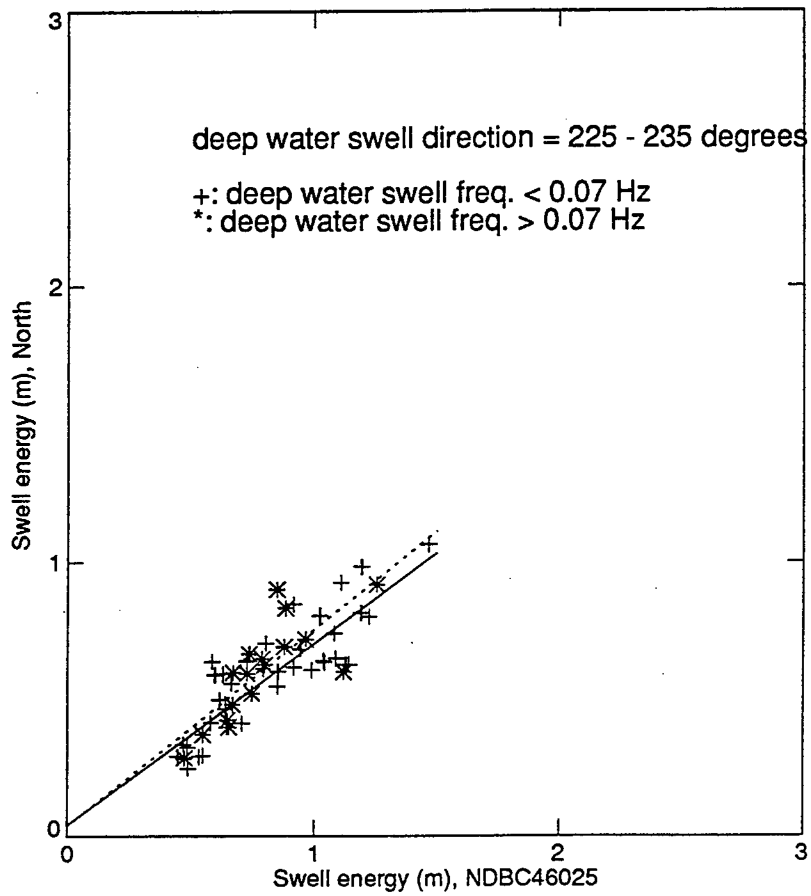
deep water swell direction = 225 - 235 degrees
+: deep water swell freq. < 0.07 Hz
*: deep water swell freq. > 0.07 Hz
Swell energy (m), North
Swell energy (m), NDBC46025
0
1
2
3

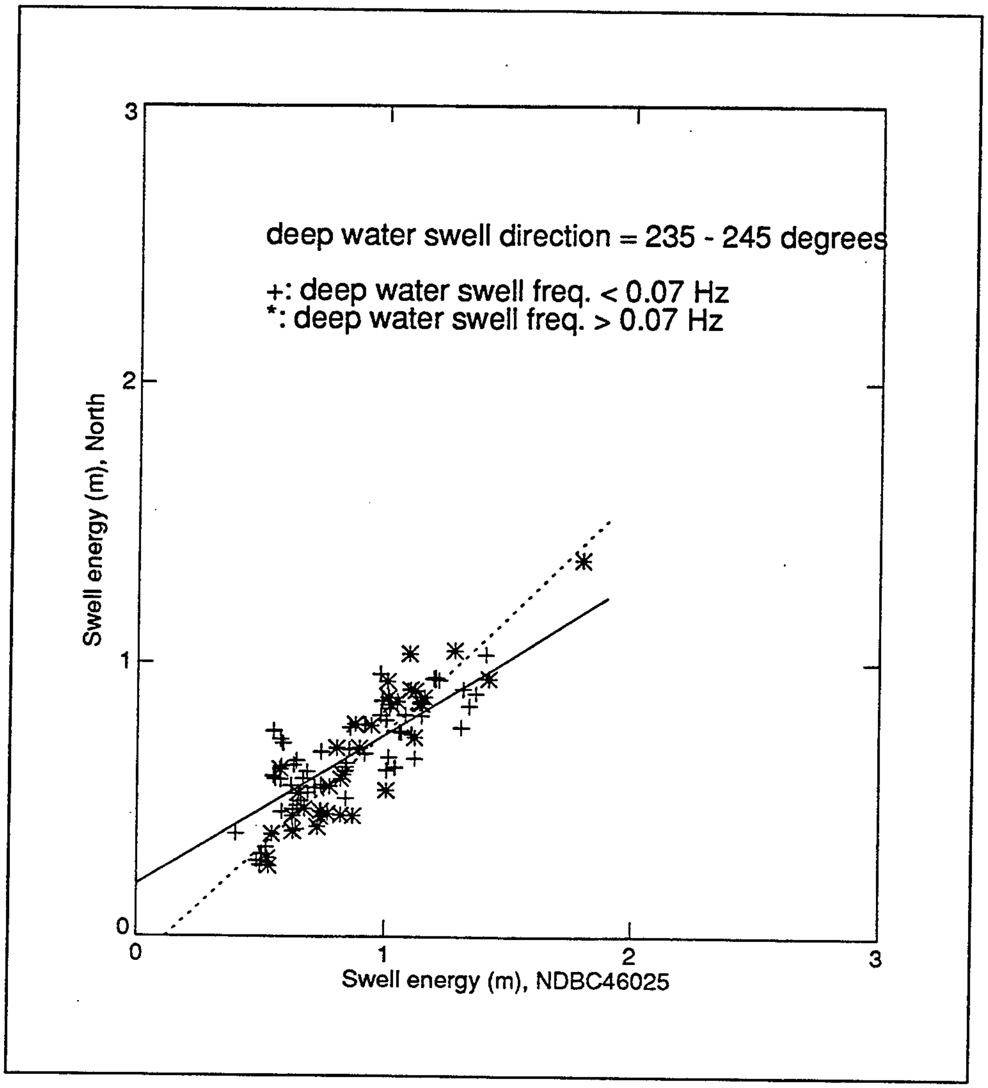
deep water swell direction = 235 - 245 degrees
+: deep water swell freq. < 0.07 Hz
*: deep water swell freq. > 0.07 Hz
Swell energy (m), North
Swell energy (m), NDBC46025
0
1
2
3
0
1
2
3

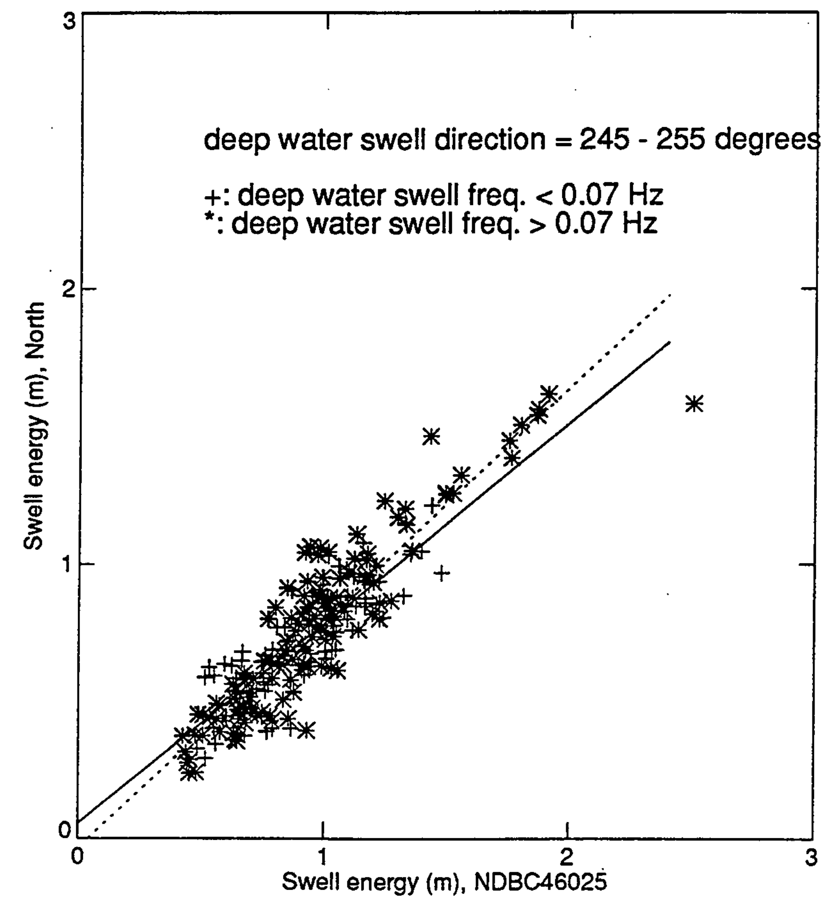
deep water swell direction = 245 - 255 degrees
+: deep water swell freq. < 0.07 Hz
*: deep water swell freq. > 0.07 Hz
Swell energy (m), North
Swell energy (m), NDBC46025
0
1
2
3
0
1
2
3

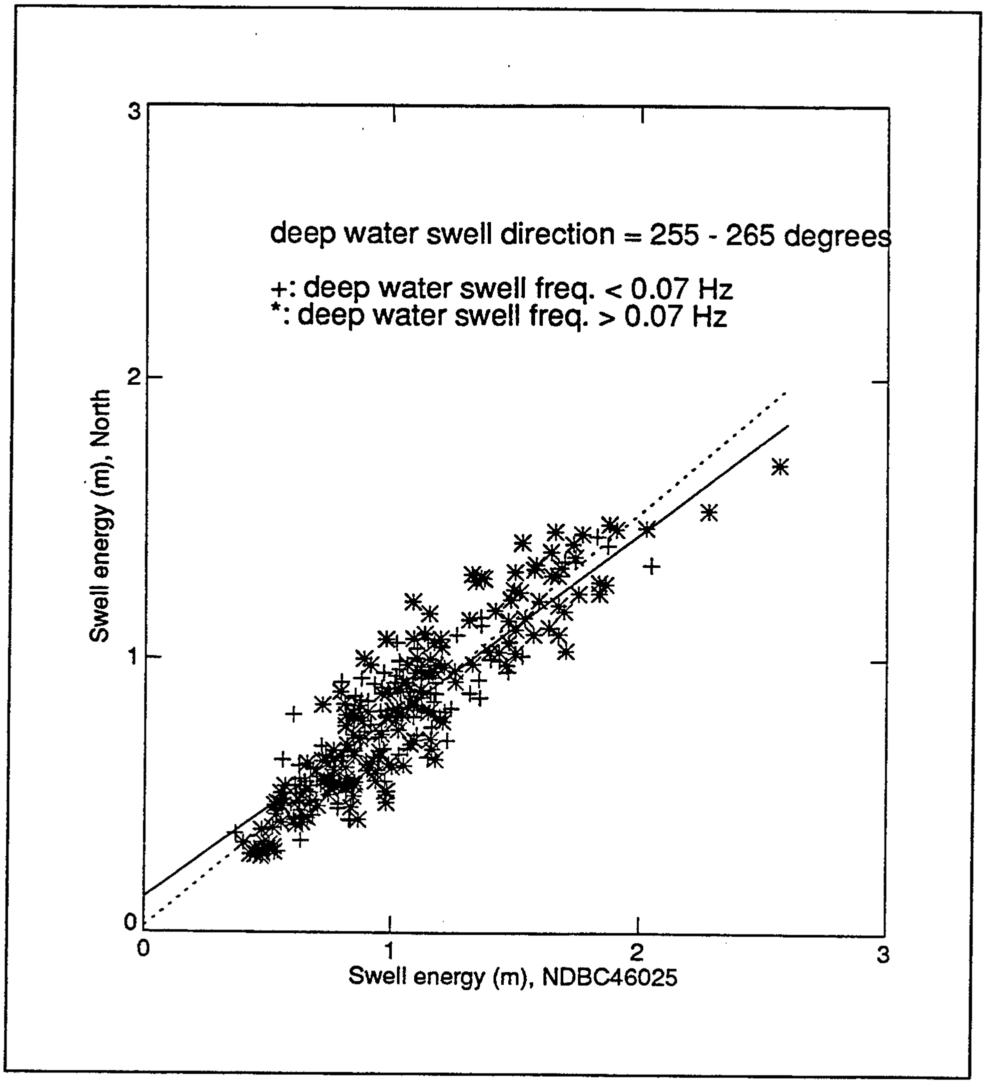
deep water swell direction = 255 - 265 degrees
+: deep water swell freq. < 0.07 Hz
*: deep water swell freq. > 0.07 Hz
Swell energy (m), North
Swell energy (m), NDBC46025
0
1
2
3
0
1
2
3

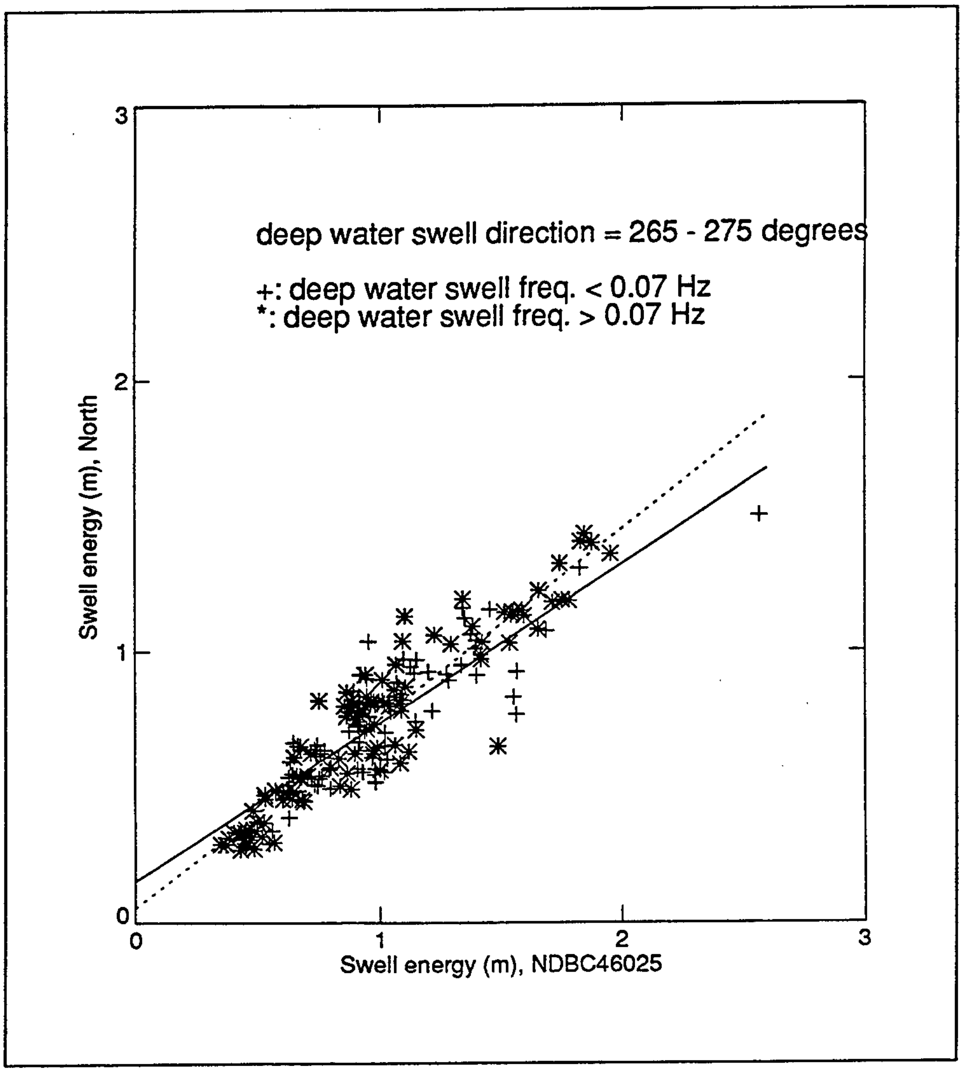
deep water swell direction = 265 - 275 degrees
+: deep water swell freq. < 0.07 Hz
*: deep water swell freq. > 0.07 Hz
Swell energy (m), North
Swell energy (m), NDBC46025
0
1
2
3
0
1
2
3

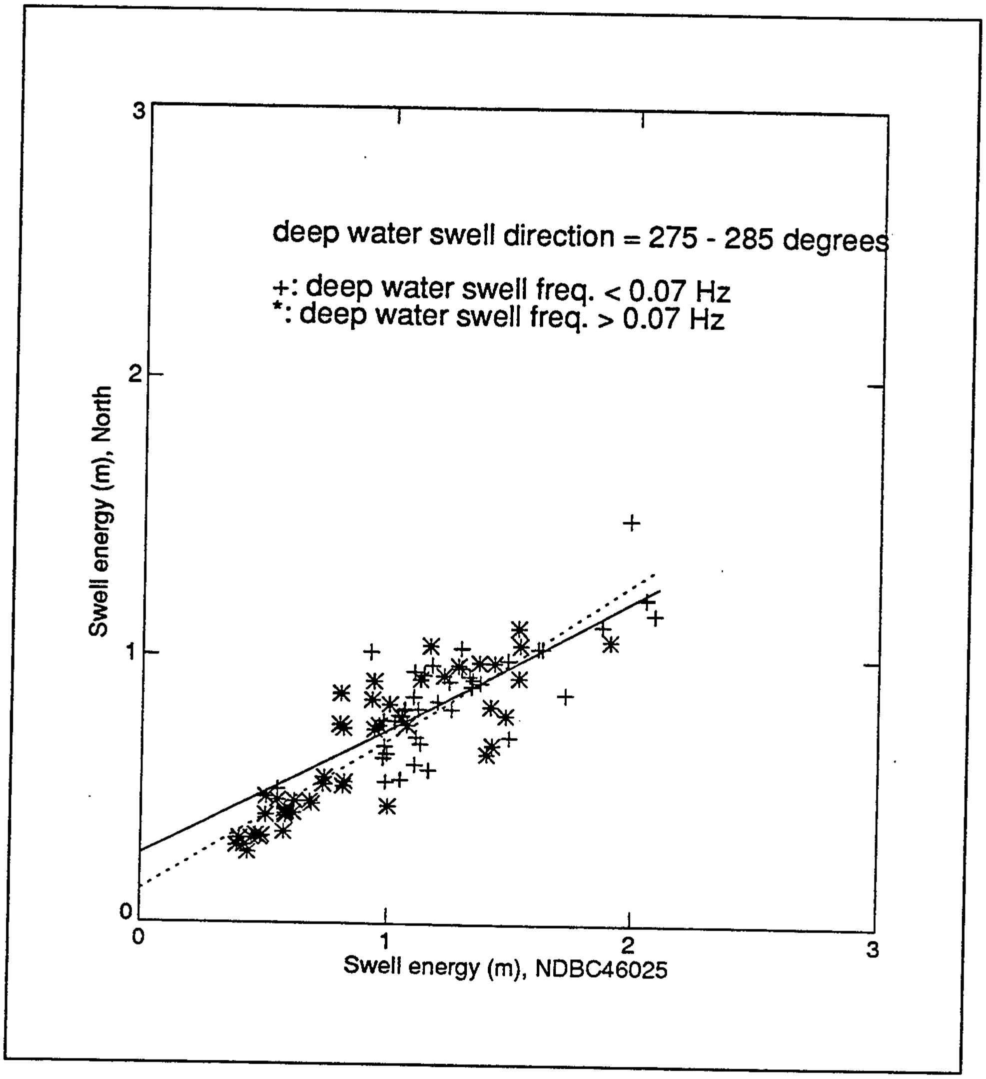
deep water swell direction = 275 - 285 degrees
+: deep water swell freq. < 0.07 Hz
*: deep water swell freq. > 0.07 Hz
Swell energy (m), North
Swell energy (m), NDBC46025
0
1
2
3
0
1
2
3

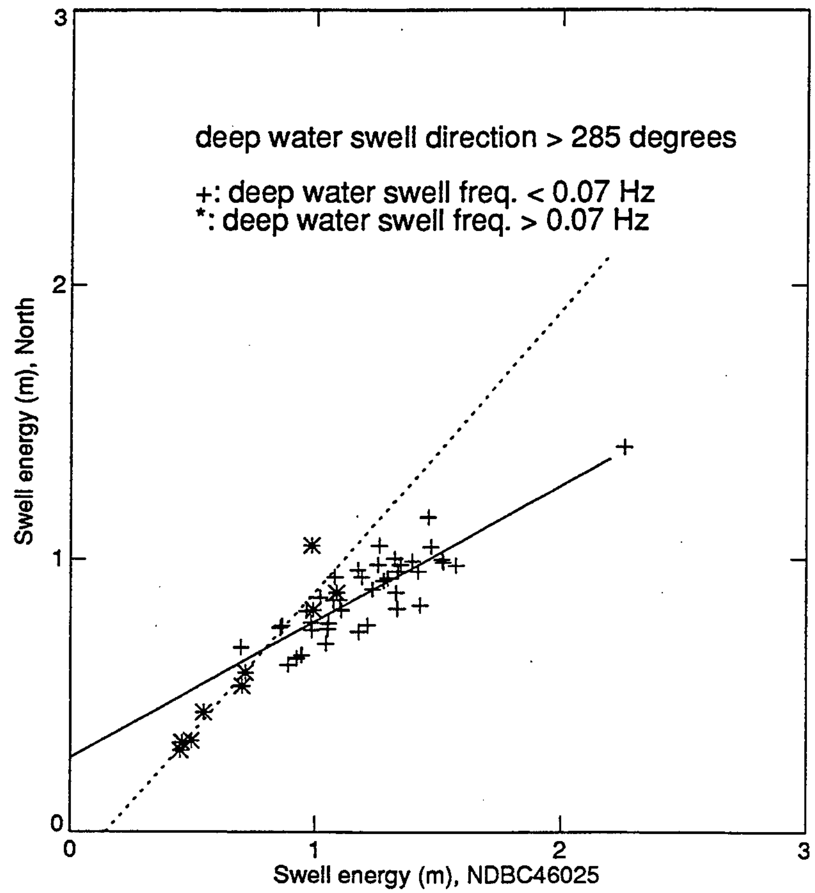
deep water swell direction > 285 degrees
+: deep water swell freq. < 0.07 Hz
*: deep water swell freq. > 0.07 Hz
Swell energy (m), North
Swell energy (m), NDBC46025
0
1
2
3

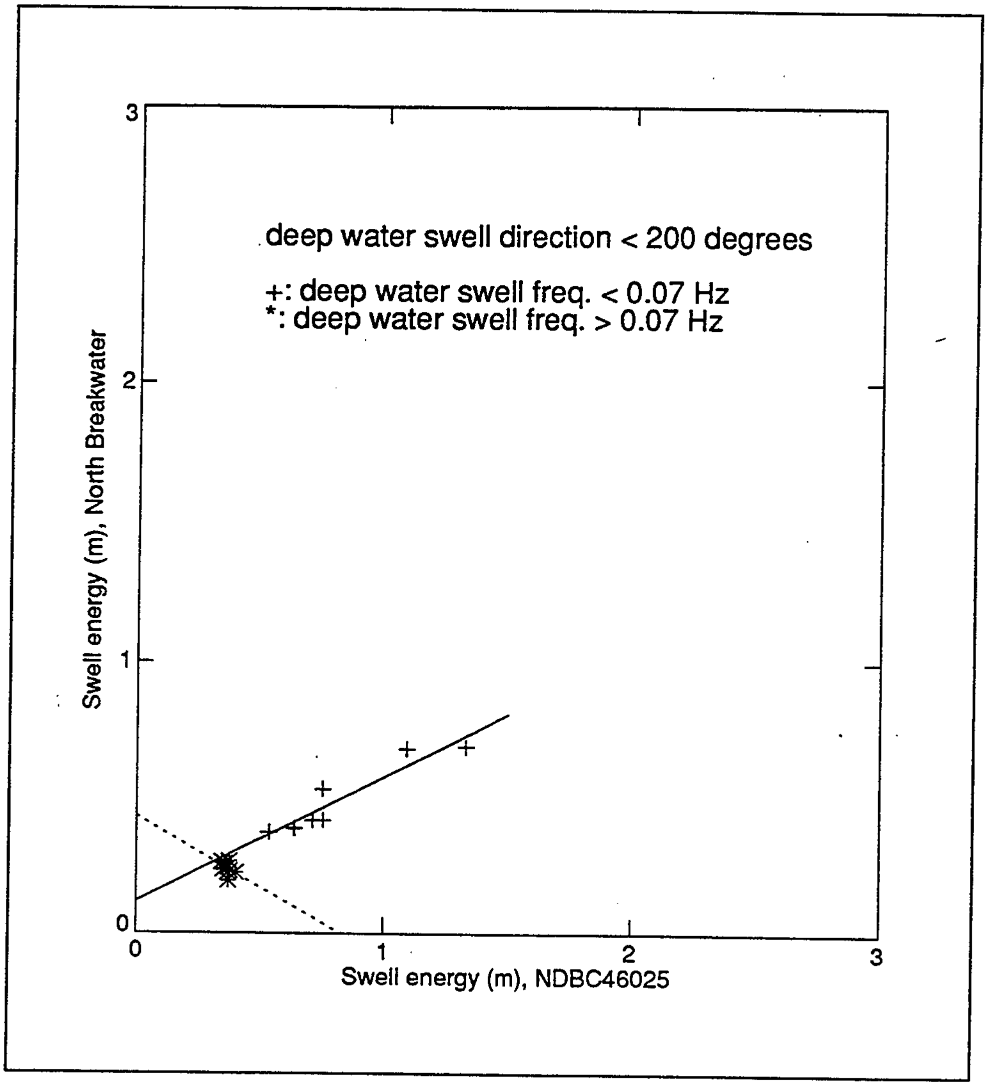

deep water swell direction < 200 degrees
+: deep water swell freq. < 0.07 Hz
*: deep water swell freq. > 0.07 Hz
Swell energy (m), North Breakwater
Swell energy (m), NDBC46025
0
1
2
3

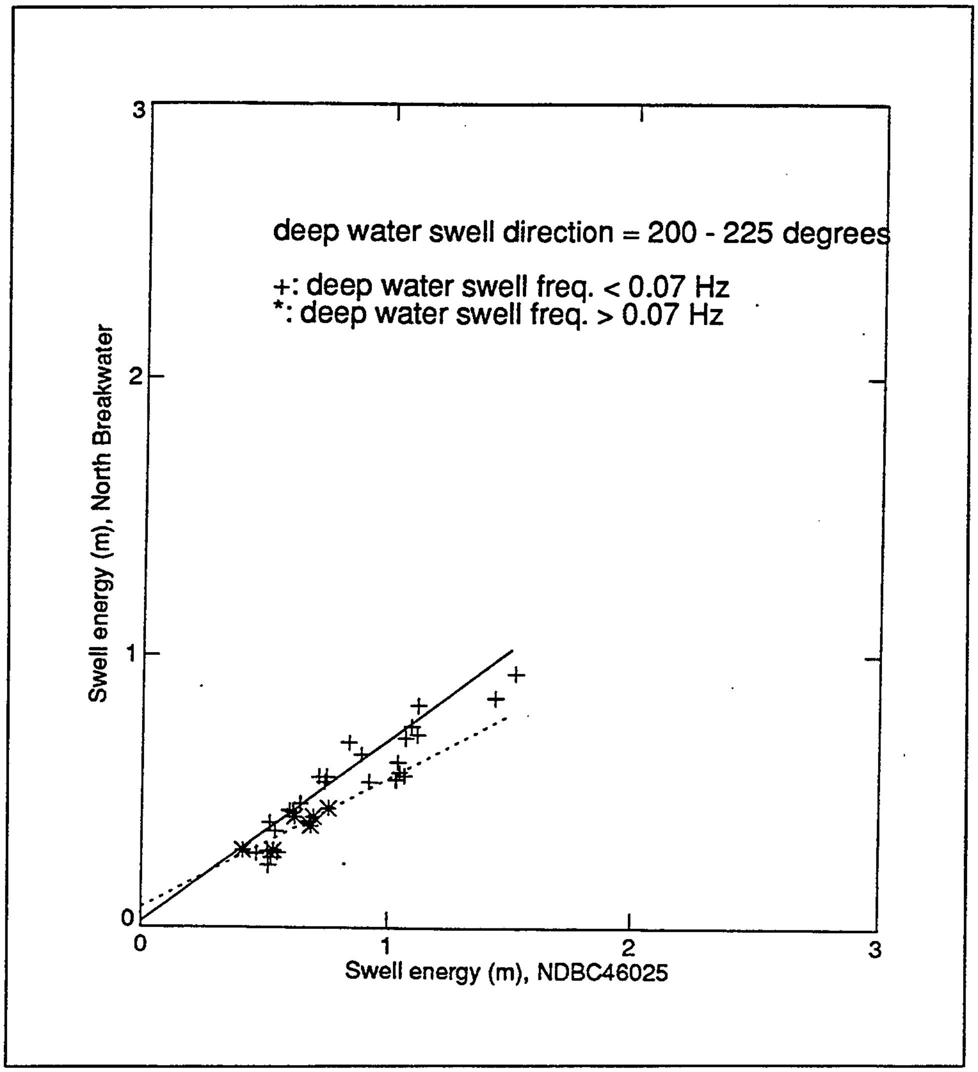

deep water swell direction = 200 - 225 degrees
+: deep water swell freq. < 0.07 Hz
*: deep water swell freq. > 0.07 Hz
Swell energy (m), North Breakwater
Swell energy (m), NDBC46025
0
1
2
3

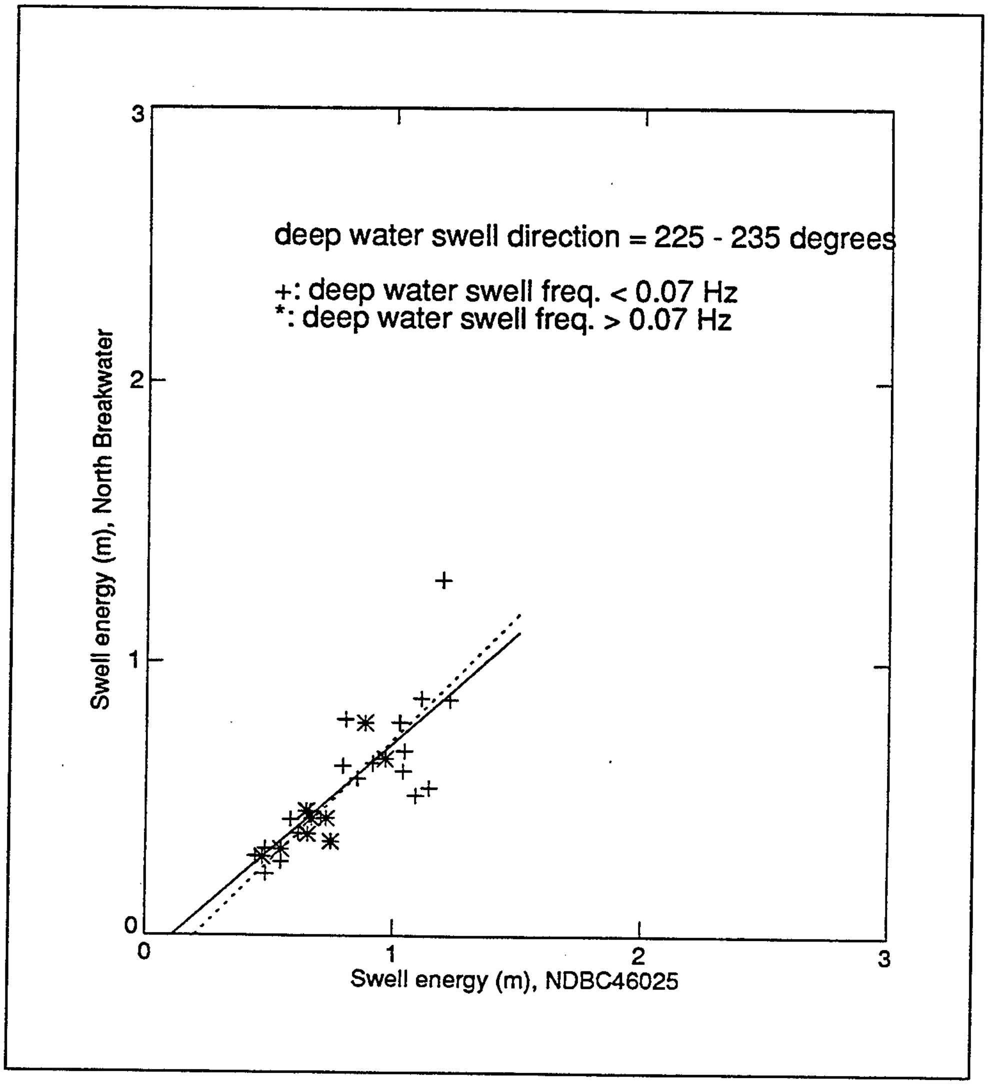

deep water swell direction = 225 - 235 degrees
+: deep water swell freq. < 0.07 Hz
*: deep water swell freq. > 0.07 Hz
Swell energy (m), North Breakwater
Swell energy (m), NDBC46025
0
1
2
3

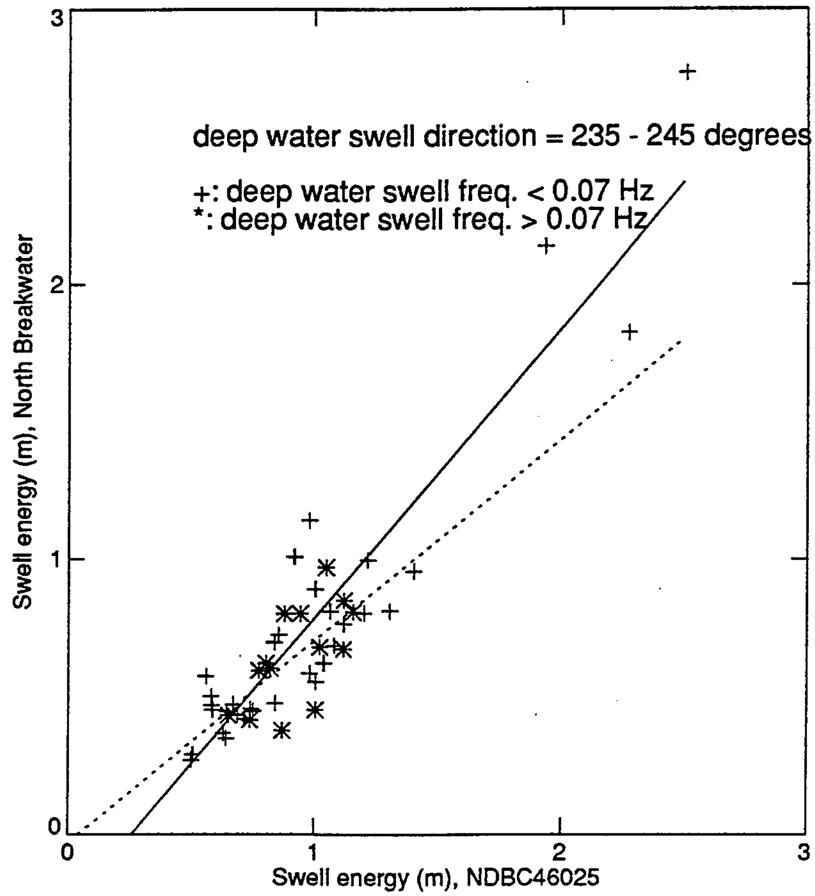
deep water swell direction = 235 - 245 degrees
+: deep water swell freq. < 0.07 Hz
*: deep water swell freq. > 0.07 Hz
Swell energy (m), North Breakwater
Swell energy (m), NDBC46025
0
1
2
3
0
1
2
3

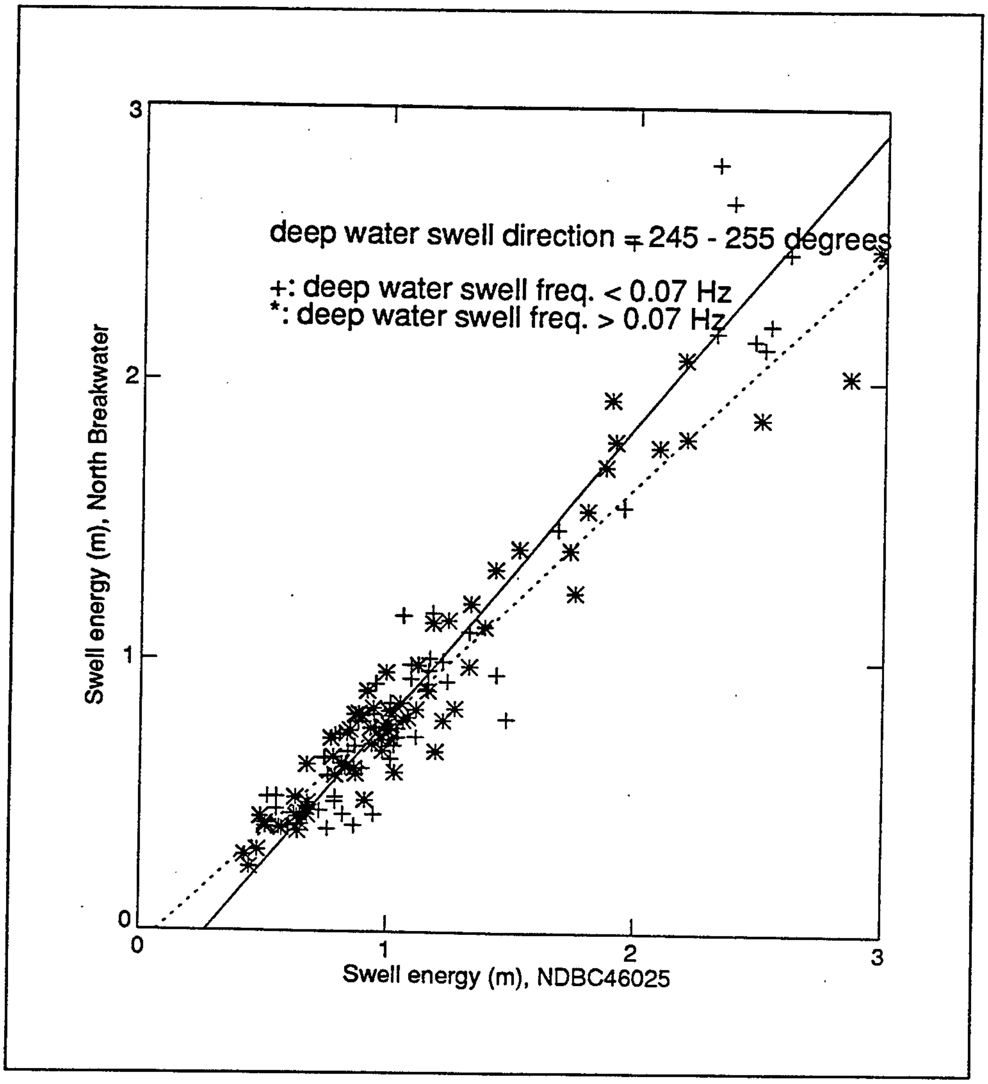
deep water swell direction = 245 - 255 degrees
+: deep water swell freq. < 0.07 Hz
*: deep water swell freq. > 0.07 Hz
Swell energy (m), North Breakwater
Swell energy (m), NDBC46025
0
1
2
3
0
1
2
3

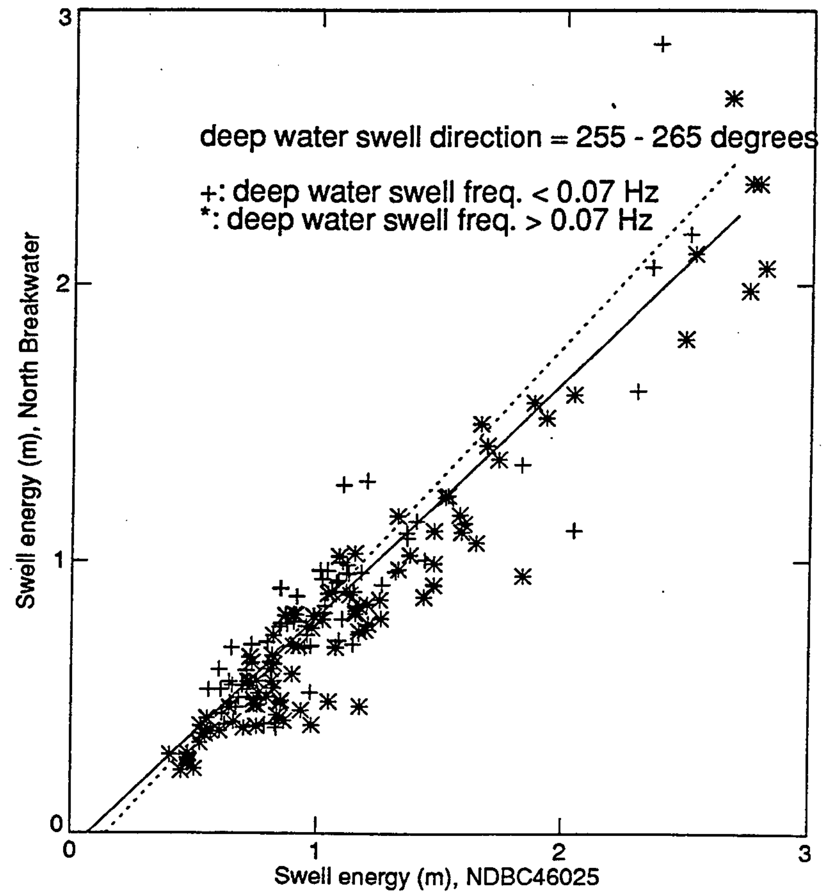
deep water swell direction = 255 - 265 degrees
+: deep water swell freq. < 0.07 Hz
*: deep water swell freq. > 0.07 Hz
Swell energy (m), North Breakwater
Swell energy (m), NDBC46025
0
1
2
3
0
1
2
3

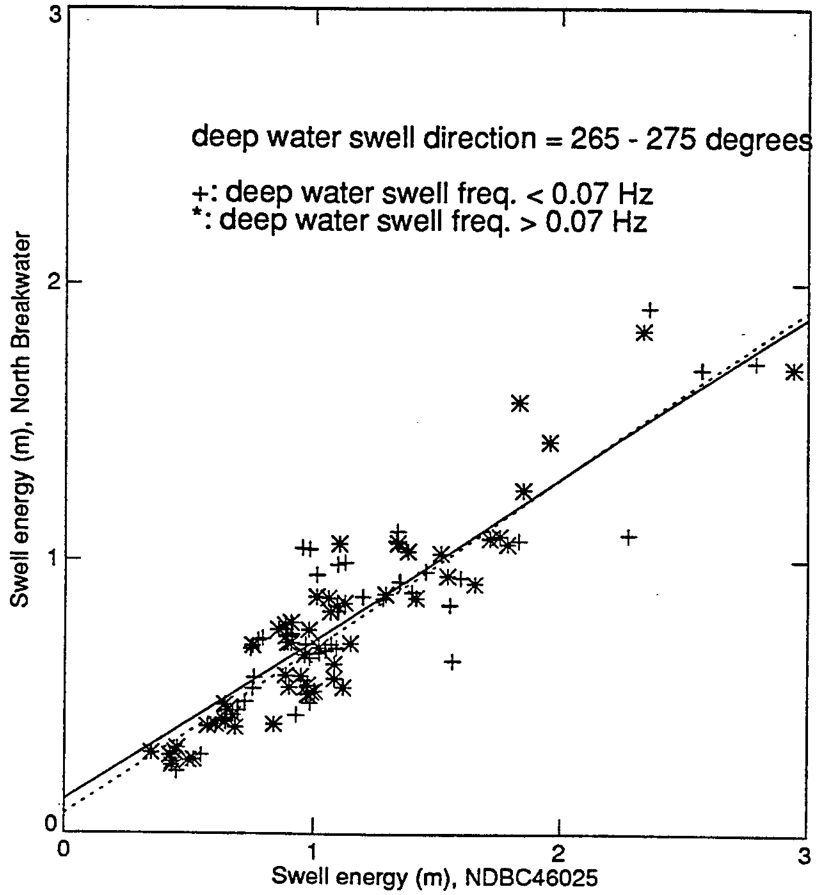
deep water swell direction = 265 - 275 degrees
+: deep water swell freq. < 0.07 Hz
*: deep water swell freq. > 0.07 Hz
Swell energy (m), North Breakwater
Swell energy (m), NDBC46025
0
1
2
3
0
1
2
3

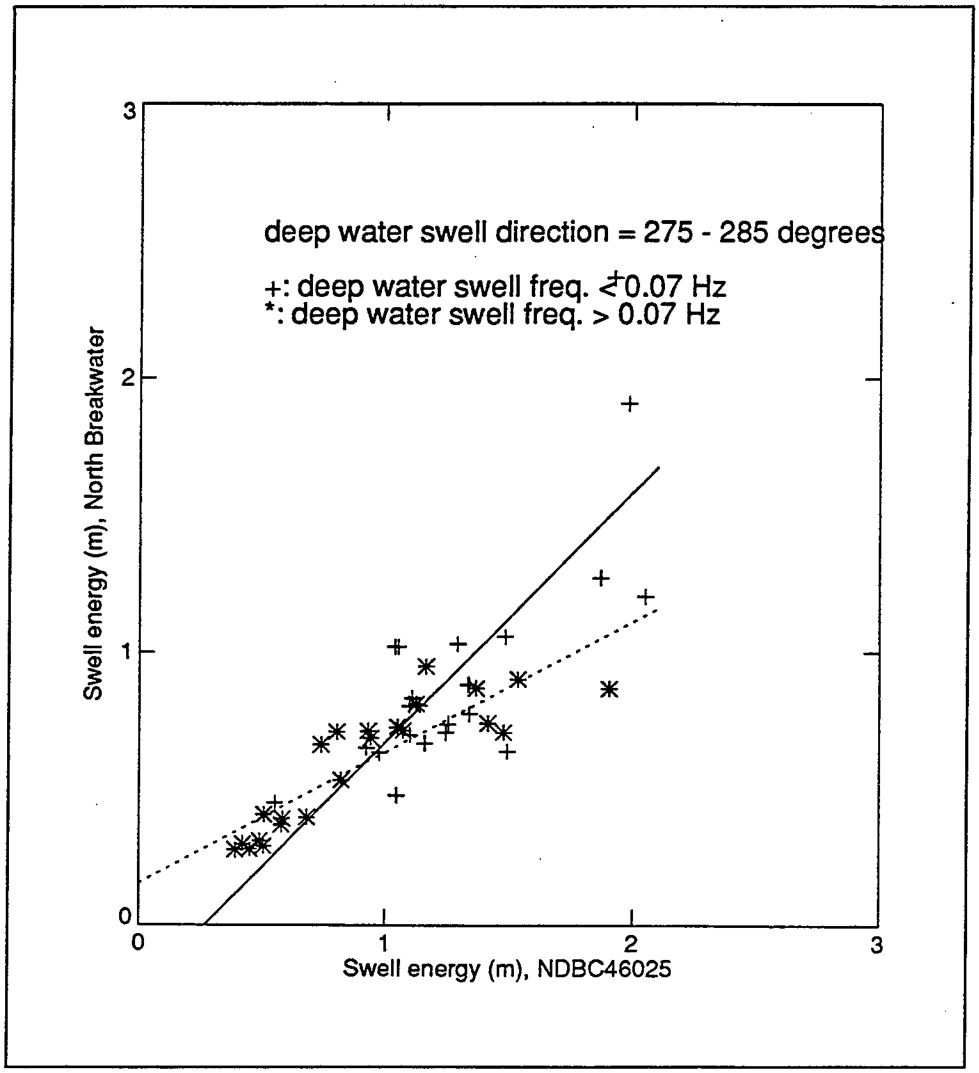
deep water swell direction = 275 - 285 degrees
+: deep water swell freq. < 0.07 Hz
*: deep water swell freq. > 0.07 Hz
Swell energy (m), North Breakwater
Swell energy (m), NDBC46025
0
1
2
3

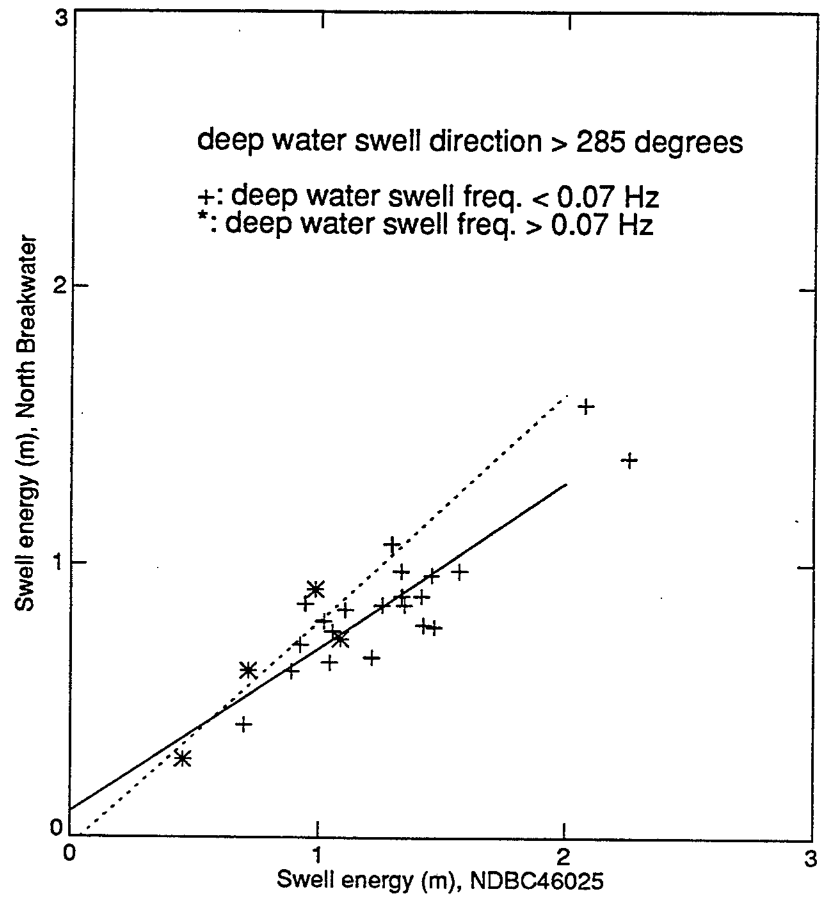

deep water swell direction > 285 degrees
+: deep water swell freq. < 0.07 Hz
*: deep water swell freq. > 0.07 Hz
Swell energy (m), North Breakwater
Swell energy (m), NDBC46025
0
1
2
3

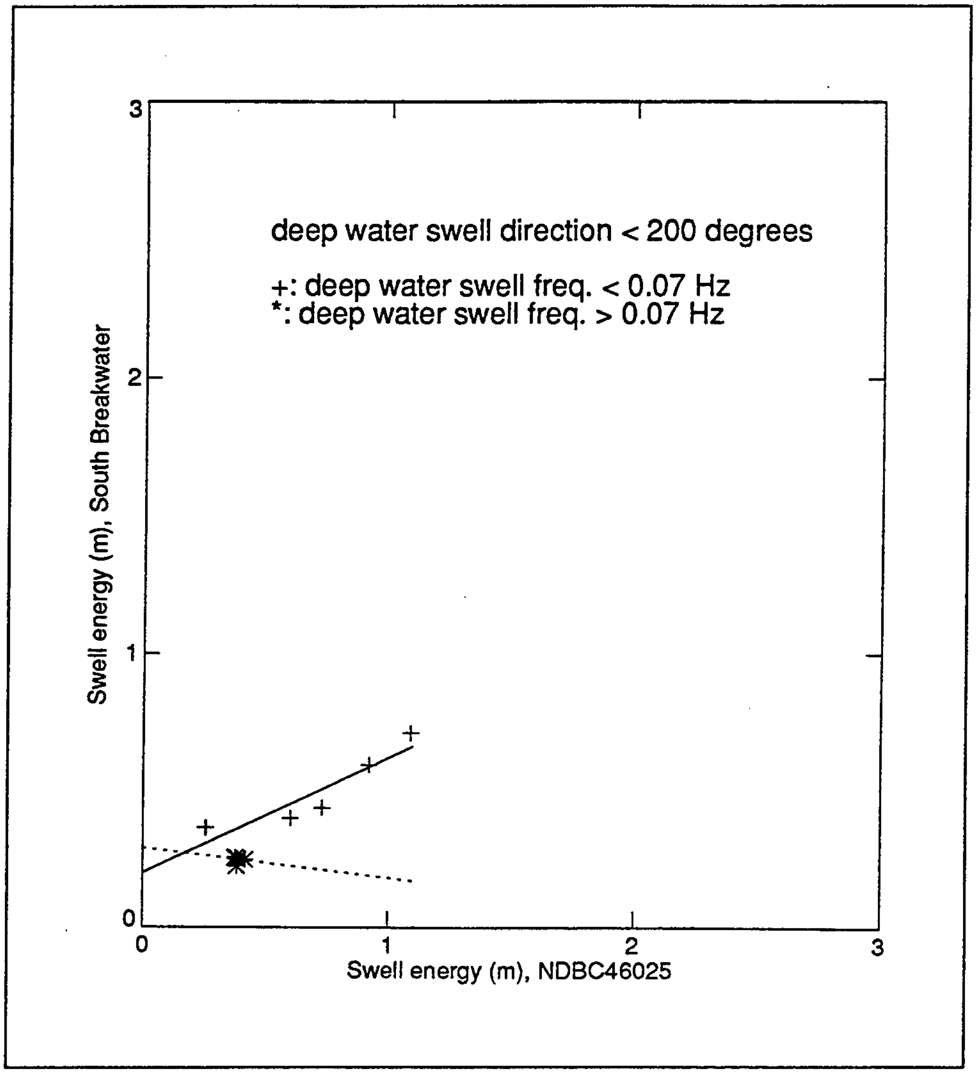
deep water swell direction < 200 degrees
+: deep water swell freq. < 0.07 Hz
*: deep water swell freq. > 0.07 Hz
Swell energy (m), South Breakwater
Swell energy (m), NDBC46025
0
1
2
3
0
1
2
3

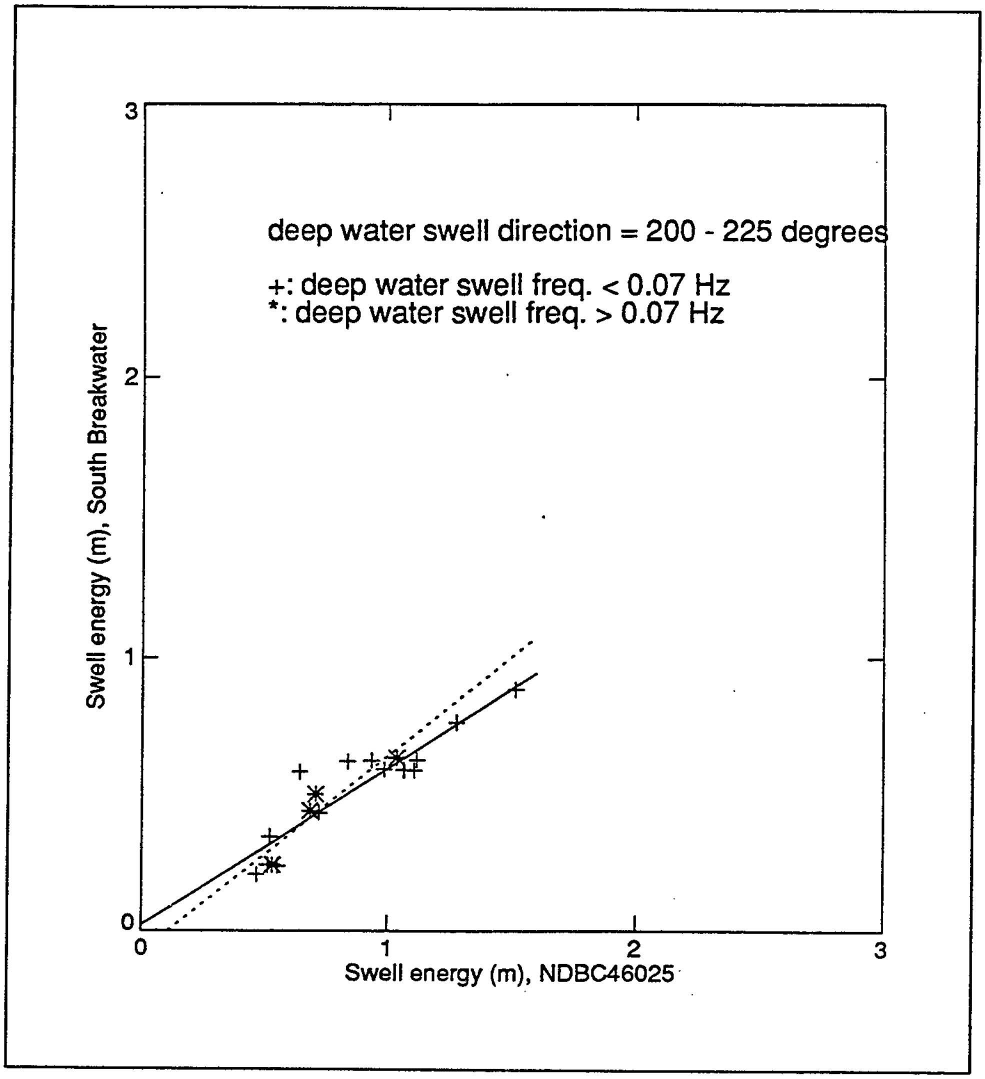

deep water swell direction = 200 - 225 degrees
+: deep water swell freq. < 0.07 Hz
*: deep water swell freq. > 0.07 Hz
Swell energy (m), South Breakwater
Swell energy (m), NDBC46025
0
1
2
3
0
1
2
3

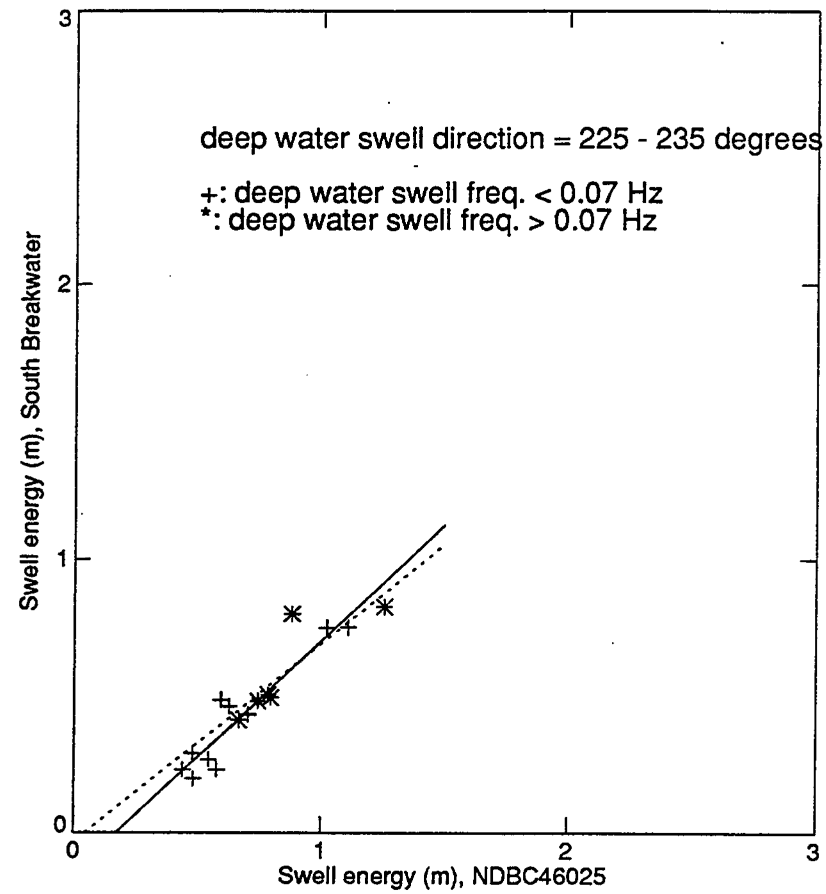

deep water swell direction = 225 - 235 degrees
+: deep water swell freq. < 0.07 Hz
*: deep water swell freq. > 0.07 Hz
Swell energy (m), South Breakwater
Swell energy (m), NDBC46025
0
1
2
3

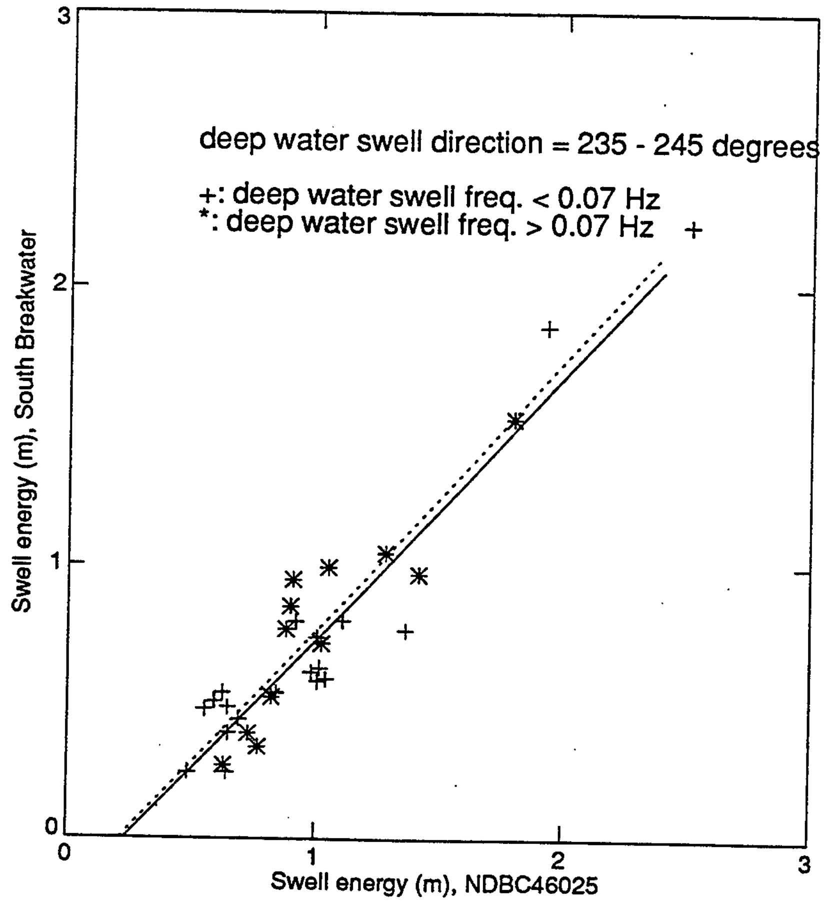
deep water swell direction = 235 - 245 degrees
+: deep water swell freq. < 0.07 Hz
*: deep water swell freq. > 0.07 Hz
Swell energy (m), South Breakwater
Swell energy (m), NDBC46025
0
1
2
3
0
1
2
3

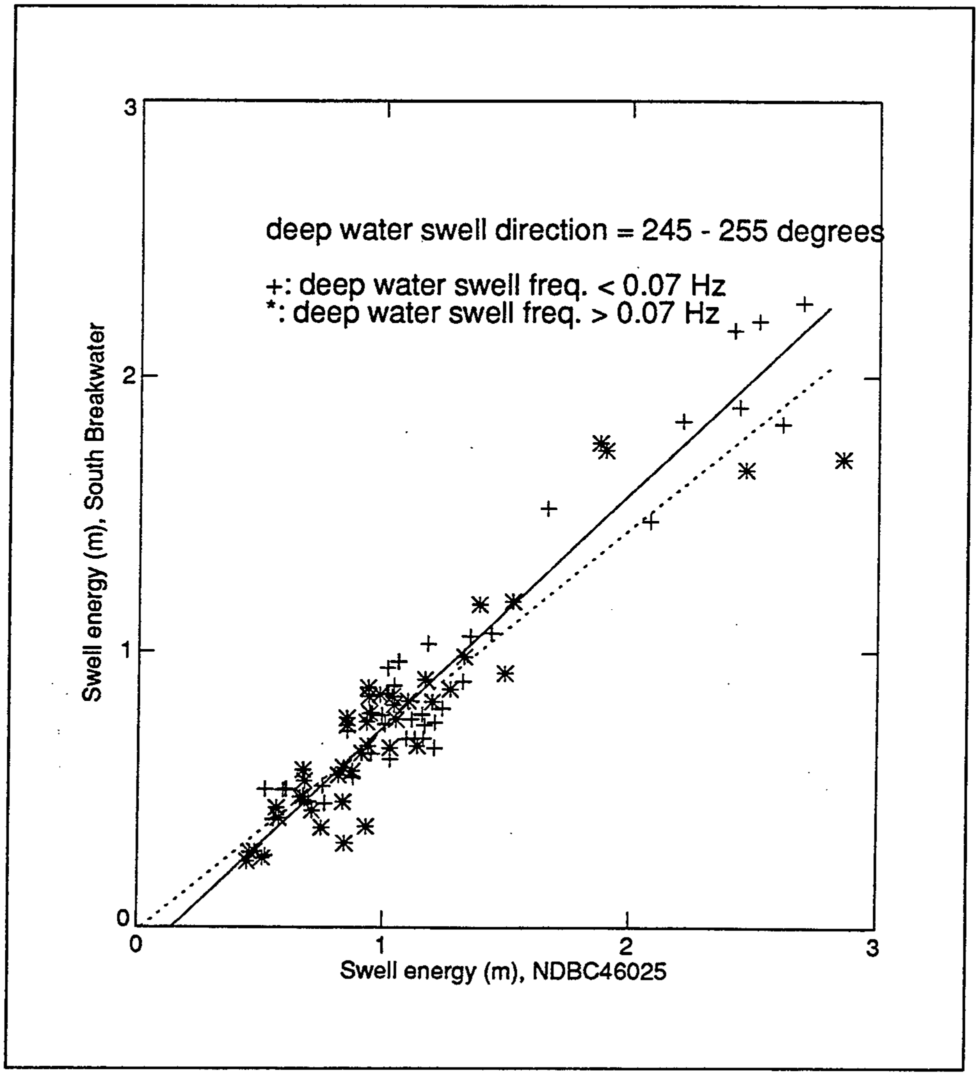
deep water swell direction = 245 - 255 degrees
+: deep water swell freq. < 0.07 Hz
*: deep water swell freq. > 0.07 Hz
Swell energy (m), South Breakwater
Swell energy (m), NDBC46025
0
1
2
3
0
1
2
3

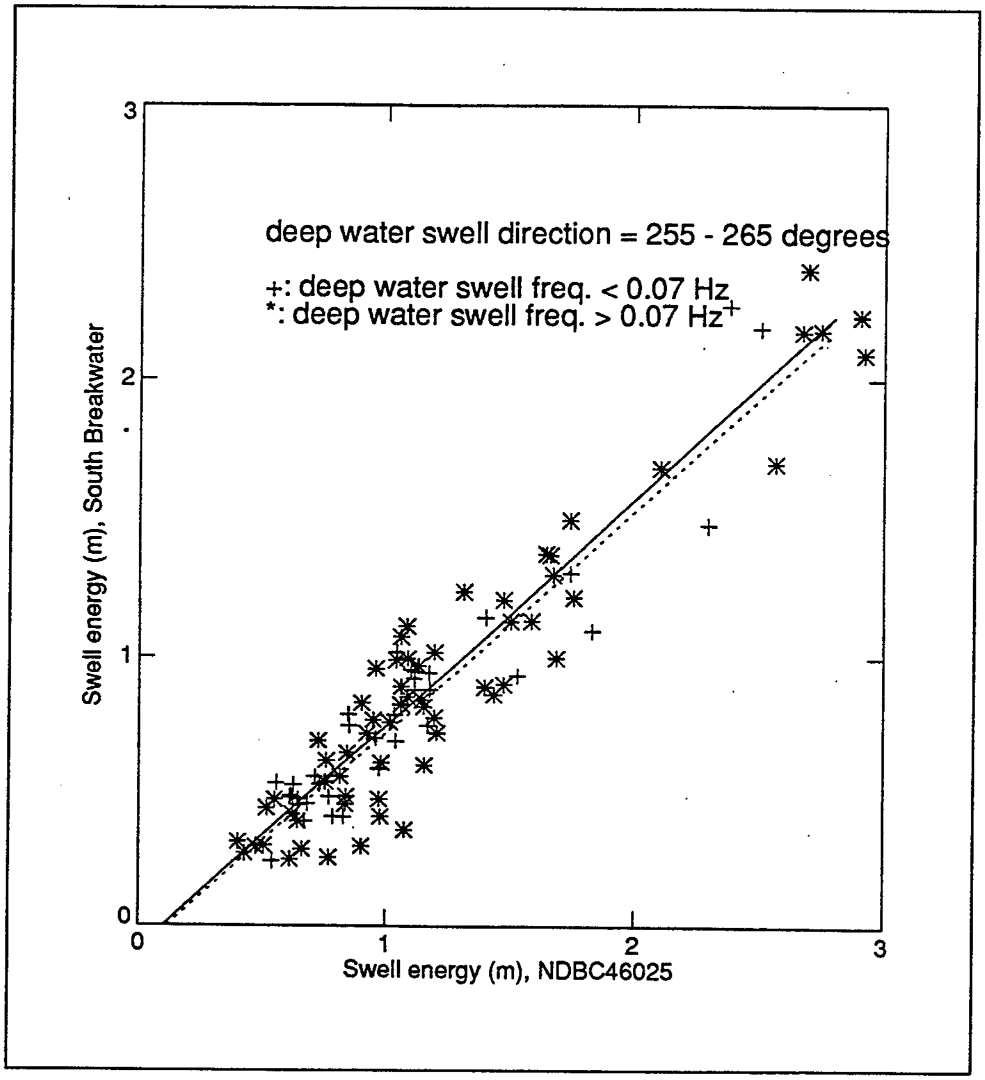

deep water swell direction = 255 - 265 degrees
+: deep water swell freq. < 0.07 Hz
*: deep water swell freq. > 0.07 Hz
Swell energy (m), South Breakwater
Swell energy (m), NDBC46025
0
1
2
3
0
1
2
3

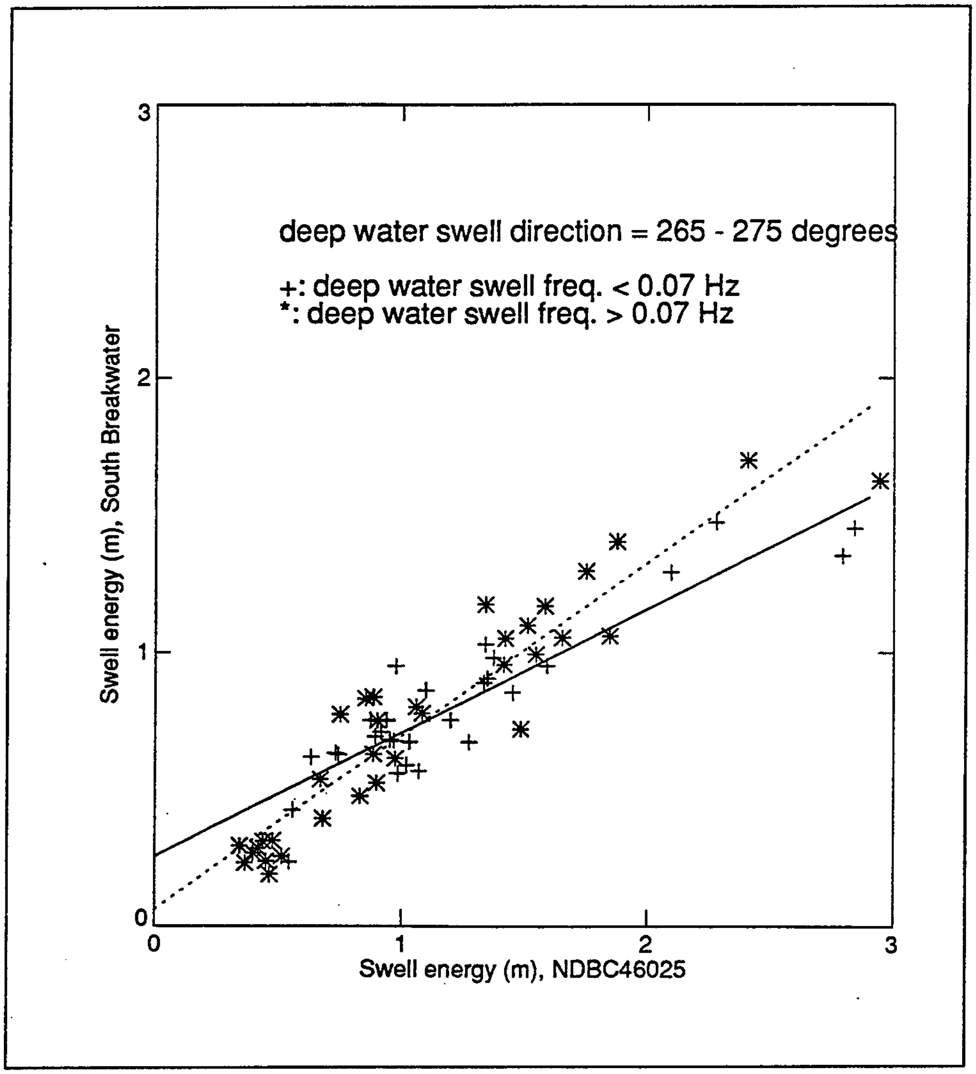
deep water swell direction = 265 - 275 degrees
+: deep water swell freq. < 0.07 Hz
*: deep water swell freq. > 0.07 Hz
Swell energy (m), South Breakwater
Swell energy (m), NDBC46025
0
1
2
3
0
1
2
3

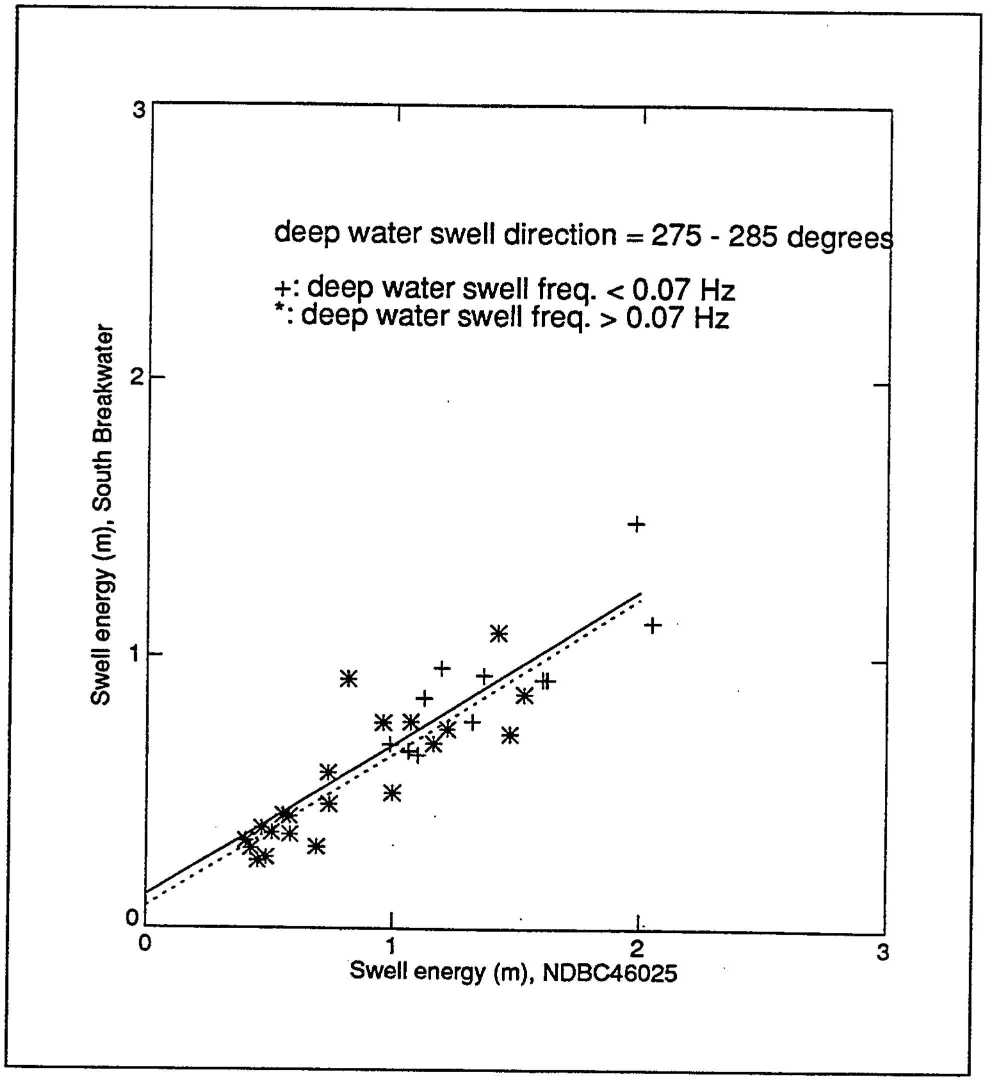
deep water swell direction = 275 - 285 degrees
+: deep water swell freq. < 0.07 Hz
*: deep water swell freq. > 0.07 Hz
Swell energy (m), South Breakwater
Swell energy (m), NDBC46025
0
1
2
3
0
1
2
3

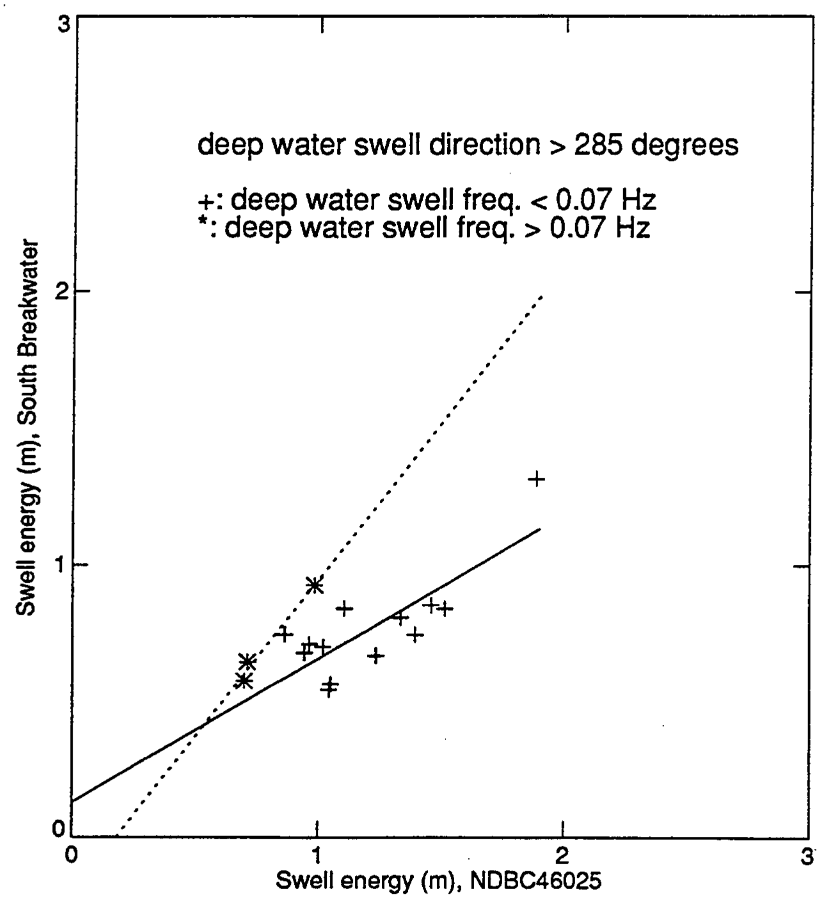

deep water swell direction > 285 degrees
+: deep water swell freq. < 0.07 Hz
*: deep water swell freq. > 0.07 Hz
Swell energy (m), South Breakwater
Swell energy (m), NDBC46025
0
1
2
3

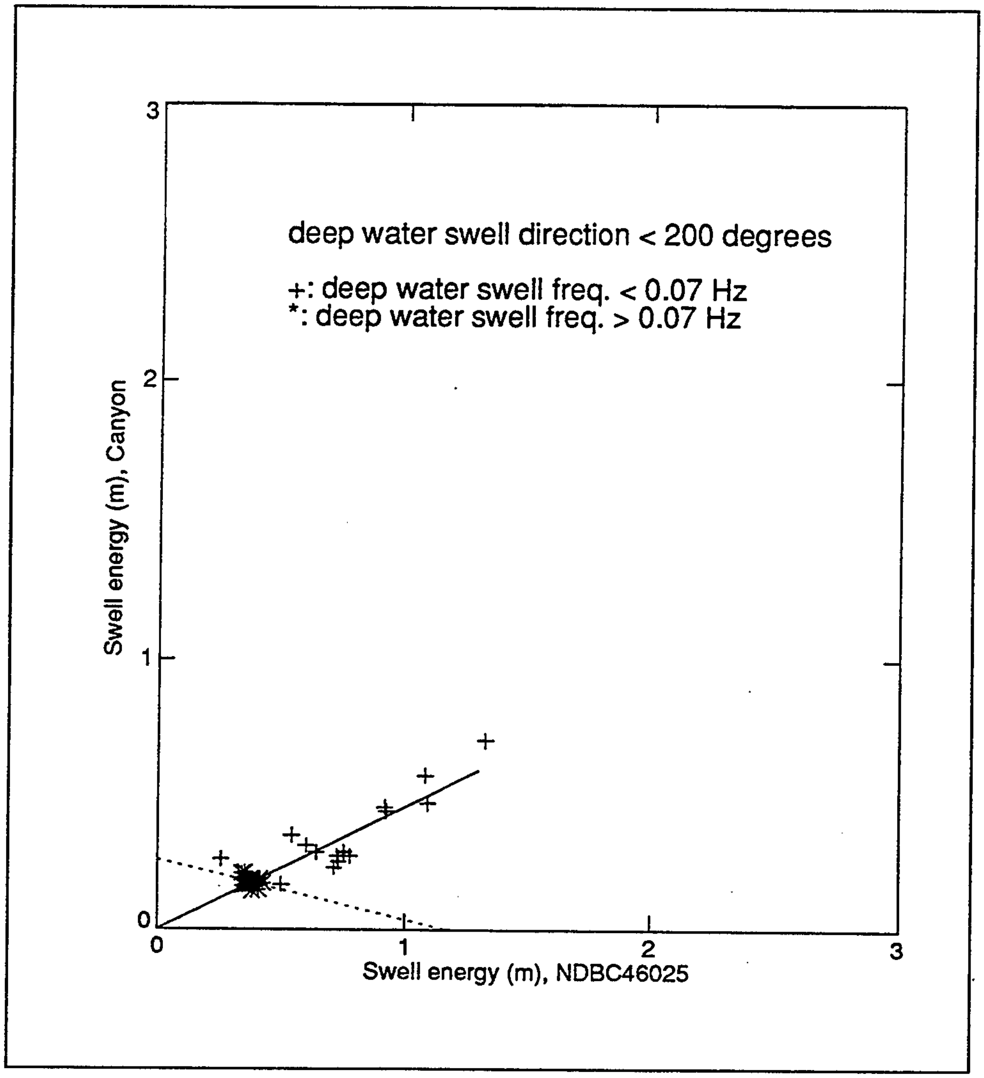
deep water swell direction < 200 degrees
+: deep water swell freq. < 0.07 Hz
*: deep water swell freq. > 0.07 Hz
Swell energy (m), Canyon
Swell energy (m), NDBC46025
0
1
2
3

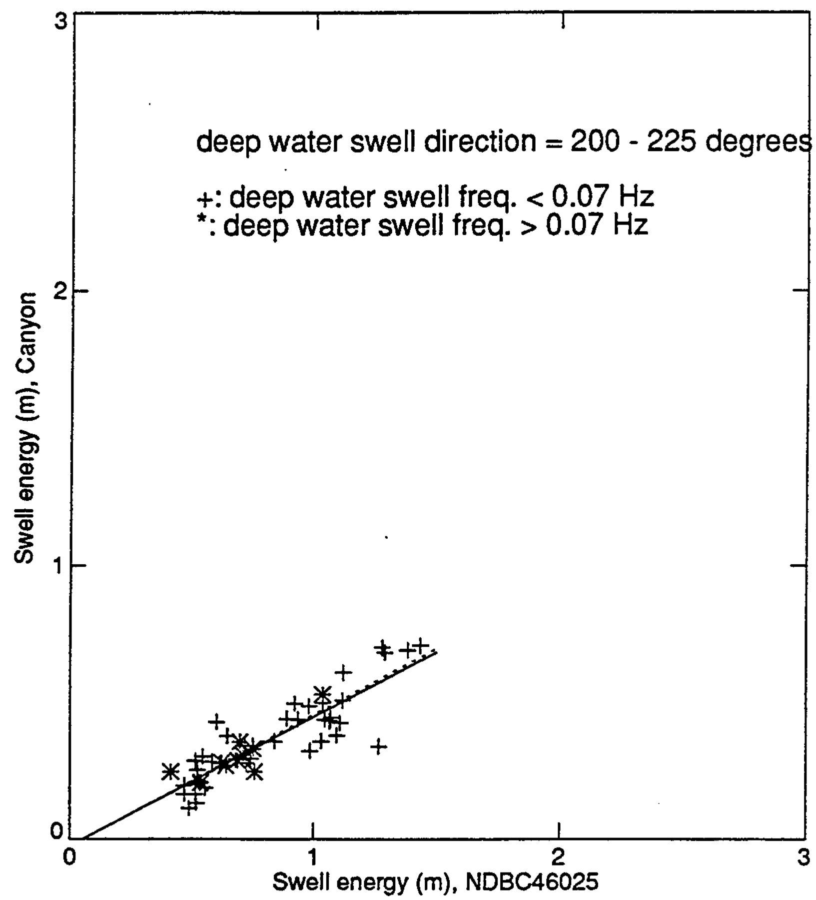
deep water swell direction = 200 - 225 degrees
+: deep water swell freq. < 0.07 Hz
*: deep water swell freq. > 0.07 Hz
Swell energy (m), Canyon
Swell energy (m), NDBC46025
0
1
2
3
0
1
2
3

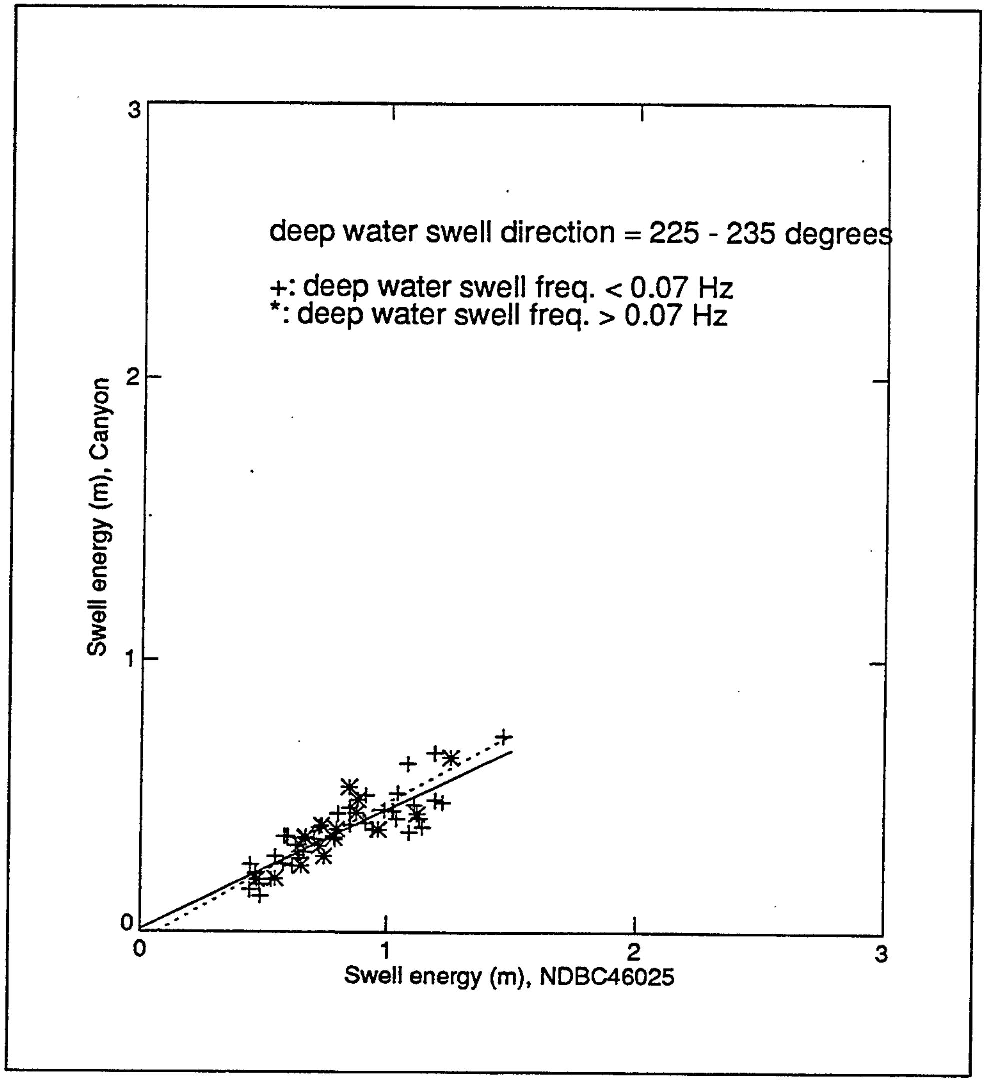

deep water swell direction = 225 - 235 degrees
+: deep water swell freq. < 0.07 Hz
*: deep water swell freq. > 0.07 Hz
Swell energy (m), Canyon
Swell energy (m), NDBC46025
0
1
2
3

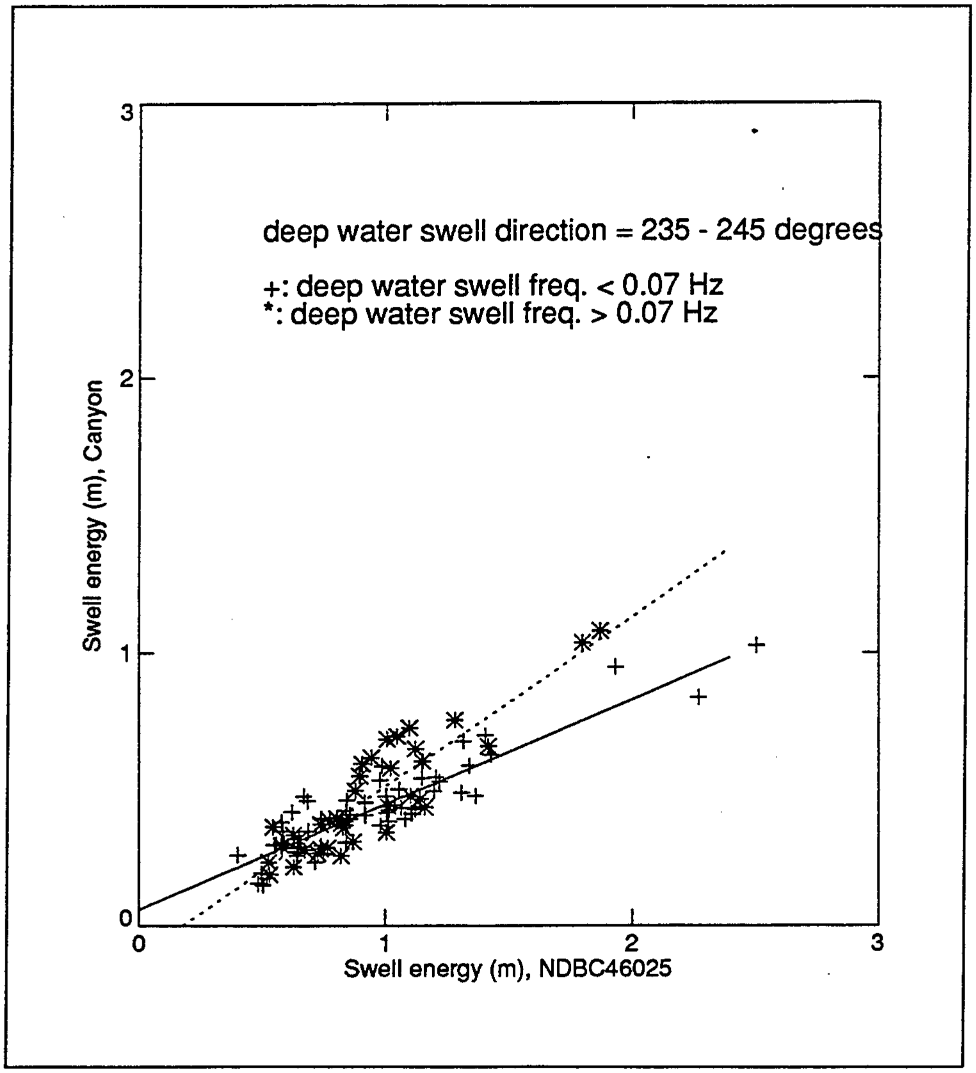
deep water swell direction = 235 - 245 degrees
+: deep water swell freq. < 0.07 Hz
*: deep water swell freq. > 0.07 Hz
Swell energy (m), Canyon
Swell energy (m), NDBC46025
0
1
2
3

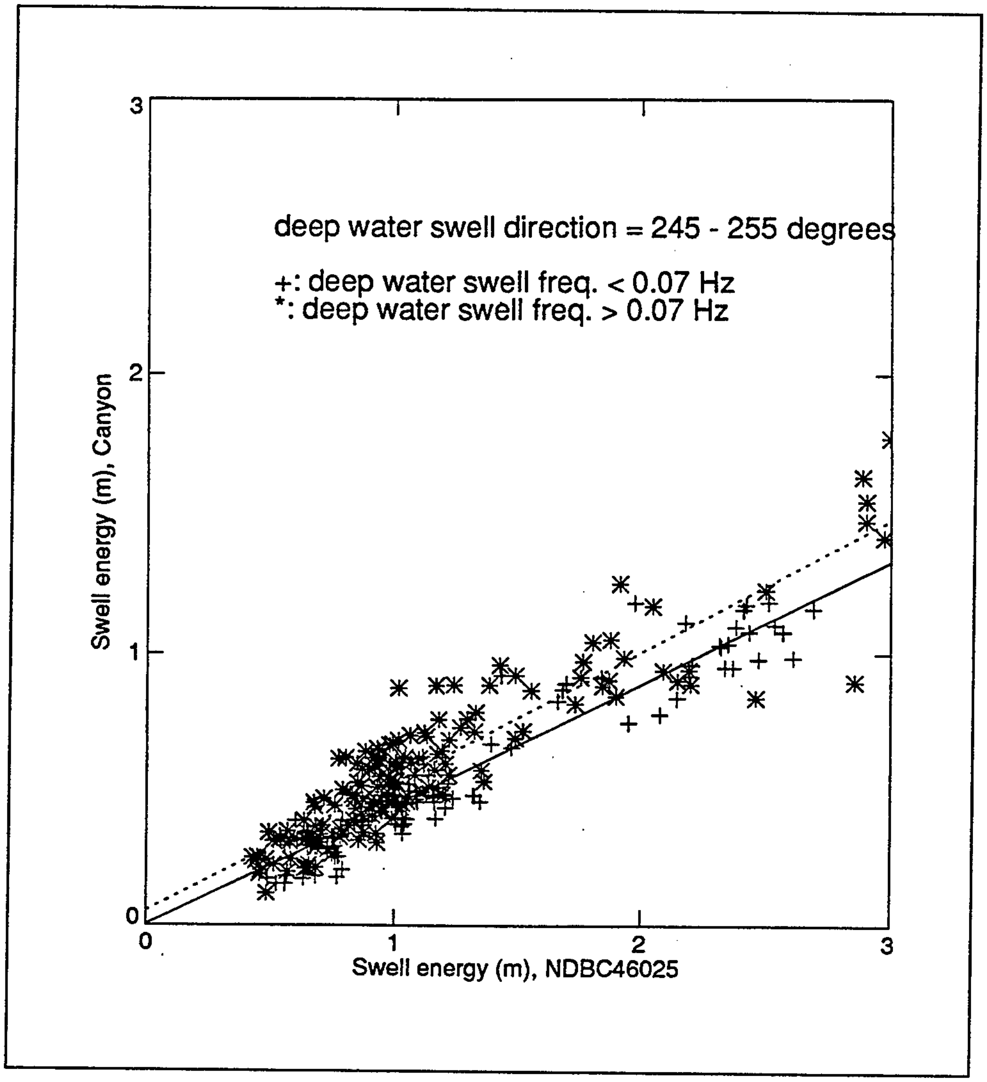

deep water swell direction = 245 - 255 degrees
+: deep water swell freq. < 0.07 Hz
*: deep water swell freq. > 0.07 Hz
Swell energy (m), Canyon
Swell energy (m), NDBC46025
0
1
2
3
0
1
2
3

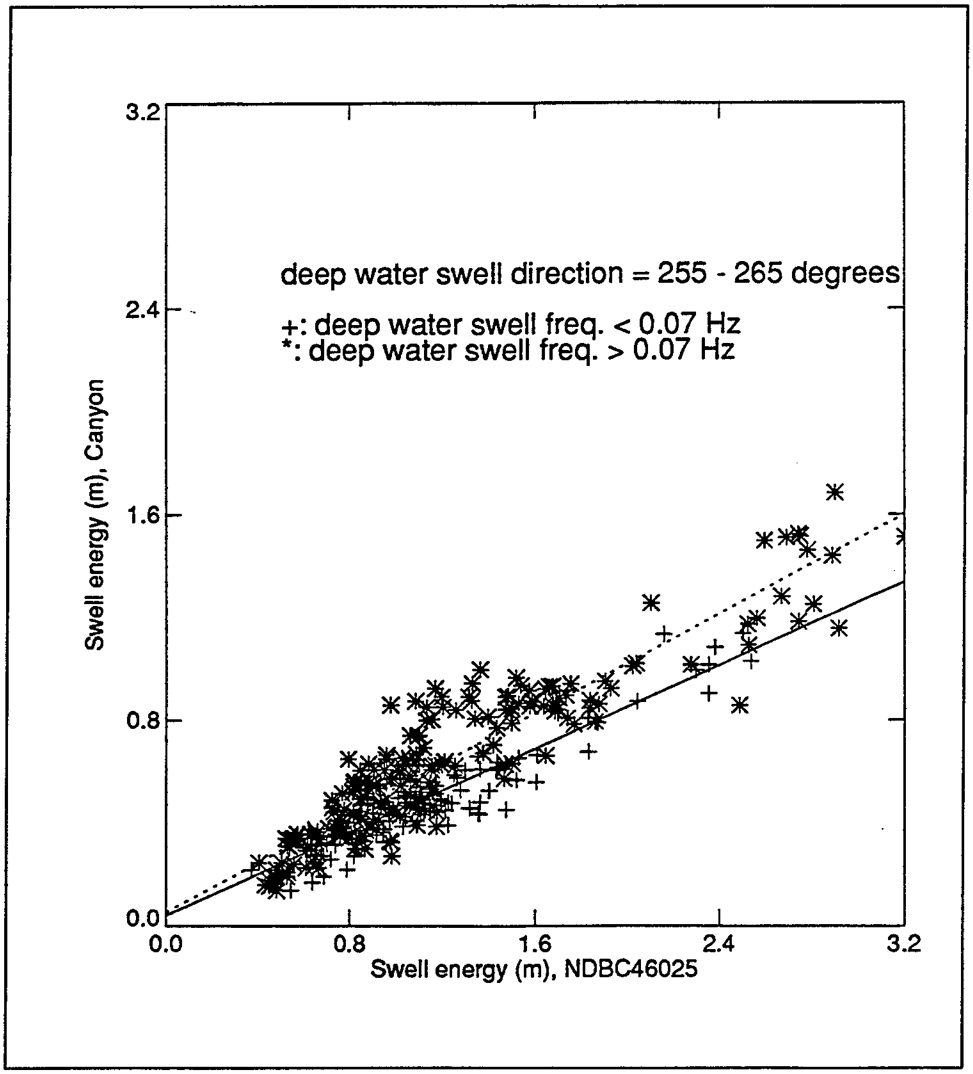

3.2
2.4
1.6
0.8
0.0
0.0
0.8
1.6
2.4
3.2
deep water swell direction = 255 - 265 degrees
+: deep water swell freq. < 0.07 Hz
*: deep water swell freq. > 0.07 Hz
Swell energy (m), Canyon
Swell energy (m), NDBC46025

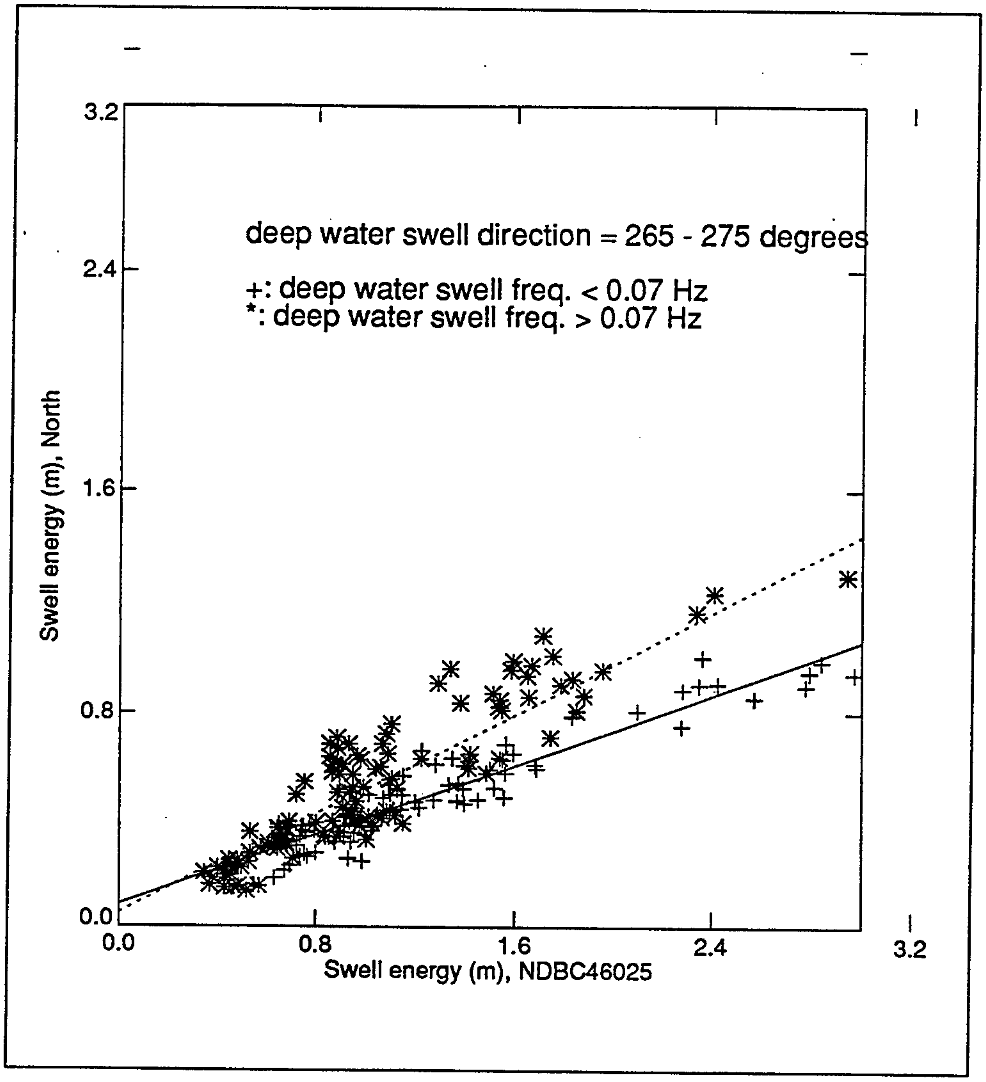

deep water swell direction = 265 - 275 degrees
+: deep water swell freq. < 0.07 Hz
*: deep water swell freq. > 0.07 Hz
3.2
2.4
1.6
0.8
0.0
Swell energy (m), North
0.0
0.8
1.6
2.4
3.2
Swell energy (m), NDBC46025

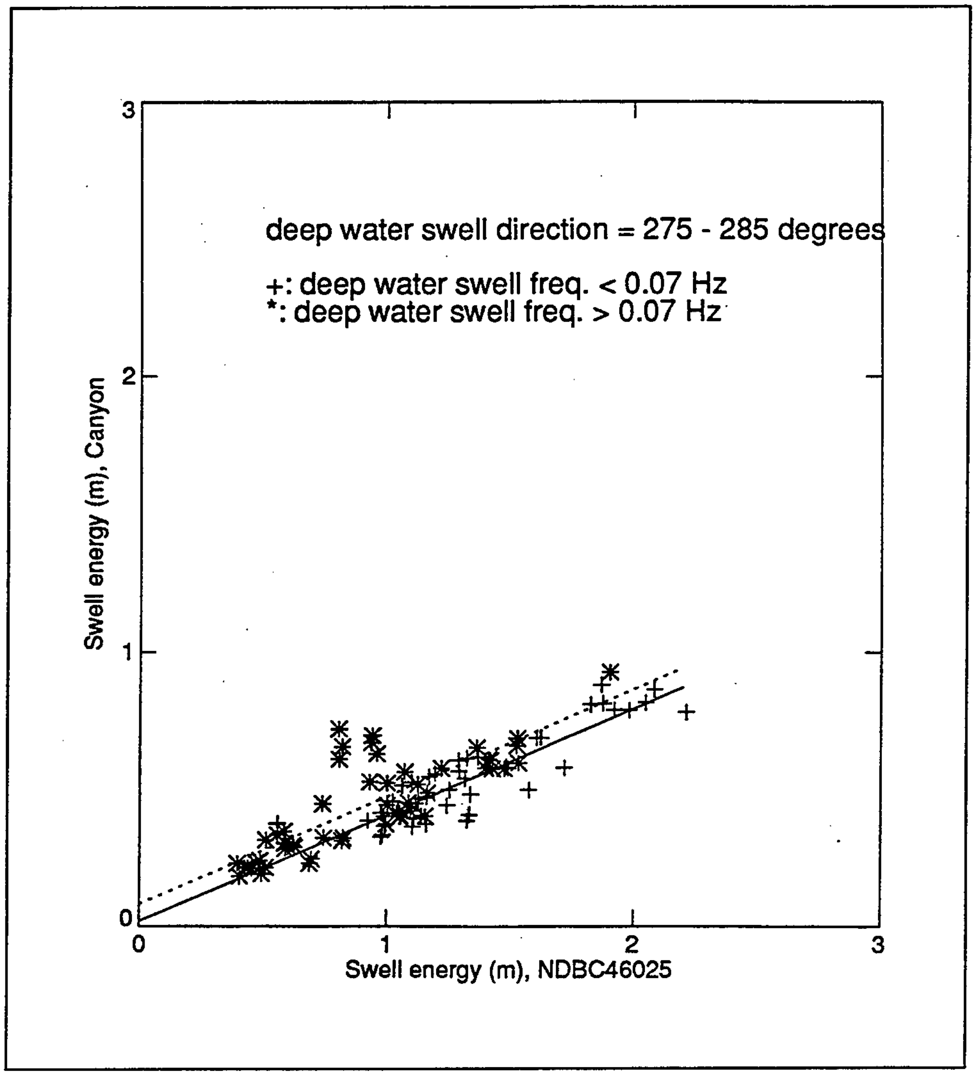

deep water swell direction = 275 - 285 degrees
+: deep water swell freq. < 0.07 Hz
*: deep water swell freq. > 0.07 Hz
Swell energy (m), Canyon
Swell energy (m), NDBC46025
0
1
2
3

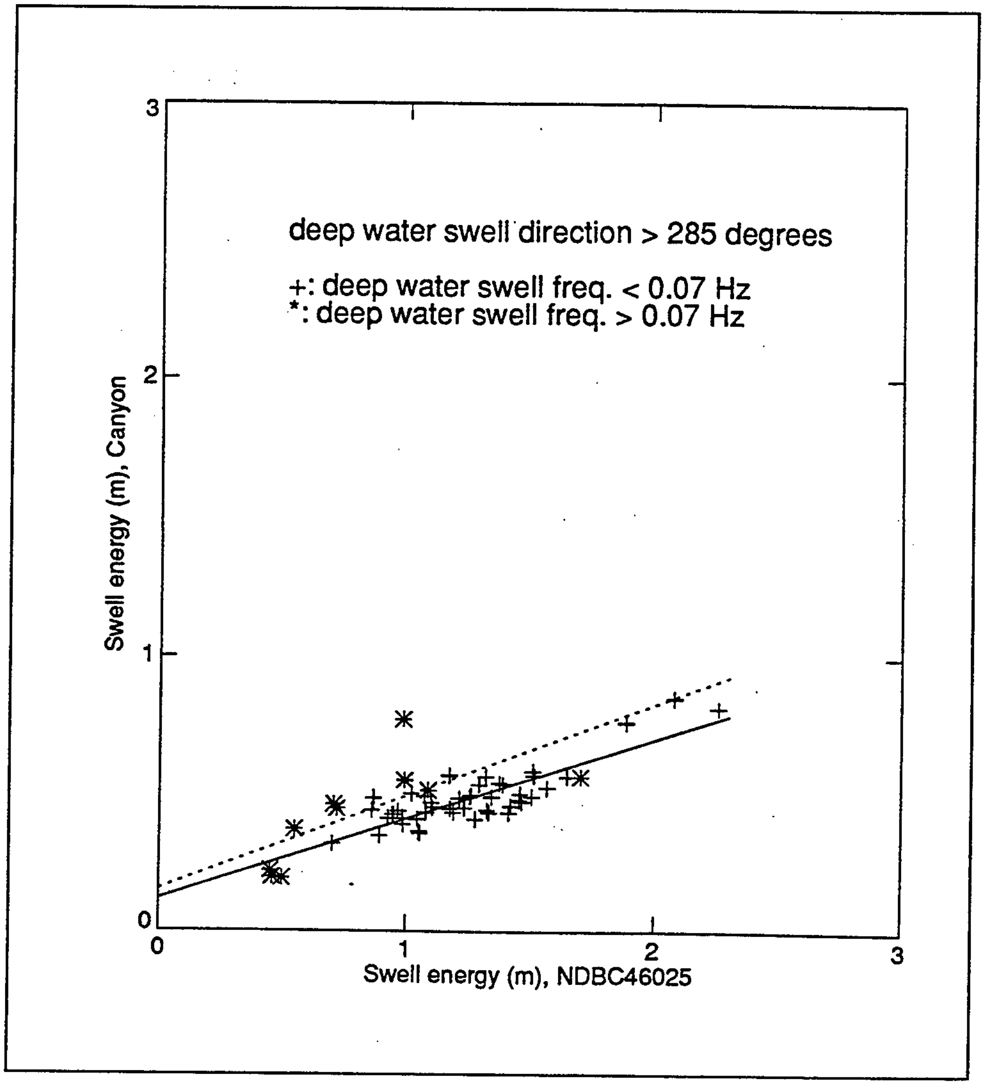
deep water swell direction > 285 degrees
+: deep water swell freq. < 0.07 Hz
*: deep water swell freq. > 0.07 Hz
Swell energy (m), Canyon
Swell energy (m), NDBC46025
0
1
2
3
0
1
2
3

REPORT DOCUMENTATION PAGE

Form Approved
OMB No. 0704-0188

1. AGENCY USE ONLY *(Leave blank)*

2. REPORT DATE
July 1998

3. REPORT TYPE AND DATES COVERED
Final report

4. TITLE AND SUBTITLE
Wave Refraction at Redondo Beach, California (Comparison of Field Measurements with Models)

5. FUNDING NUMBERS

6. AUTHOR(S)
Joon P. Rhee, William D. Corson

7. PERFORMING ORGANIZATION NAME(S) AND ADDRESS(ES)
U.S. Army Engineer Waterways Experiment Station
3909 Halls Ferry Road
Vicksburg, MS 39180-6199

8. PERFORMING ORGANIZATION REPORT NUMBER
Technical Report CHL-98-16

9. SPONSORING/MONITORING AGENCY NAME(S) AND ADDRESS(ES)
U.S. Army Corps of Engineers
Washington, DC 20314-1000

10. SPONSORING/MONITORING AGENCY REPORT NUMBER

11. SUPPLEMENTARY NOTES
Available from National Technical Information Service, 5285 Port Royal Road, Springfield, VA 22161.

12a. DISTRIBUTION/AVAILABILITY STATEMENT
Approved for public release; distribution is unlimited.

12b. DISTRIBUTION CODE

13. ABSTRACT *(Maximum 200 words)*

The U.S. Army Corps of Engineers has investigated various measures for storm damage reduction at Redondo Beach/King Harbor, CA. Numerical models have been used to investigate the effects of local bathymetry on the transformation of deepwater swell. Documents produced by the U.S. Army Engineer District, Los Angeles, point out discrepancies between these model computations and observations during actual storms in 1983 and 1988. The Los Angeles District also questioned the accuracy of theoretical models in general, for areas of complex bathymetry such as Redondo Beach, and argued that the results from the RCPWAVE model "misrepresent actual conditions." There has been a growing consensus to call for the testing of model capabilities. This report responds to that call, and compares results from the refraction model RCPWAVE to measured waves near the Redondo breakwaters. The study also compares results from the spectral refraction model STWAVE against the same measurements. Results of these comparisons are as follows:

a.. Computations from both RCPWAVE and STWAVE are in poor agreement (low correlation coefficients) with the field measurements for $H > 1.5$ m.

b. RCPWAVE tends to overestimate wave heights in general.

c. STWAVE wave heights appear to be more accurate than RCPWAVE, but their underestimations may be unacceptable in some cases.

(Continued)

14. SUBJECT TERMS
Numerical modeling
RCPWAVE model
Redondo Beach, California
STWAVE model
Wave refraction

15. NUMBER OF PAGES
87

16. PRICE CODE

17. SECURITY CLASSIFICATION OF REPORT	18. SECURITY CLASSIFICATION OF THIS PAGE	19. SECURITY CLASSIFICATION OF ABSTRACT	20. LIMITATION OF ABSTRACT
UNCLASSIFIED	UNCLASSIFIED		

NSN 7540-01-280-5500

Standard Form 298 (Rev. 2-89)
Prescribed by ANSI Std. Z39-18
298-102

13. (Concluded).

d. Both the field measurements and the model computations indicate no significant tidal influence on wave transformation.

e. Field measurements fail to support the wave-height relationship $H = kH_o$ inherent in the model computations.

f. Correlation changes significantly with increasing measured wave height. Therefore, extrapolation of the present results beyond those measured (3.3 m for maximum H_0) requires caution.